AN INVESTIGATION OF THE THERMAL STRUCTURE IN THE VICINITY OF IPOD SITES 417 and 418

by

DANIEL ALLEN GALSON

B.S. Massachusetts Institute of Technology (1979)

SUBMITTED IN

PARTIAL FULFILLMENT

OF THE REQUIREMENTS FOR THE

DEGREE OF MASTER OF SCIENCE

at the

MASSACHUSETTS INSTITUTE OF TECHNOLOGY

August, 1979

Signature of Author..
Department of Earth and Planetary Sciences, August 17, 1979

Certified by..
Thesis Supervisor

Accepted by..
Chairman, Departmental Committee on Graduate Students

AN INVESTIGATION OF THE THERMAL STRUCTURE IN THE VICINITY OF IPOD SITES 417 AND 418

by

Daniel Allen Galson

Submitted to the Department of Earth and Planetary Sciences on August 17, 1979 in partial fulfillment of the requirements for the degree of Master of Science

ABSTRACT

We have obtained a suite of 53 closely spaced acoustically navigated heat flow measurements on well sedimented 110 Ma crust in the northwest Atlantic Ocean (25^{o}N, 68^{o}W; 950 kms south of Bermuda). Their mean and standard deviation are 1.17 HFU (49.0 mW/m^2) and .08 (3.3), respectively. The temperature gradients increased asymptotically with depth in a remarkably consistent fashion; a 10% perturbation in gradient was seen at a depth of 1 m in the sediment column. This perturbation was less than a few percent at a depth of 2 m in the sediment column. These observations can be explained by either a step increase in water temperature of a few hundredths of a degree at the sediment interface 1 month prior to the measurements or by an oscillatory temperature change at the sediment interface with a maximum amplitude

of a few hundredths of a degree and a 1 month period. The mean, based on the asymptotic temperature gradient, is close to the 1.18 HFU (49.4 mW/m^2) predicted by lithospheric cooling models that incorporate an exponential decrease in heat flow with increasing age for the older oceanic basins (i.e. plate models). The average basement depth (corrected for sediment loading), of the 10 by 20 km IPOD (International Phase of Ocean Drilling) survey area is within 135 m of that predicted by these same cooling models, well within the predicted scatter of the depth-age relationship. Hence, it appears that the thermal anomaly which caused the formation of the Bermuda Rise may not currently be significantly affecting the shallow thermal structure of the lithosphere 950 kms south of the island.

The heat flow measurements were made with a new digitally recording instrument, the operating characteristics and limits of which we discuss. The instrument has a maximum temperature sensitivity of .00017 $^{\circ}C$ and a maximum depth (pressure) sensitivity of .06 m. Generally, the temperature resolution was not better than ±.0005 $^{\circ}C$ due to either cable leakage or electronic path effects (instrument noise).

Thesis Supervisor: R.P. Von Herzen

Title: Senior Scientist, Woods Hole Oceanographic Institution

ACKNOWLEDGEMENTS

I am grateful to my thesis advisor, Dick Von Herzen for his understanding, patience and helpful advice. I am thankful to John Sclater for providing me with financial support for much of the time I spent working on this thesis, for initially encouraging me into the discipline of observational heat flow, and for much beneficial advice in my three years as an undergraduate and a graduate student at MIT.

I would like to acknowledge John Crowe and Ken Green who were always willing to answer questions and provide criticism. Ken Green also did some of the initial data processing. Lawrence Hobbie was responsible for obtaining all of the thermal conductivity measurements, for many grammatical improvements in the final version of the text, and for drafting the final version of some of the figures. Jim Akens was responsible for running the heat flow program during the cruise.

Finally, I am grateful to Dorothy Frank and Laura Willard who each typed part of the final draft of the text, and to Jamie MacEachern who typed the final version of all of the tables.

A special acknowledgement must go to my family, who provided me with endless amounts of much needed encouragement, warmth and advice.

TABLE OF CONTENTS

LIST OF FIGURES

LIST OF TABLES

I INTRODUCTION

Fifty-five closely spaced measurements of heat flow were obtained in the vicinity of IPOD sites 417 and 418 during Leg 2 of the Atlantis II cruise #97 in February of 1978. Fifty of the measurements were obtained during 4 multipenetration 'pogo' probe stations. The remaining 5 measurements were deep piston cores. The mean and standard deviation of the 53 reliable measurements are respectively, 1.17 HFU (μcal/cm^{2}s) and .08. The two drill sites were occupied for five months (20 November 1976 to 21 April 1977, Glomar Challenger Legs 51-53) and are located at the southern part of the Bermuda Rise, slightly north of the Vema Gap on oceanic floor connecting the Nares and Hattaras abyssal plains (figure 1). A drilling summary is given in Table 1 and the results of the drilling have been presented by Donnelly, Francheteau et al. (1977), Bryan, Robinson et al. (1977), and Flower, Salisbury et al. (1977).

The heat flow measurements were taken in conjunction with seismic reflection experiments carried out using a .66 liter (40 cubic inch) airgun and a single hydrophone towed within a few hundred meters of the seafloor. These results are presented elsewhere (Purdy et al., 1979).

A bathymetry contour map was made of the 10 by 20 kilometer survey area using data from a conventional 3.5 kHz echo sounder (figure 2). Superimposed on this map are the

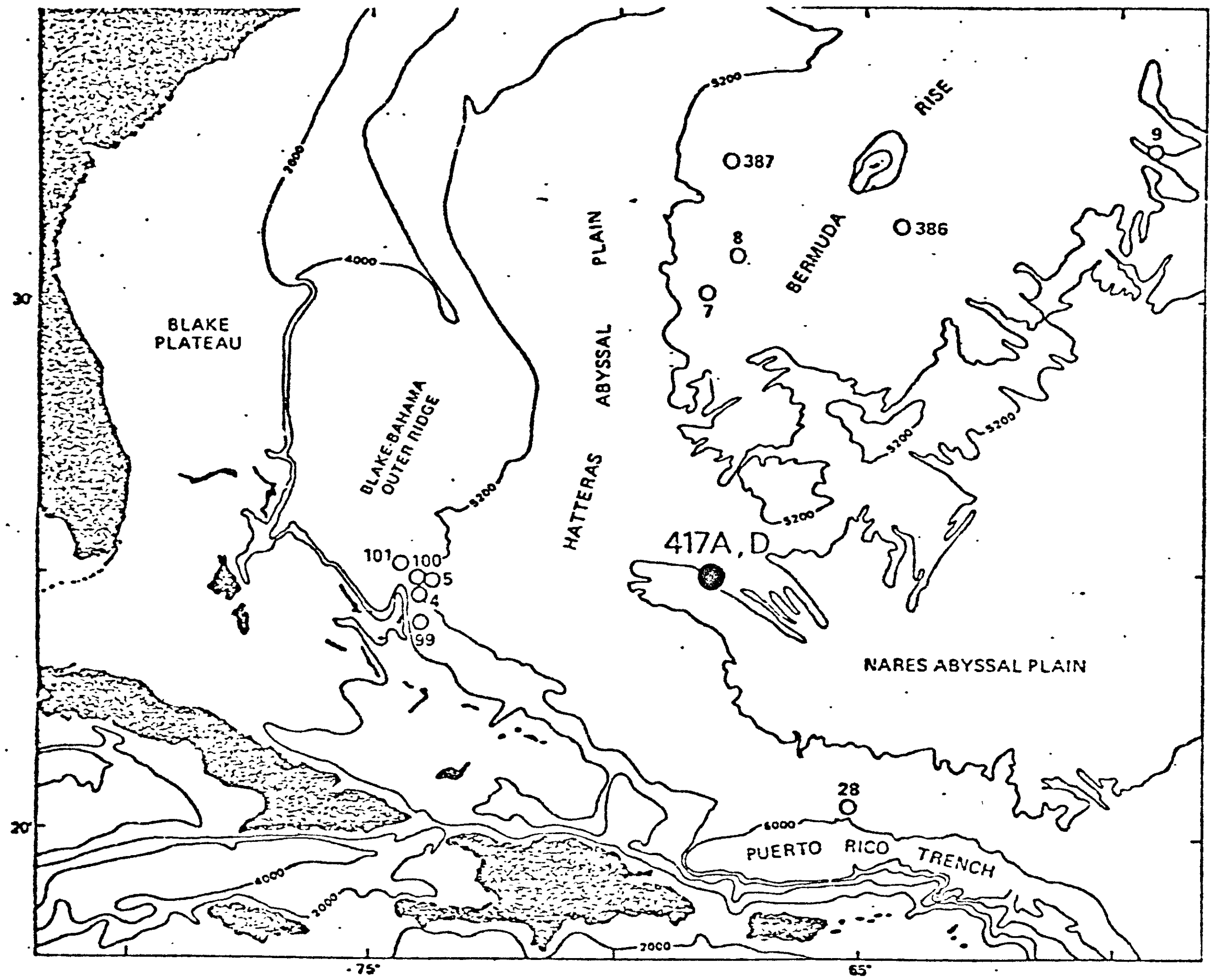

Index Map of the Western Atlantic Basin showing Locations of Deep Sea Drilling Sites

Figure 1

Table 1

Drilling Data from IPOD Sites 417 and 418

Hole	Latitude(N)	Longitude(W)	Depth(m)	Penetration (m) Sediment	Basement	Total
417A	25°06.63'	68°02.48'	5468	211	206	417
417D	25°06.69'	68°02.82'	5482	343	363	708
418A	25°02.08'	68°03.44'	5511	324	544	868
418B	25°02.08'	68°03.45'	5514	320	10	330

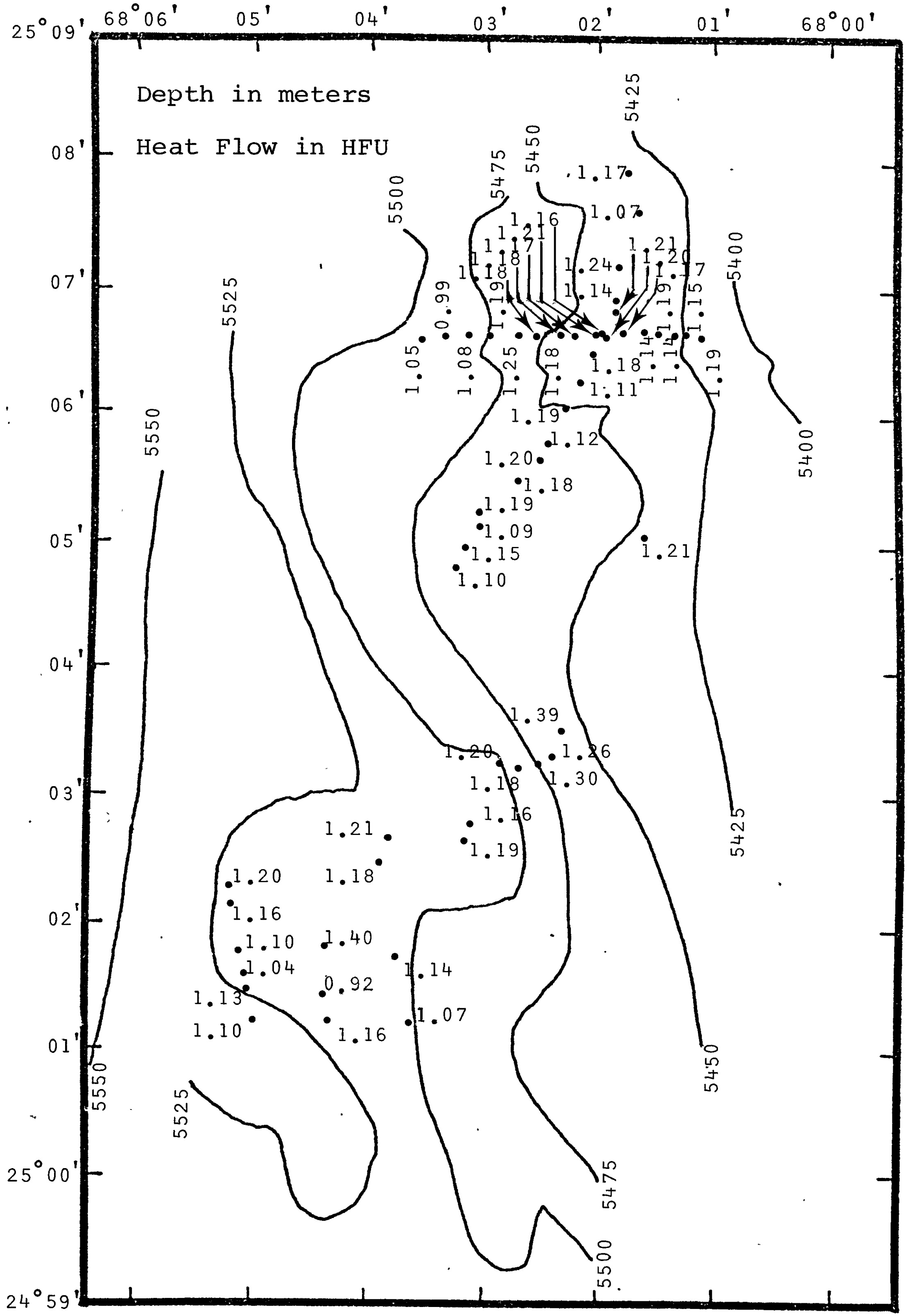

Bathymetry and Heat Flow Map of the Survey Area

Figure 2

53 reliable heat flow values. Ship tracks, most of which were navigated using acoustic transponders, are shown in figure 3. The bathymetry map shows a gentle slope towards the west with total seafloor relief of about 150 meters in the survey area.

Previous work in the area has been done at IPOD survey site AT 2.3 and is reported by Harkins and Groman (1976). No previous heat flow measurements have been taken in the exact survey area although Gerard *et al*. (1962), Reitzel (1963), Langseth *et al*. (1966) and Bookman *et al*. (1973) have presented discussions of measurements obtained within a few 100 kms of the survey area.

This paper will briefly report on the instrumentation and operations used in the collection of the measurements. A discussion is given of data reduction techniques and possible sources of error in the heat flow values. Finally, we present a discussion and interpretation of the measurements.

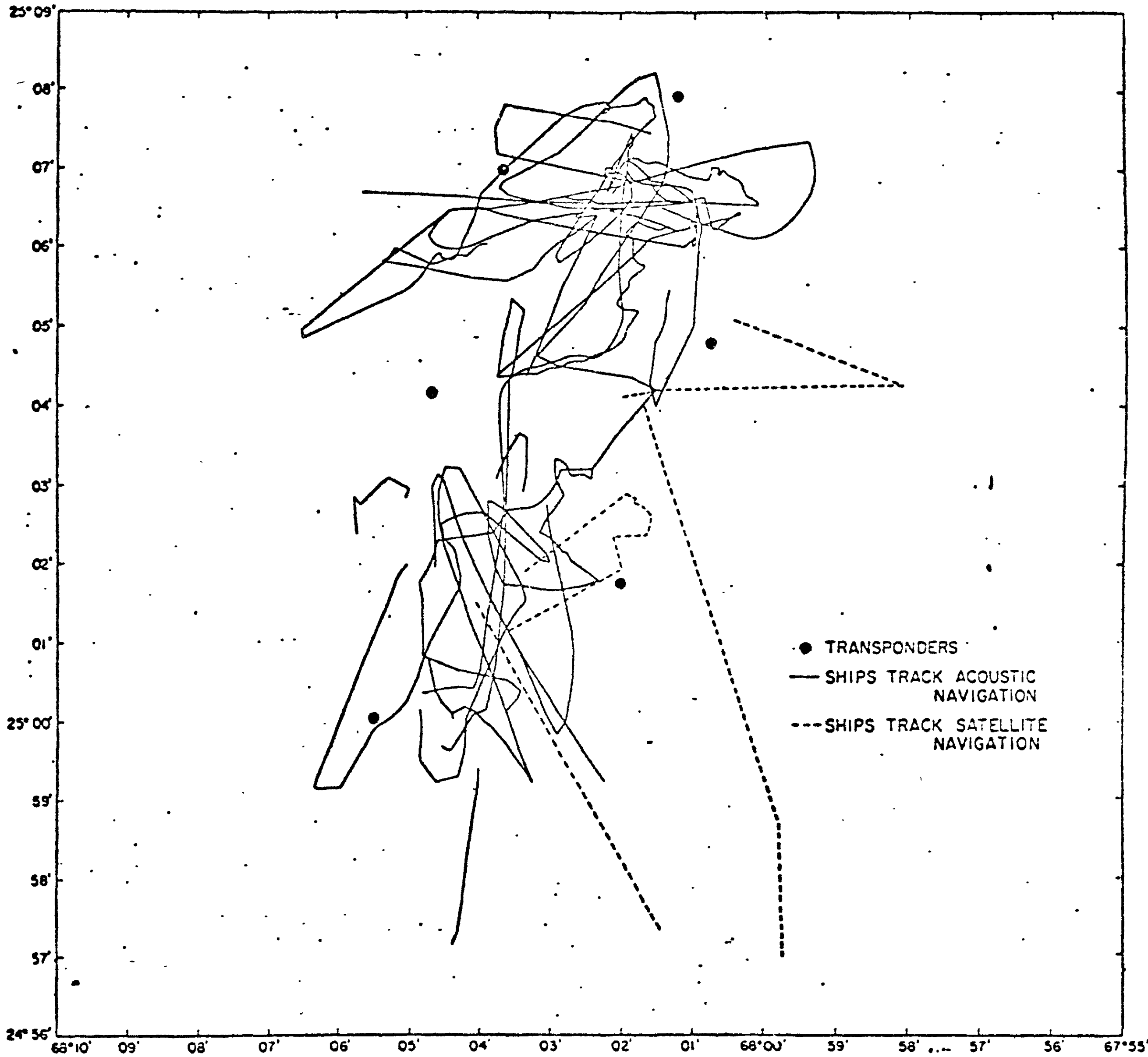

Ship Tracks Along Which Depth Data was Gathered for the Construction of a Bathymetry Map

Figure 3

II INSTRUMENTATION AND METHODS

Due to recent advances in instrumentation, both in navigation and in the design of the heat flow apparatus, new standards should soon be set for the reporting of thermal gradient measurements at sea.

Navigation

Precise navigation was obtained using a network of transponders laid out in the configuration shown in figure 3. When within the range of the transponder net, an independent determination of the position of the heat flow instrument could be made by the use of a transponder relay (hereafter referred to as 'fish') placed a short distance up the wire from the instrument. This distance was either 200 meters or 1000 meters. The configuration is shown in figure 4. A description of the Woods Hole Oceanographic Institution's acoustic navigation system (known as ACNAV) is given by Hunt et al. (1974).

When inside the range of the net, the relative position of the fish or of the ship could be determined to within ±25 meters (Purdy et al., 1979). However, the absolute accuracy of the locations is limited by our ability to determine the absolute positions of the transponders. These positions are calculated from satellite fixes collected during the survey operations. Hence, the absolute accuracy of the fish and ship locations is estimated to be ±100 meters (Purdy et al.,

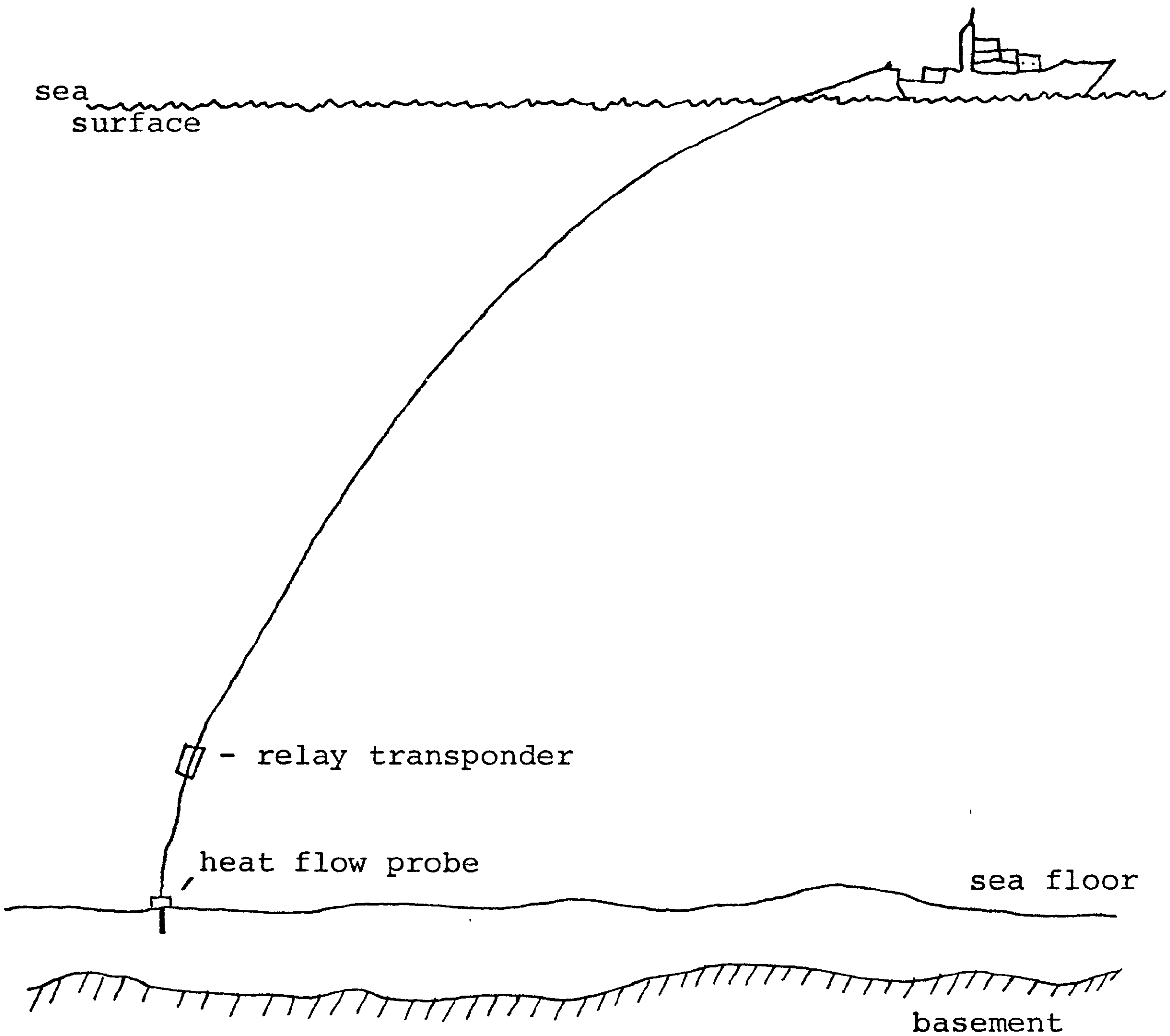

Ship - Relay Transponder - Heat Flow Probe
Configuration

Figure 4

1979). This represents a considerable improvement over the accuracy of more conventional satellite fixes, radar fixes and Loran fixes. For some of the heat flow stations, the fish was either not used or was out of the range of the transponder net. In these cases, the position of the heat flow instrument was estimated from an analysis of ship/fish separations for stations in which acoustic navigation data was available for the fish. A discussion is postponed to the section on data reduction.

Thermal Gradient Measurements

Until recently, most oceanic heat flow measurements were obtained with analog recording devices, such as that described by Langseth (1965). With recent electronic improvements, the capability has been developed to utilize a digitally recording instrument. The Woods Hole Oceanographic Institution's digital heat flow instrument (DHF2), designed by Paul Murray and built by Jim Akens, was used for all of the measurements. Figure 5 shows 2 photographs of the instrument, taken at different angles.

The thermistors used are of the standard type; their resistance is sensed by a Wheatstone bridge whose output is an analog voltage. Figure 6 shows a simplified version of this part of the circuitry. V_o is the output voltage and is equal to $G \cdot (V_+ - V_-)$ where G is the gain of the Op-Amp. R_2 is a variable fixed precision resistor. R_x is the thermistor

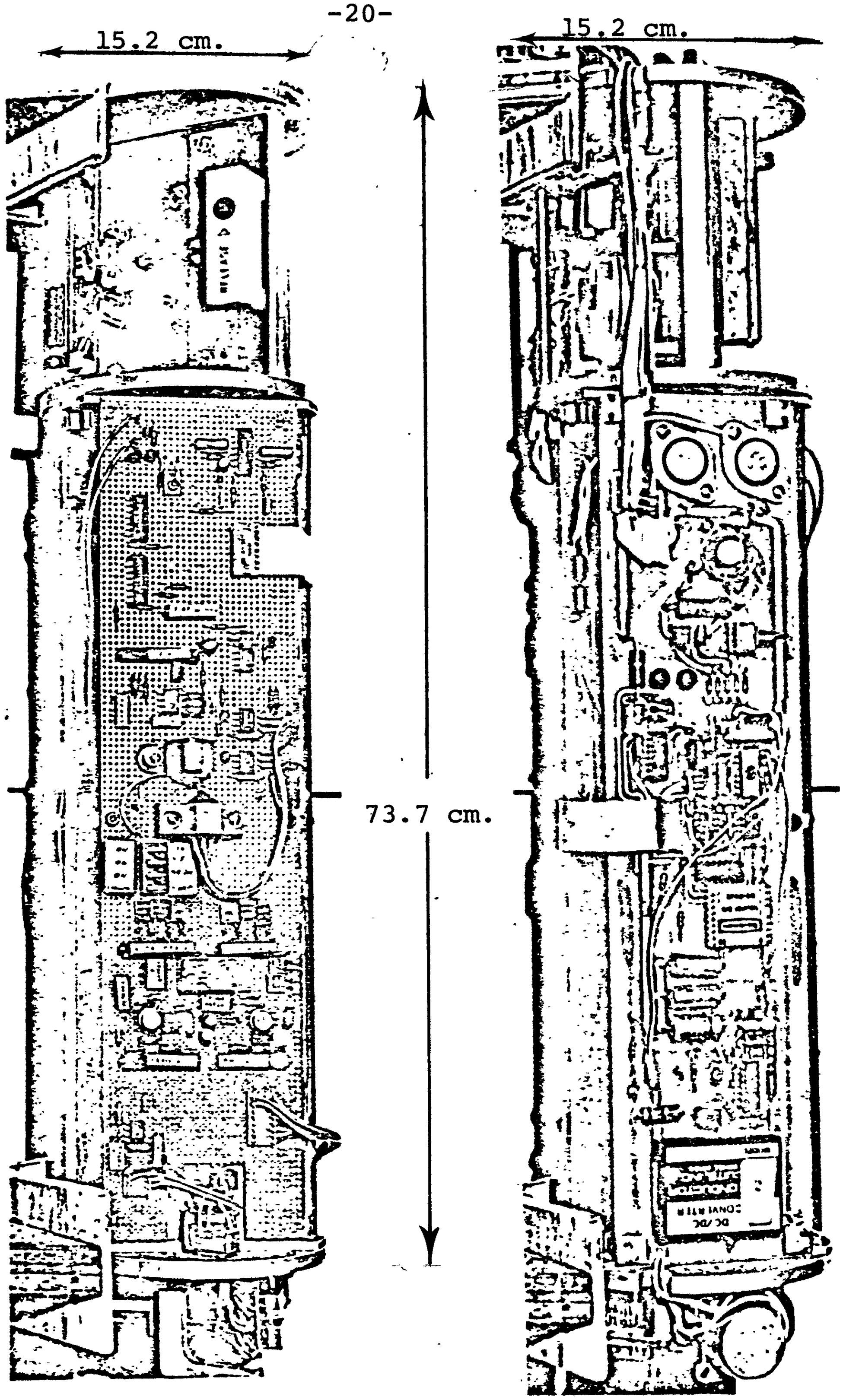

Two Views of the DHF2

Figure 5

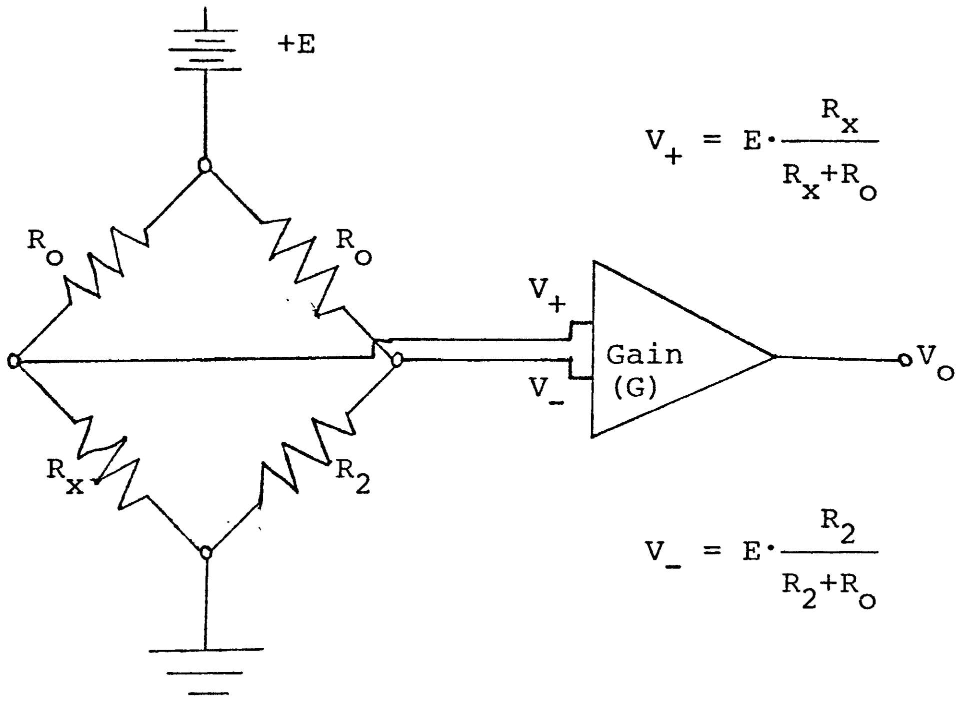

$$V_+ = E \cdot \frac{R_x}{R_x + R_o}$$

$$V_- = E \cdot \frac{R_2}{R_2 + R_o}$$

$$V_o = G \cdot (V_+ - V_-)$$

$$= G \cdot E \cdot \left(\frac{R_x}{R_x + R_o} - \frac{R_2}{R_2 + R_o}\right)$$

Thermistor Resistance (R_x) to Voltage Conversion
Via a Wheatstone Bridge Circuit

Figure 6

resistance to be sensed. R_o is a constant resistance, typically equal to 20,000 ohms. E is typically on the order of 1 Volt. We have,

$$V_+ = E \cdot \frac{R_x}{R_x + R_o} \quad ; \quad V_- = E \cdot \frac{R_2}{R_2 + R_o}$$

hence,

$$V_o = G \cdot E \cdot (R_x \cdot (R_x + R_o)^{-1} - R_2 \cdot (R_2 + R_o)^{-1})$$

It is desirable to have the R_x/V_o transfer function as linear as possible. From the form of the equation, we can see that greater linearity is achieved if R_o is large compared to R_x. However, as R_o is increased, the gain of the Op-Amp must also be increased so as to maintain an output voltage of approximately the same magnitude. Unfortunately, increasing the gain of the Op-Amp will introduce new nonlinearities into the R_x/V_o transfer.

With previous instruments, the analog voltage was measured by the deflection of a galvanometer, which was recorded optically on film or on a paper tape strip chart recorder. However, via a voltage to frequency (V to F) converter, DHF2 records a serial data stream digitally on an internal cassette tape. Essentially, the V to F converter is a circuit which sends out a pulse with a frequency which is dependent on the input voltage. The time interval between pulses is clocked by a 12 bit digital counter circuit. The output of the counter circuit is recorded on the tape as a 12 bit number of 'counts.'

Figure 7a is a simplified block diagram of the operation of the instrument. A slightly expanded version is given in figure 7b. The pinger output is a 12 kHz signal which is telemetered to the ship and which is received, decoded and subsequently displayed by a Precision Graphic Recorder (PGR). The PGR data, although not as precise as that recorded on the tape, provides an excellent backup in case of tape or V to F failure. Furthermore, it allows the scientist to continuously monitor the temperatures and pressures being recorded by the heat flow instrument.

The principal characteristics of the device are as follows. Each data word consists of 12 bits, which allows a resolution of 1 part in 2^{12} (1:4096). The instrument is equipped with a pressure sensor and has inputs for time, tilt, pressure, a zero scale calibration resistance, from 4 to 8 thermistors and a full scale calibration resistance. The record length is 28 seconds, in which time the instrument accepts, in the above order, information from all of these variables with a 2 second lapse between the recording of each variable. The first thermistor (the water thermistor on this cruise) and the clock pulse are recorded twice. Unfortunately, the tilt variable was not operational on this cruise. The temperatures and pressures recorded are aver-

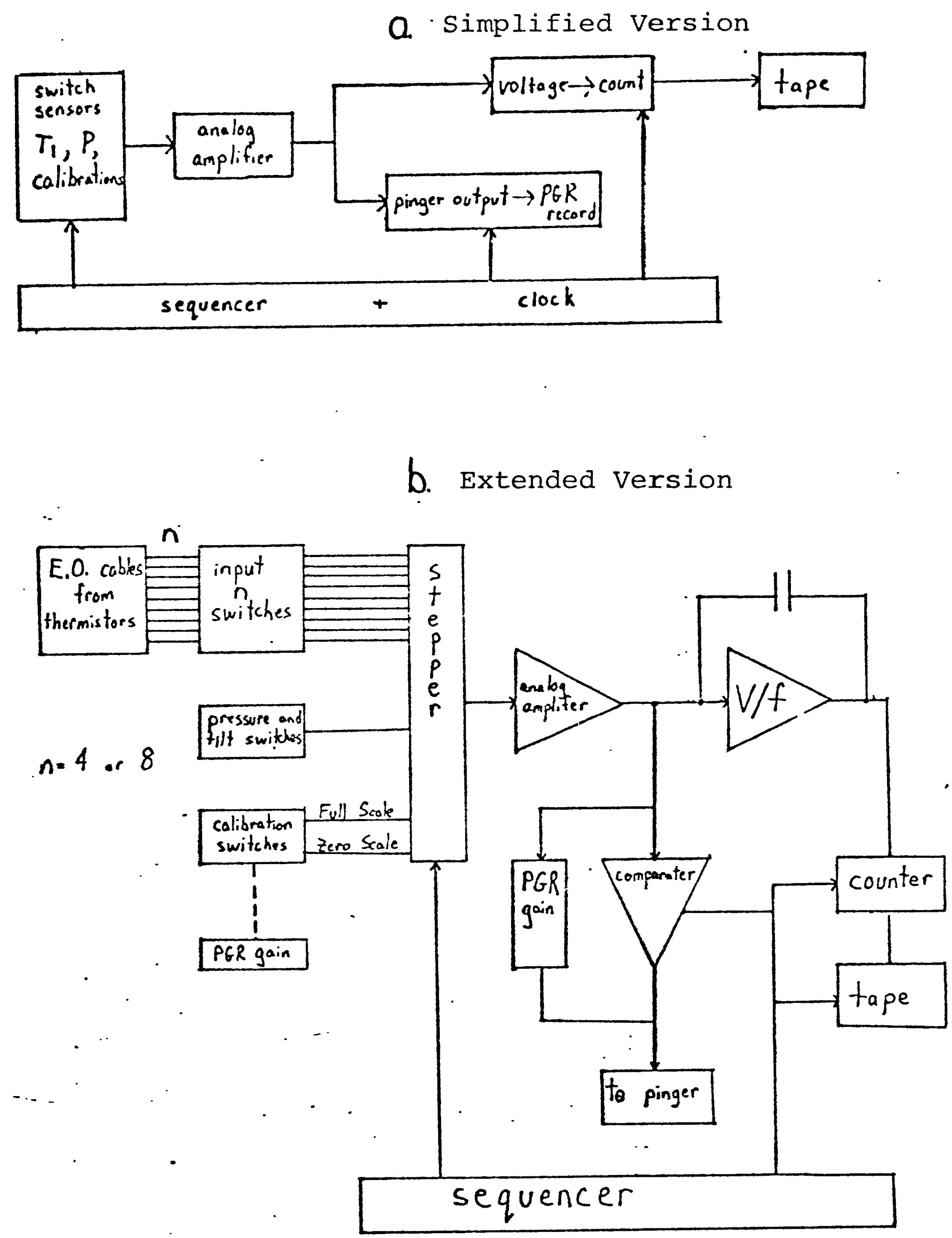

Figure 7

Block Diagrams of the Operation of the DHF2 ages over 1 13/16 second intervals. For situations when fewer than 8 thermistors are used (e.g., pogo probe stations), the instrument can sample a given thermistor more than once each 28 second record.

The allowable sensitivity of the digital recording of pressure and temperature is determined by a combination of the following factors: the actual depth and sediment temperatures, the automatic rollover to 0 of the number of counts after 4096 is reached, and the instruments upper-scale limit of 13.5 rollovers (55296 usable counts). The temperature counts were set to rollover at intervals of approximately .7 °C. This corresponds to a least significant bit of .00017 °C. The thermistors used to measure temperature have a characteristic resistance change on the order of 200 ohms/deg near 2 °C, which decreases as temperature increases. Thus, the least significant bit corresponds to a resistance change of .034 ohms. Rollovers occur approximately every 141 ohms. Pressure rolls over every 246 meters corresponding to a least significant bit of .06 meters. For the first 4 stations of the cruise, the pressure sensitivity was actually .09 meters. This was changed to .11 meters for the last 5 stations because a sensitivity of .09 meters resulted in an off-scale pressure near bottom.

The meaningful recording life of the battery is at least 20 hours. Station 6, during which 19 thermal gradient measurements were obtained, alone exhausted 16 hours of battery life. Good results were obtained up until the time the battery died. On the other hand, during station 10, dying batteries resulted in a measurement with noise level slightly above average. In fact, the instrument actually stopped recording while the probe was still in the sediments (but fortunately, after thermal equilibrium had been reached).

For data reduction purposes, a thermistor count can be converted back to an actual resistance by utilizing our knowledge of the instrument design characteristics. The equations which are used in this conversion can be derived from the bridge and V to F circuits characteristic of the instrument. They are as follows:

$$R(\text{ohms}) = \frac{R_o}{\frac{a}{N-b} - 1} \qquad \text{where,}$$

$$a = \frac{F - Z}{C - D} \quad ; \quad b = \frac{(F \cdot D) - (Z \cdot C)}{D - C}$$

$$\text{and, } C = (1 + R_o/R_F)^{-1}; \; D = (1 + R_o/R_z)^{-1}$$

N is the number of counts corresponding to a given resistance. R_o is a constant resistance, generally equal to 20,000 ohms. R_z and R_F are zero and full scale fixed precision calibration resistances, and Z and F are the number of counts corresponding to these resistances. R_z and R_F are known constants which are pre-set on the instrument before any station whereas Z and F may fluctuate slightly with respect to time due to instrument noise or weak batteries.

It is R_Z and R_F to which the thermistor readings are compared. R_Z and R_F were on the order of 5000 ohms and were typically different by 90.5 ohms corresponding to voltage and frequency differences of approximately .16 volts and 1385 hertz respectively. It is clear that the counts versus resistance relationship is dependent on the values of Z and F. Typically, the relationship is linear to better than 99 percent.

The nonlinearity inherent in the counts to resistance conversion should be primarily due to the transfer characterisitics of the V to F converter. With the electronics available today, the bridge circuit should be able to be made linear to within a few tenths of a percent. It is our belief that the linearity of the counts to resistance conversion could be greatly increased if the V to F conversion chip were replaced by an analog to digital (A to D) conversion chip. Such a chip would cost about $200 (Fajans, personal communication).

As would be the case with analog instruments, the thermistors were preselected to have closely matching resistances around 2 °C, the temperature expected for the bottom water. Empirical constants, α, β, and γ, which describe the temperature dependency of the thermistors are used in the equation: $T = (\alpha + \beta \cdot \ln R + \gamma \cdot (\ln R)^3)^{-1}$ to determine a temperature once the resistance has been calculated. In this equation, the temperature is given in degrees Kelvin for a resistance given in ohms. For the thermistors which we used, α, β, and γ had a range of $(.127-.133)\cdot 10^{-2}$, $(.260-.269)\cdot 10^{-3}$ and $(.137-.148)\cdot 10^{-6}$ respectively. From these values and the form of the temperature-resistance relationship, it can be seen that the conversion from counts to temperature has a high degree of linearity for a range of temperatures.

We conclude with a work on the future of the digital heat flow instrument. At the time of the Atlantis II 97 cruise, major technical advancements were being made in the instrument design. However, the basic operating system described here is still applicable to the more updated versions of the instrument. Green (in preparation) and Murray (in preparation) will describe in more detail the updated and improved versions of the DHF2 currently in use. George Pelletier, the technician responsible for building the current instrument, has remarked that the DHF5 has operating characteristics that are an order of magnitude better than those of the DHF2. Furthermore, he believes that the operating characteristics of the DHF5 will be improved upon by another order of magnitude, pending the design and marketing of more advanced electronic components.

The thermal gradient probes were of two conventional designs. Five of the measurements were taken with piston cores with the thermistor probes mounted in outrigger fashion on the outside of the core barrel. As many as 7 thermistors could penetrate the sediment to a maximum of 12 meters depth with this apparatus. Fifty of the measurements were obtained using a 3 meter long multipenetration pogo probe with 3 externally mounted thermistors at distances of .5, 1.5, and 2.5 meters beneath the weight stand (Von Herzen and Anderson, 1972). Both types of apparatus have a thermistor attached to the outside of the heat flow instrument casing. This thermistor measures the water temperature 1 meter off the bottom during the heat flow measurement. All of the thermistors used have thermal time constants on the order of a few seconds (Von Herzen et al., 1970).

There still exist uncertainties as to the temperature and pressure characteristics of the electronics and battery, and of the magnitude of resistances at connections, of the E.O. cables and elsewhere in the electronics. Hence, it is difficult to determine the absolute error associated with an individual water temperature or sediment temperature determination. However, this error is probably less than ±.02 °C as evidenced by the distribution of thermistor temperatures along the probe at times when we felt they should be at the same temperature. Because of continuous cable leakage, the temperature determinations from the sediment thermistors have relative errors associated with them that there were as great as ±.012 °C but which were generally less than ±.001 °C. Instabilities of the sediment thermistors due to causes other than leakage were probably negligible. In theory, the deeper penetrating cores should yield more accurate thermal gradient determinations because temperature perturbations of the sediment-water interface die out exponentially with increasing depth. If cable leakage does not occur, it should be possible to obtain relative temperature determinations accurate to at least .00025 °C, the smallest estimated error with leakage. As previously mentioned, the temperature sensitivity of the instrument is almost exactly 1 count to .00017 °C; this provides an absolute lower bound for the precision of the sediment thermistors.

Thermal Conductivity Measurements

For the 5 piston cores, thermal conductivities were measured every 50 centimeters using the needle probe technique described by Von Herzen and Maxwell (1959). Additionally, conductivities were measured every 50 centimeters in the 1.53 meter long gravity cores. The accuracy of an individual conductivity measurement is related to the calibration of the needle, the thermal state of the core at the time of measurement and the validity of the approximations assumed by Von Herzen and Maxwell (1959). Figure 8 depicts three representative plots of data produced from piston core 1 for the equilibrium temperature/time extrapolations. As can be seen in the examples shown in figure 8, most of the points for individual conductivity measurements fall along a straight line, indicating a high degree of precision.

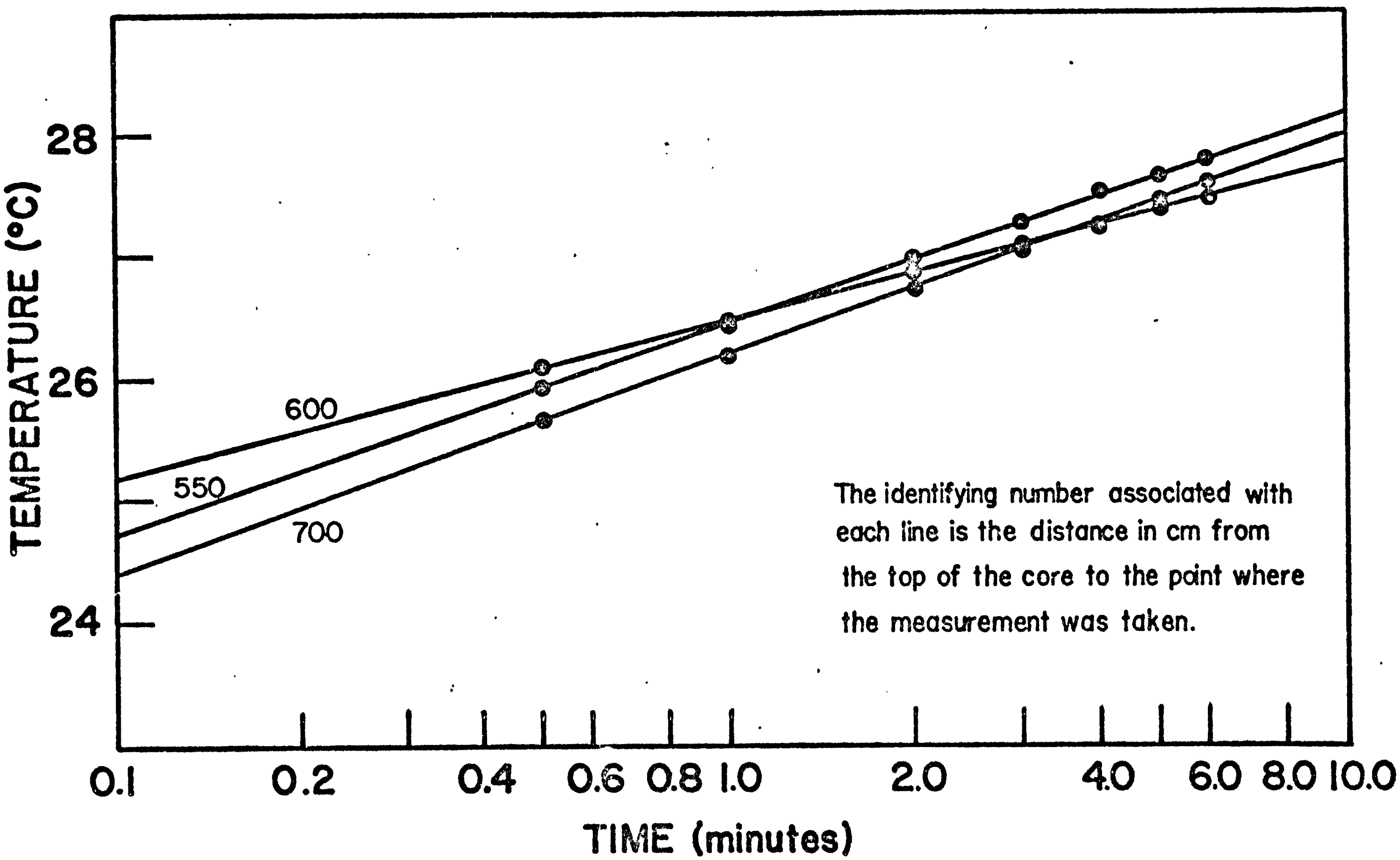

Figure 8

Thermal Conductivity Equiblibrium Extrapolations From Piston Core 1

Due to environmental factors difficult to control, it is likely that the cores were not in a state of exact thermal equilibrium at the time the conductivity measurements were taken. The following envronmental disturbances were noted by Lawrence Hobbie, who was responsible for obtaining the conductivity measurements. They were afterthoughts and are included here, primarily to serve as cautions for future investigators.

1) The table on which the measurements were taken was next to a window which received a great deal of sun. On bright days, the air temperature around the table was on the order of several degrees warmer than elsewhere in the dimly lit storage room. During the later measurements, a piece of cardboard was used to cover the window. However, although the sunlight no longer fell directly on the cores as it had in some earlier measurements, the air around the table was probably still slightly warmer than elsewhere in the room.

2) The cores were stored on a low shelf, which appeared to keep them cooler than the average ambient air temperature in the rest of the room. For some measurements, the cores had only a few minutes to warm up to the ambient air temperature while resting on an adjacent table.

Thus, during the conductivity measurements, it is possible that the temperature of the entire core was changing for a reason other than the heat input from the needle probe. Hobbie noted certain other factors which might have served to give erroneous conductivity measurements. They are:

3) In some cases the cores on which measurements were to be made the following day were brought to a place by the work table and leaned vertically against a rack. It was thought that this would insure that the cores were at the same temperature as the ambient air surrounding the work table. However, becasuse the cores were leaned vertically, the water in the cores might have migrated to the lower end. Furthermore, in at least one case, the core was raised abruptly from the vertical to a horizontal position and, consequently, a part of the core (not the plastic liner) shifted its position by a few centimeters.

Hence, the fluid part of the core may not have been properly distributed at the time of the conductivity measurement, yielding an erroneous value.

4) Because of a lack of electrical sockets in the room, the voltmeter which was used as a source of heat input for the conductivity measurements had to rely on its battery for power. Although the voltmeter's battery was recharged between measurements, the battery may still have weakened slightly in the course of a measurement.

Hobbie notes that this effect was unlikely to have produced noticeable inaccuracies in the measurements because the temperature/time extrapolations all plotted as straight lines. Finally,

5) Occasionally measurements were taken quite near the end of a core section.

The implications of this are that the needle probe could have entered an air pocket, hence producing a misleading conductivity measurement.

The scatter in conductivity along a given core is, however, thought to be greater than the errors which are introduced by these various effects; hence, no account was taken of them. Von Herzen and Maxwell (1959) estimate an error of 3 to 4 percent for a given needle probe measurement from an analysis of possible errors in calibration and random errors on repeated measurements.

At heat flow stations where no core was taken, it was not possible to independently determine a thermal conductivity. For the pogo probe stations, conductivities were assumed from an analysis of the nearby cores.

III DATA REDUCTION

Introduction

This section and Appendices A through E explain the procedure used in going from the digitally recorded thermistor data on the cassette tape to actual heat flow values. The appendices contain information relevant to the computer processing while we explain here our method of converting from processed temperature data to heat flow values. A detailed error analysis of the data is given as well. Discussion is then given to our method of finding the geographical location of each heat flow measurement. Finally, we show how the conversion of digital pressure readings to actual depths is accomplished. The computer programs and machine command statements given in the appendices were designed for the Woods Hole Oceanographic Institition's Sigma 7 computer system.

Steps 1, 2, 3 and 4: A Brief Preview

These four steps in the data reduction process, described in detail in Appendices A through E, encompass the procedure necessary to convert the raw digital data into a workable format. Step 1 explains how the transformation from the cassette tape to a 9-track tape occurs. Gross errors in the digital data are located and processed during this step. During step 2, the digital data are segmented into intervals that each contain one thermal gradient measurement. In step 3, we show how these intervals can be plotted; such plots serve as an excellent first order indicator of measurement quality. Finally, in step 4 we discuss how the digital thermistor data was converted to temperature data.

Step 5: Conversion of Temperature Data to Heat Flow Values--Error Analysis

The first three steps have been straightforward application of computer programming techniques. At this point, we will describe not only the rather simple conversion of temperature data to thermal gradients, but also our method for determining the error associated with an individual heat flow measurement.

Equilibrium Temperature Determination

Five piston core stations were occupied resulting in 3 reliable measurements of heat flow, and 4 pogo probe stations were run resulting in an additional 50 reliable measurements of the thermal gradient. In the determinations of absolute temperatures, slightly different methods were used for the 2 probe types. However, several important steps in the data reduction process including the entire error analysis scheme were the same for both piston core and pogo probe measurements. The estimated errors associated with individual temperature determinations were obtained as explained below. Ideally, both shortly before penetration and after pullout from a thermal gradient measurement, the probe will be held motionless in the water column, on the order of a few hundred meters above the bottom. Because of the near isothermal nature of the bottom water in the deep seas, the entire length of the the probe is hopefully at the same temperature during these holding periods. Hence, at these times the thermistors should all be recording exactly the same temperature. However, this is generally not the case due to various factors such as cable leakage, varying lengths (and hence resistances) of the E.O. cables, and other path effects. At these times then, temperature corrections can be determined so that all of the thermistors effectively record the same temperature. These corrections can then be applied to the temperatures recorded while the thermistor probes are not at the same temperature, such as during a thermal gradient measurement. Determining these correction terms both before and after a thermal gradient measurement is one way of estimating the error in the measurement due to instrument drift and cable leadage. In some cases, these holding periods were not well defined. For these cases, we effectively generated isothermal conditions by averaging thermistor temperatures over several consecutive cycles.

Another source of error in the sediment temperature determinations is introduced if the probe is pulled out of the sediments or disturbed before the thermistors have had time to come to thermal equilibrium. In this case, the error can be reduced by extrapolating the observed temperature decay to equilibrium using the theory described by Bullard (1954). The exact penetration time must be known. The temperature decay is then plotted against 1/t on normal graph paper. Equilibrium is reached as time goes to infinity or, equivalently, as 1/t goes to 0. Because of the thermistor characteristics, a series of points will be plotted through which a straight line can be drawn, intersecting the 1/t equals 0 axis at some equilibrium temperature. Only in exceptional cases was an equilibrium extrapolation capable of reducing an estimated sediment temperature error. For a few measurements in which thermal equilibrium was reached, checks were performed in order to determine whether the extrapolations resulted in the same temperature as the chosen values at equilibrium. All such checks agreed to within the estimated error of the temperature determination.

Further sources of error are the instability of the thermistor reading during the equilibrium, pre-penetration and post-pullout times chosen. These instabilities as well as deviations from straight line plots during equilibrium extrapolations can all be due to either leakage or instrument drift and noise. Each thermistor temperature was recorded twice (water temperature 3 times) every 28 second recording cycle during pogo probe stations. The instrument noise was less for the later sequence of data (e.g.

appendices, tables B1 and D1, figure C3). Hence for all of these measurements, we used the temperatures recorded during the 5, 6, 7 and 8 switching positions. However, for penetration 8 of station 2, we found it necessary to use both data sets in the equilibrium extrapolations because of the short measurement time.

Hence, to obtain errors on temperature measurements, we looked closely at two factors, one short-term and one long-term. Both of the following problems can result from cable leakage, a frequent problem when taking oceanic heat flow measurements. For each measurement, we estimated the stability of each thermistor at equilibrium and while it was held in the water column before and after the measurement (short-term errors). Furthermore, for each thermistor we calculated correction terms for both of these holding periods. We estimate the average error due to a change in the value of the correction terms from before to after the measurement as 1/2 of the magnitude of this change (long-term error). In extreme cases, the variations in these correction terms was much greater than the instabilities noted over shorter observation times (e.g., equilibirum, holding periods). In these cases, the error in the temperature during equlibrium was estimated solely on the basis of this variation. Typically, the instability errors and longer term errors were of the same order. In these cases, the total error was estimated as a weighted average of the three short-term instabilities noted above and 1/2 of the long-term change of one thermistor with respect to another. It bears reiteration that all of the errors described can be due to either leakage or instrument noise and are all somewhat related. Hence, our error estimates have a certain degree of subjectivity to them.

During the holding periods, the temperatures recorded by the piston core probe thermistors and by the pogo probe thermistors exhibited different behaviors. For the piston cores, the sediment thermistors were observed to read the same temperature to within ±.01 °C. However, at a given holding time, the water thermistor recorded a temperature between .04 °C and .07 °C less than the mean temperature recorded by the sediment thermistors. Hence to determine correction terms, we first found the mean value recorded by the reliable sediment thermistors. We then corrected both the sediment thermistors and the water thermistor to this value.

For the pogo probe stations, we observed that the bottom water temperatures recorded by the water thermistor agreed well with the corrected bottom water temperatures determined from the piston core probe water thermistor. Hence, during the holding periods, we simply corrected all of the sediment thermistors so that they agreed with the temperature recorded by the water thermistor. No correction was applied to the water thermistor temperatures. This was done to establish agreement between the water temperatures recorded by the piston core probe thermistors and the pogo probe thermistors. We note that all of the pogo probe E.O. cables leaked in varying degrees throughout the cruise.

To determine the error due to a change over the course of a measurement in the temperature recorded by one thermistor with respect to another, we first were able to look only at the sediment thermistors. This was due to our method of calculating correction terms. In certain cases, if we noticed that these changes all had the same sign, and had magnitudes larger than .001 ^{o}C, we assumed that the changes were partially due to leakage of the water thermistor's cable. We then reduced our error estimate of these changes by an amount that was the same for all of the sediment thermistors. This amount was chosen based on our estimates of the temperature effect of this leakage and from the observed sign of the effect. After performing all of this analysis, we noticed that the temperatures recorded by the lower 2 sediment thermistors on the probe typically had associated errors of ±.0005 ^{o}C with only an occassional error as great as ±.01 ^{o}C. Hence, the cables of these thermistors appear to have leaked, but with a generally minimal affect on the path resistance (and hence temperature).

Table 2 shows a typical example (station 7, penetration 1) of our method of determining the temperature errors. It was not possible to make a reliable estimate of the stability of the water thermistor during equilibrium for any of the stations. Generally, the water temperature recorded displayed a rise on the order of .01 °C over the course of a measurement. We postulate that this is due to a phenomenon whereby as the probe penetrates, it stirs up the top of the sediment pile around the probe. Hence, the lowermost few meters of bottom water are heated by interactions with the warmer sediments. The water temperatures we have chosen are those that were recorded during or 1 cycle after penetration.

We calculated interval temperature gradients from our corrected temperature data whenever possible. For the 4 pogo probe stations, a computer program was developed that could calculate the 2-interval gradients as well as the total gradient (Appendix E). Furthermore, we tried other methods of converting the raw temperature data to thermal gradients. For example, during the pre-penetration and post-pullout holds, we first averaged all 4 of the thermistor temperatures. Then we calculated a temperature correction for each thermistor as the difference between its actual value and this average value. We applied these correction terms to the

Table 2

Pogo Probe Temperature Gradients - Error Estimates

Explanation	Station 7	Penetration 1		
	water	2	3	4
Thermistor penetration depth (m)	+1	-.5	-1.5	-2.5
equilibrium temperature (°C)	2.1212	2.1350	2.1828	2.2382
stability (°C)				
equilibrium	?	±.0005	±.0005	±.0005
pre-penetration hold	±.00025	±.00025	±.001	±.0005
post-pullout hold	±.00025	±.0005	±.0003	±.0005
magnitude and direction of drift with respect to water thermistor (°C)	--	±.001	±.0005	±.0005
Total error (°C)		±.0005	±.0005	±.0005

temperatures recorded by the thermistors at thermal equilibrium while in the sediment column. The temperature gradients calculated from this method of data reduction were different from those calculated by the previous method by an amount that was within the estimated error of the gradient. Hence, we feel justified in using the first method.

Piston Core Heat Flow

Heat flow is defined as the product of a temperature gradient with the thermal conductivity over the interval of the gradient. Hence, the errors introduced with the conductivity measurements are important in determining the total error of the heat flow measurement. The piston corer never penetrated to its full length. Furthermore, the amount of core recovered was always less than the estimated amount of penetration from mudmark indications.

In order to determine the real locations of the conductivity measurements and thermistors in the sediment column, we did as explained below. For each core we first plotted all of the temperature gradients on a temperature/depth graph. We then adjusted the thermistor depths until the line representing the mean gradient crossed through the water temperature at the sediment-water interface. This located the thermistors in the sediment column by giving us an idea of the depth of penetration. We assumed that the top of the sediment column was lost during penetration. Hence, the conductivity measurements obtained are thought to be made on sections of the core recovered from the depth of deepest penetration to a depth less than this by an amount equal to the total length of core recovered. We show the temperature versus depth plot alongside the conductivity versus depth plot for all 5 piston core stations in figure 9. The circled conductivity points were taken from the gravity core.

Similar temperature versus depth plots were made for the pogo probe measurements. Figure 10 shows some representative examples (including station 7, penetration 1). In deriving these graphs we assumed full penetration of the probe. Strictly speaking, the amount of total penetration varies within $\pm$.25 meters, and can be determined in the same manner as was done for the piston core stations. However, we did not do this because the $\pm$.25 meter variation does not affect our final results or interpretation.

For the piston core stations, we calculated the heat flow and errors as explained below. We first calculated interval thermal gradients g_i and e_i. The g_i were calculated using our best estimates of the equilibrium temperatures. The e_i were then calculated as the maximum variation in the gradient possible with the given errors on temperature. For each core we then found a weighted

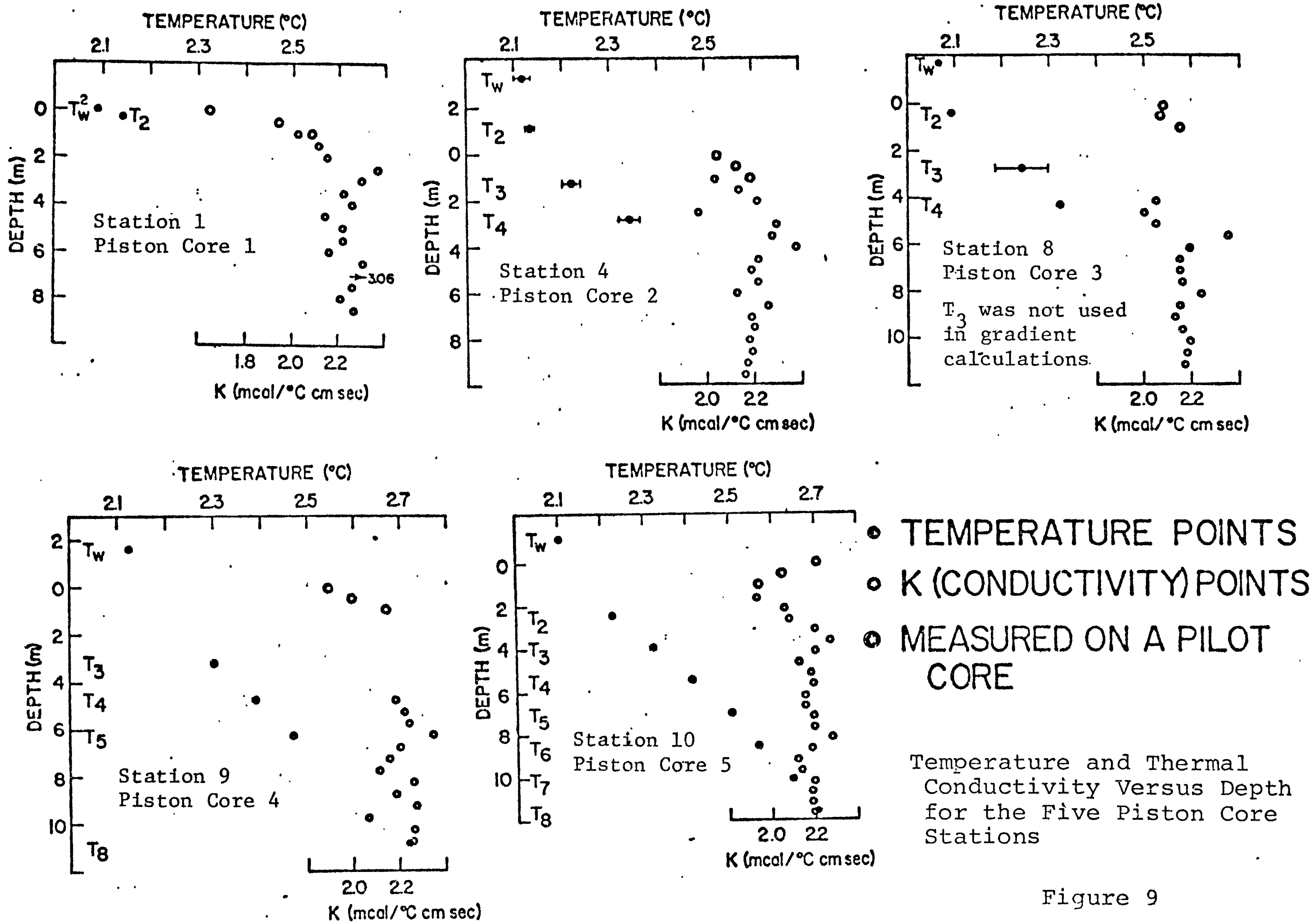

Temperature and Thermal Conductivity Versus Depth for the Five Piston Core Stations

Figure 9

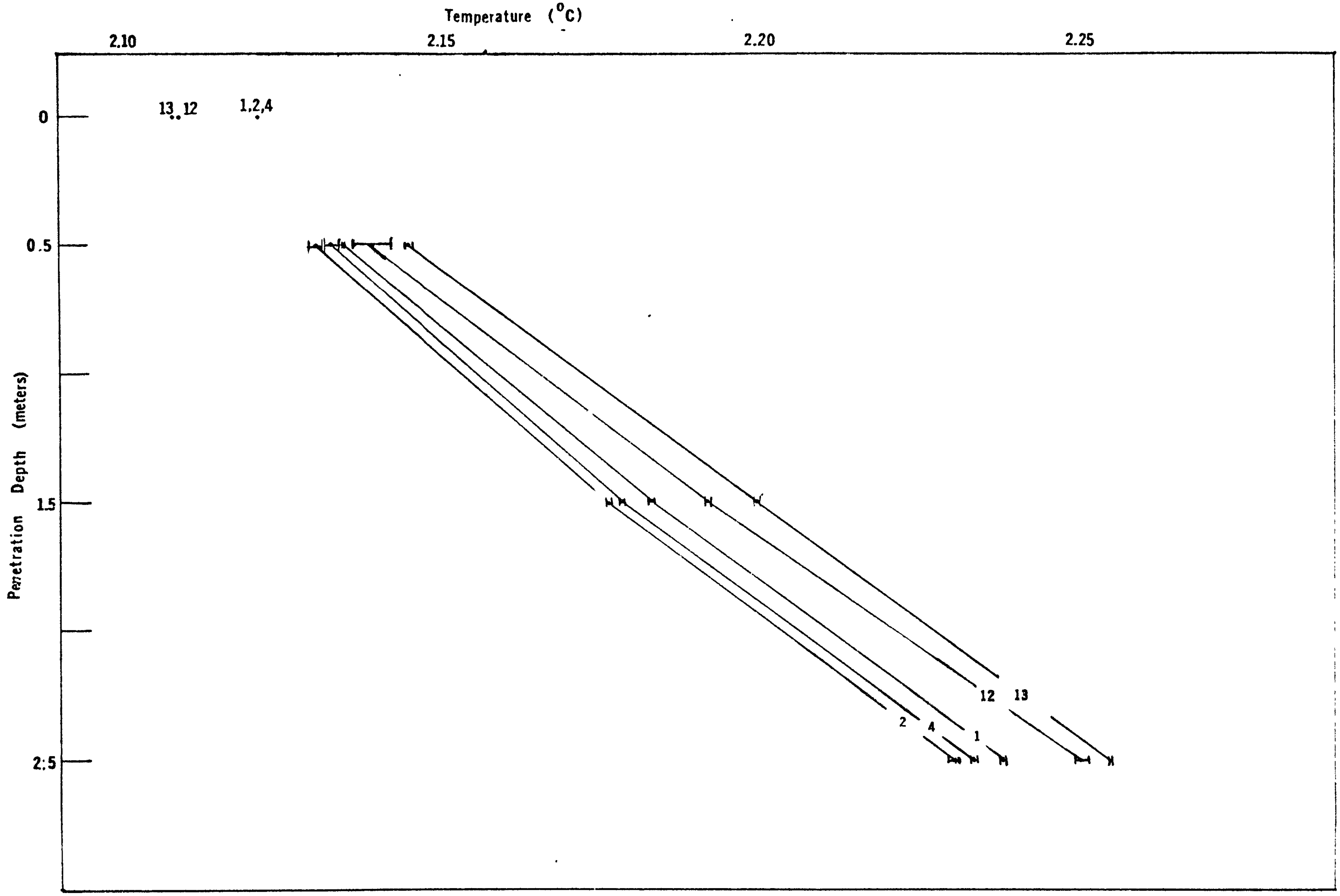

Figure 10

Some Representative Pogo Probe Temperature Versus Depth Plots - Station 7 mean gradient (g) and a weighted mean error (e) from the interval gradients and errors. Within the frequency of our sampling interval, the thermal conductivity data show no significant variation with depth. A mean harmonic conductivity was found utilizing all of the measuremnts that fell within the depth range of the thermistors used for the gradient calculations. The error on this mean conductivity (K) was taken to be the standard deviation (σ) of all of the measurements. This error is typically much larger than the error in temperature gradient. Following Von Herzen and Anderson (1972), we found a fractional error in thermla conductivity (FEK) as $\sigma/K + .02$. The factor of .02 takes into account systematic biases of the needle probe used for the measurements. The total error (E) in heat flow (Q) was calculated as,

$$E = \{(FEK)^2 + (FEG)^2\}^{1/2} \cdot Q$$

where (FEG) is the fractional error in the temperature gradient e/g. Table 3 is a summary of the 5 piston core stations including location, ocean depth, bottom water temperature, penetration of deepest reliable thermistor, total number of conductivity values used and their harmonic mean and standard deviation, number of thermistors used to calculate the temperature gradient, temperature gradient with error, and heat flow with error.

Table 3

Summary AII97-2 Piston Core Heat Flow Stations

sta.#	core#	Lat.(N)	Long.(W)	Corr. Depth(m)	W[1]	Pen.[2]	#K[3]	K[4]	#th[5]	dT/dz[6]	HF[7]	Q[8]
1	1	25°01.43'	68°02.20'	5484	2.09	0.25	2	1.79 ± .22	1	1.93 ± .05	+3.45 ± .49	A
4	2	25°01.80'	68°02.62'	5482	2.13	2.80	3	2.17 ± .13	2	.77 ± .41	1.62 ± .87	A
8	3	25°04.95'	68°01.44	5434	2.07	4.30	4	2.07 ± .07	2	.587 ± .10	1.21 ± .21	A
9	4	25°06.67'	68°01.58	5433	2.07	10.83	13	2.21 ± .07	4	.546 ± .019	1.21 ± .06	A
10	5	25°01.29'	68°04.33	5513	2.10	11.53	20	2.18 ± .05	7	.534 ± .015	1.16 ± .04	A

\+ unreliable value - temperature gradient was obtained by using penetration depth from mudmark indication and water temperature ~ 15 meters above seafloor (see text)

[1] W=bottom water temperature given in °C.

[2] Pen.=depth of lowermost thermistor used in calculation of temperature gradient

[3] #K=number of conductivity determinations obtained over the temperature gradient interval

[4] K=harmonic mean conductivity ± standard deviation $.10^3$ cal/°C cm s

[5] #th=number of thermistors used for temperature gradient calculation

[6] dT/dz=temperature gradient ± error $.10^3$ °C/cm

[7] HF=heat flow in $\mu cal/cm^2$ s

[8] Q=environmental evaluation after Sclater et al. (1976)

Three of the piston core stations were plagued with thermistors that did not work properly. Only the thermistor located .55 meters beneath the corehead was operational throughout the first station. The depth of penetration from the mudmark indication was estimated as 8.85 meters and this station was unique in that a 9.15 meter (30 feet) long core barrel was used. Hence, we estimate the depth of penetration of this thermistor as .25 meters. The water temperature recorded by this thermistor approximately 15 meters off the bottom (1 cycle before penetration) was 2.0920 $\pm$ .002 ^{o}C. As shall later be explained, the bottom water was not always isothermal, showing slight increases or decreases in temperature through at least the lowermost 30 meters. However, because we could find no systematic magnitudes or directionality in this depth range, we assumed isothermal conditions in this case. The equilibrium temperature was 2.1402 $\pm$ .003 ^{o}C. The nearest two conductivity measurements were at .05 and .5 meters depth. A value of 1.79 $\pm$ .22 $\cdot 10^{-3}$ cal/^{o}C$\cdot$cm$\cdot$s was obtained.

The heat flow was calculated

as 3.45$\pm$.49 HFU. However, because this value is different from the more reliable piston core measurements by a factor of 3 and because a small mislocation of the thermistor depth will greatly affect the temperature gradient, we have chosen to ignore the measurement.

Station 4, piston core 2 had 4 working thermistors, located at distances of 1.32, 3.67, 5.25 and 9.62 meters from the corehead. Unfortunately, the lowermost thermistor leaked so severely that the associated temperature errors were unreasonably large. Furthermore, the uppermost thermistor could not have penetrated the sediments since its equilibrium temperature agreed with the water temperature to within .0022°C. The remaining 2 thermistors, at estimated sediment depths of 1.22 and 2.80 meters, were disturbed throughout the measurement and produced somewhat unreliable equilibrium temperatures. Hence, the heat flow value of 1.62$\pm$.87 HFU is also a poor estimate of the regional heat flux.

During station 8, piston core 3 four sediment thermistors were operational, the lowermost of which leaked so severely as to make it unusable. Of the remaining three thermistors, at estimated sediment depths of .4, 2.32 and 4.30 meters, the middle thermistor had leakage related temperature errors far greater in magnitude than the other two thermistors (Figure 9). Hence, we have used only two thermistors in obtaining our heat flow value of 1.21±.21 HFU.

Fortunately, station 9, piston core 4 and station 10, piston core 5 produced somewhat more reliable heat flow values than did the first 3 piston core stations. Station 9 had 5 working sediment thermistors, which were estimated to lie at depths of 1.70, 3.21, 4.74, 6.27 and 10.83 meters in the sediment column. Upon shipboard recovery of the coring apparatus, it was observed that the uppermost sediment thermistor was severely bent, and that the connecting chain to the gravity corer was quite muddy. Apparently, the chain had wrapped itself around the piston core while the instrument package was lowered through the water column. This prevented a proper trip of the piston core. Nevertheless, the piston core was able to slowly drive itself into the sediments. From the sediment thermistor temperature data, we deduced that penetration occurred over a several-cycle period. Because the uppermost sediment thermistor apparently received an uncalculable amount of heat input from extraneous sources, we have not used it in our thermal gradient calculations. We feel that the calculated value of 1.21±.06 HFU is a reliable estimate of the regional heat flux.

Station 10 had 7 working sediment thermistors, which were estimated to lie at depths of 2.40, 3.91, 5.44, 6.97, 8.50, 10.00 and 11.53 meters in the sediment column. The only problems encountered in the data reduction were with instrument noise; as remarked in the Instrumentation section, the battery died before pullout. Thus, we had no check as to the amount of leakage or instrument drift that might have occurred over the course of the measurement. With the exception of the lowermost interval gradient, we feel that the linearity of the interval gradients is one check of the reliability of the heat flow measurement. The fact that the calculated heat flow of 1.16$\pm$.04 HFU agrees closely with the values obtained at stations 8 and 9 is further evidence of the reliability of the measurement. Hence, from the measurements obtained at stations 8, 9, and 10, we estimate the regional heat flux to be on the order of 1.2 HFU.

Pogo Probe Heat Flow

The two deep piston core measurements are inherently more accurate estimators of the heat flow at depth than the 2.5 meter pogo probe measurements for two reasons. The thermal conductivity can be measured from the recovered core sediments for the piston core stations whereas it has to be assumed using nearby core samples for the pogo probe stations. Secondly, as already noted, the temperature perturbation due to a recent change in conditions at the sediment-water interface dies out exponentially with depth in the sediment column.

Although leakage was at times a problem, all three sediment thermistors worked during the 4 pogo probe stations with the exception of the first 7 penetrations of station 2. The lowermost thermistor, 2.5 meters below the weight stand, was not operational during these measurements. Tables 4a-d list the temperature gradients which we calculated between thermistors 2 and 3, 3 and 4, and 2 and 4. The notable feature of these tables is the consistency of the data. The mean and standard deviation for 42 gradients in the interval .5 to 1.5 meters depth are respectively, $.479 \cdot 10^{-3}$°C/cm and $.051 \cdot 10^{-3}$. In the interval 1.5 to 2.5 meters depth, the mean and standard deviation for the same 42 measurements are, respectively, $.537 \cdot 10^{-3}$ °C/cm and $.036 \cdot 10^{-3}$ We have excluded the first 7 penetrations, station 2 and penetration 3a, station 6. The latter measurement was a clear case of the upper thermistor failing to penetrate the sediments. The small but consistent nonlinearity of these relatively shallow measurements is remarkable. They are in most cases larger than can be explained by the errors in temperature alone. Only 4 measurements exhibited gradients which did not increase with depth.

We first looked for an explanation of these data under the assumption that the heat flow through the sediments is constant with depth. In general, one expects the thermal

Table 4a

Station 2 Pogo 1 - Interval Temperature Gradients

$dT/dz \cdot 10^3$ °C/cm

penetration	2-3(.5-1.5 m)	3-4(1.5-2.5 m)	2-4(.5-2.5 m)
1	.589 ± .06	.647 ± .078	
2	.5292 ± .008	.587 ± .026	
3	.5501 ± .010	.608 ± .023	
4	.494 ± .03	.552 ± .048	assumed lower
5	.5011 ± .012	.559 ± .030	gradients
6	.4840 ± .008	.542 ± .026	(see text)
7	.4992 ± .008	.557 ± .026	
8	.5235 ± .014	.6539 ± .010	.5887 ± .014
9	.3081 ± .005	.4296 ± .013	.3689 ± .013

Table 4b

Station 3 Pogo 2 - Interval Temperature Gradients

penetration	$dT/dz \cdot 10^3$ °C/cm 2-3 (.5-1.5m)	3-4(1.5-2.5)	2-4(.5-2.5m)
1	.4886 ± .014	.5613 ± .008	.5250 ± .015
2	.5039 ± .009	.5399 ± .008	.5219 ± .006
3	.4409 ± .005	.5139 ± .008	.4774 ± .109
3a	.474 ± .04	.484 ± .04	.479 ± .01
4	.4307 ± .110	.5257 ± .019	.4782 ± .109
5	.4381 ± .130	.5132 ± .015	.4757 ± .125

Table 4c

Station 6 Pogo 3 - Interval Temperature Gradients

penetration	dT/dz · 10^3 °C/cm 2-3(.5-1.5m)	3-4(1.5-2.5 m)	2-4(.5-2.5m)
1	.5284 ± .010	.5636 ± .009	.5460 ± .009
2	.4819 ± .013	.5503 ± .008	.5161 ± .015
3	.4796 ± .005	.5310 ± .005	.5053 ± .005
3a	.4438 ± .005	+.5014 ± .023	
4	.4773 ± .013	.5469 ± .011	.5121 ± .014
5	.6414 + .045(-.135)	.4976 ± .025	.5684 ± .040 (-.130)
6	.3610 ± .115	.5803 ± .020	.4706 ± .105
7	.4352 ± .016	.5323 ± .012	.4838 ± .012
8	.4888 ± .015	.5586 ± .015	.5237 ± .010
9	.4548 ± .065	.5497 ± .015	.5022 ± .070
10	.4790 ± .011	.5174 ± .008	.4982 ± .011
11	.4709 ± .009	.5534 ± .012	.5121 ± .013
12	.474 ± .02	.522 ± .02	.498 ± .02
13	.5268 ± .084	.5587 ± .013	.5427 ± .089
14	.4915 ± .014	.5492 ± .006	.5204 ± .013
15	.5785 ± .084	.5574 ± .007	.5680 ± .083
16	.4860 ± .013	.5076 ± .008	.4968 ± .011
17	.4635 ± .009	.5367 ± .009	.5001 ± .008
18	.4331 ± .008	.5135 ± .009	.4733 ± .006

+ assumed gradient (see text)

Table 4d

Station 7 Pogo 4 - Interval Temperature Gradients

penetration	dT/dz·10³ 2-3 (.5-1.5m)	°C/cm 3-4(1.5-2.5m)	2-4(.5-1.5m)
1	.4783 ± .010	.5540 ± .010	.5162 ± .010
2	.4525 ± .008	.5383 ± .010	.4954 ± .008
3	.4621 ± .005	.5341 ± .005	.4981 ± .005
4	.4575 ± .013	.5557 ± .008	.5066 ± .015
5	.423 ± .110	.533 ± .100	.493 ± .190
6	.495 ± .090	.545 ± .010	.520 ± .090
7	.5004 ± .065	.5405 ± .015	.5205 ± .070
8	.4874 ± .025	.5638 ± .010	.5256 ± .025
9	.4783 ± .023	.5467 ± .013	.5125 ± .020
10	.4631 ± .021	.5519 ± .015	.5075 ± .018
11	.4989 ± .035	.5510 ± .010	.5250 ± .035
12	.5291 ± .035	.5824 ± .015	.5558 ± .040
13	.5438 ± .012	.5539 ± .008	.5489 ± .010
14	.5112 ± .015	.5040 ± .010	.5076 ± .015
15	.4758 ± .088	.4598 ± .016	.4678 ± .088
16	.4865 ± .024	.488 ± .013	.4873 ± .021

conductivities to also increase slightly with depth due to compaction of the sediments. The actual conductivity data seem to bear out this generalization (Figure 9); certainly, there is no characteristic decrease in conductivity within the upper few meters of sediment. Hence, we concluded that the departure from nonlinearity of the shallow temperature gradients was an artifact of disturbances created at the sediment-water interface. A standard assumption in calculating the heat flow through oceanic sediments is that the temperature of the sediment-water boundary has remained at the same temperature - that of the bottom water - for a long period of time. This assumption was clearly not valid at the time the measurements were made.

The thermal conductivity which we used to calculate heat flow for the pogo probe measurements represents the arithmetic mean of all conductivity determinations that were made in sediments which lay between 1.25 and 2.75 meters beneath the seafloor. We list these for each core in Table 5. The mean and standard deviation of the 9 conductivities are respectively, $2.14.10^{-3}$ cal/°C.cm.s and $.11.10^{-3}$.

The heat fluxes calculated from the 2 most reliable piston core measurements given in Table 3, were 1.21 HFU for station 9 and 1.16 HFU for station 10. The mean of

Table 5

Thermal Conductivities Used for Pogo Probe Stations

Station	Core	Conductivity $\cdot 10^3$ cal/°C cm s
1	1	2.11, 2.15, 2.37
4	2	2.14, 2.22, 1.97
8	3	none
9	4	none
10	5	2.06, 2.08, 2.20

depth range: 1.25-2.75 m

mean = $[\sum_{n=1}^{N} K_n]/N$ = 2.144 cal/°C cm s, N=9

standard deviation = .113

these two values is 1.185 HFU, a few percent greater than the mean heat flow which would be calculated between the two deepest pogo probe thermistors. Hence, we believe that the heat flow calculated from the temperature gradients between thermistors 3 and 4 is more representative of the heat flow at depth than that calculated from the gradients measured between thermistors 2 and 3 or 2 and 4. Furthermore, as evidenced by a slightly lower mean than the reliable piston core measurements, it is possible that the lower gradient still samples the effect of the recent temperature perturbation at the sediment-water interface. It is unfortunate that these 2 piston core measurements did not sample the temperature gradient in the upper 1 or 2 meters of the sediment column. Had gradients measured in this interval been smaller by on the order of $.06 . 10^{-3}$°C/cm from the mean calculated gradient for the piston core station, it would have strongly supported our arguments.

The mean difference between 42 of the upper and lower pogo probe gradients is $.058 . 10^{-3}$°C/cm. There were 8 measurements discussed previously in which the temperature was not measured below 1.5 meters in the sediment column. By adding this correction term to the upper gradient, we were able to obtain more reliable estimates of the deep temperature gradient. The error on these gradients was obtained by adding 1/2 of the standard deviation of the gradients actually measured at depths of 1.5 to 2.5 meters ($.018.10^{-3}$) to the error obtained for the specific gradient measured at a depth of .5 to 1.5 meters.

Table 6 is a summary of the pogo probe stations listing similar information in a similar format as was given for the piston core stations (Table 3). The error analysis was done using the same method as was used for the piston cores. The error in thermal conductivity is assumed to be the standard deviation of the 9 usable measurements. The error in thermal gradient is the difference between our best estimate of the gradient and the maximum/minimum gradient allowable with the given errors on equilibrium temperatures. The error (E) in heat flow (Q) is calculated as,

$$E = [(FEK)^2 + (FEG)^2]^{1/2}.Q$$

Step 6 - Locating the Heat Flow Stations

Locating the heat flow stations was, for the most part, a straightforward task. For 4 stations the use of an acoustic relay transponder placed a short distance up the wire from the heat flow probe simplified matters. This distance was 200 meters for station 2 and 1000 meters for stations 6, 7, and 9. We assumed that the wire hung

Table 6

Summary AII97-2 2.5 Meter Pogo Probe Heat Flow Stations

Sta.#	Pogo#	Pen.#	Lat.(N)	Long.(W)	Corr. Depth(m)	K(-10^3Cal/ΔC cm s)	dt/dz(-10^3°C/cm)	HF(HFU)	±Q
2	1	1	25° 3.370'	68° 2.255'	5457	2.14 ± .11	.647 ± .078	1.39 ± .18	A
		2	3.289'	2.301'	5464		.587 ± .026	1.26 ± .09	A
		3	3.224'	2.449'	5474		.608 ± .028	1.30 ± .09	A
		4	3.228'	2.608'	5484		.552 ± .048	1.18 ± .12	A
		5	3.261'	2.753'	5497		.559 ± .030	1.20 ± .09	A
		6	2.801'	3.041'	5505		.542 ± .026	1.16 ± .08	A
		7	2.662'	3.093'	5505		.557 ± .026	1.19 ± .08	A
		8	1.92'	4.32	5509		.654 ± .010	1.40 ± .08	A
		9	1.55'	4.37'	5514		.430 ± .013	0.92 ± .05	A
4	2	1	25° 2.41'	68° 5.08'	5517	2.14 ± .11	.561 ± .009	1.20 ± .06	A
		2	2.27'	5.07'	5514		.540 ± .008	1.16 ± .06	A
		3	1.91'	5.03'	5513		.514 ± .008	1.10 ± .06	A
		3a	1.72'	5.01'	5514		.484 ± .009	1.04 ± .06	A
		4	1.59'	5.00'	5527		.526 ± .019	1.13 ± .07	A
		5	1.35'	4.97'	5527		.513 ± .015	1.10 ± .07	A
6	3	1	25° 2.718'	68° 3.740'	5518	2.14 ± .11	.564 ± .009	1.21 ± .07	A
		2	2.533'	3.818'	5514		.550 ± .008	1.18 ± .06	A
		3	1.808'	3.728'	5502		.531 ± .005	1.14 ± .06	A
		3a	1.276'	3.639'	5502		.501 ± .005	1.07 ± .06	A
		4	7.750'	1.443'	5428		.547 ± .011	1.17 ± .06	A
		5	7.428'	1.379'	5428		.498 ± .025	1.07 ± .06	A
		6	7.011'	1.551'	5432		.580 ± .020	1.24 ± .08	A
		7	6.764'	1.609'	5434		.532 ± .012	1.14 ± .06	A
		8	6.512'	1.731'	5434		.559 ± .015	1.20 ± .07	A
		9	6.367'	1.822'	5436		.550 ± .015	1.18 ± .07	A
		10	6.158'	1.929'	5448		.517 ± .008	1.11 ± .06	A
		11	5.971'	2.048'	5452		.553 ± .012	1.19 ± .07	A
		12	5.737'	2.186'	5456		.522 ± .018	1.12 ± .07	A
		13	5.579'	2.312'	5459		.559 ± .013	1.20 ± .07	A
		14	5.395'	2.477'	5461		.549 ± .006	1.18 ± .06	A

Table 6 continued

Sta.#	Pogo#	Pen.#	Lat.(N)	Long.(W)	Corr. Depth(m)	$K(-10^3 Cal/\Delta C\ cm\ s)$	$dt/dz(-10^{3}\,{}^\circ C/cm)$	HF(HFU)	+Q
6	3	15	25° 5.183'	68° 2.312'	5464	2.14 ± .11	.557 ± .007	1.19 ± .06	A
		16	5.080'	2.818'	5463		.508 ± .008	1.09 ± .06	A
		17	4.931'	2.920'	5464		.537 ± .009	1.15 ± .06	A
		18	4.844'	3.008'	5467		.514 ± .009	1.10 ± .06	A
7	4	1	25° 6.436'	68° 0.922'	5415	2.14 ± .11	.554 ± .010	1.19 ± .06	A
		2	6.465'	1.029'	5417		.538 ± .010	1.15 ± .06	A
		3	6.478'	1.133'	5421		.534 ± .005	1.14 ± .06	A
		4	6.485'	1.265'	5425		.556 ± .008	1.19 ± .06	A
		5	6.493'	1.372'	5426		.533 ± .095	1.14 ± .21	A
		6	6.505'	1.538'	5429		.545 ± .014	1.17 ± .07	A
		7	6.503'	1.694'	5432		.541 ± .015	1.16 ± .07	A
		8	6.506'	1.811'	5436		.569 ± .010	1.21 ± .07	A
		9	6.512'	1.969'	5439		.547 ± .013	1.17 ± .07	A
		10	6.518'	2.097'	5441		.552 ± .015	1.18 ± .07	A
		11	6.520'	2.296'	5441		.551 ± .010	1.18 ± .06	A
		12	6.532'	2.437'	5445		.582 ± .015	1.25 ± .07	A
		13	6.528'	2.669'	5455		.554 ± .008	1.19 ± .06	A
		14	6.536'	2.851'	5460		.504 ± .010	1.08 ± .06	A
		15	6.545'	3.044'	5472		.460 ± .016	0.99 ± .06	A
		16	6.557'	3.236'	5481		.488 ± .013	1.05 ± .06	A

+ environmental evaluation after Sclater *et al.*

vertically below the transponder. With the exception of penetrations 1, 7, 8 and 9 of station 2, we were able to directly interpolate the fish position from the processed acoustic navigation data. It was necessary to extrapolate the fish position backwards and forwards in time in order to obtain locations for, respectively, penetrations 1 and 7. Penetrations 8 and 9, station 2; penetrations 1, 2, 3, 3a, 4 and 5, station 3; and stations 1, 4, 8 and 10 (piston core measurements) did not have fish navigation data. For the piston cores, we relied on a combination of satellite fixes and acoustic navigation data for the ship in calculating their locations.

We attempted to develop an empirical relationship between ship position and fish position for the remaining 8 pogo probe measurements. Table 7 lists the acoustically navigated ship position for all of the 55 heat flow measurements. During stations 2 and 6, the heat flow probe was raised to the ship in order to perform maintenance work and then relowered. This occurred between penetrations 7 and 8 for station 2 and between penetrations 3a and 4 for station 6. For the purposes of the following discussion, we have divided both stations 2 and 6 into two groups, separated by a raising and subsequent relowering of the probe. We divided the 8 unlocated pogo probe measurements into two groups: those that occurred during a first lowering (penetration 7, station 2; penetration 1,

Table 7

ACNAV Ship Positions During Heat Flow Measurements

	Latitude(N)	Longitude(W)
S-1 C-1		
1	25° 1.431'	68° 2.195'
S-2 P-1		
1	25° 3.165'	68° 2.427'
2	3.079'	2.615'
3	3.236'	2.794'
4	3.339'	2.934
5	3.119'	2.921'
6	2.393'	3.223'
7	2.189'	2.858'
8	.905'	4.727'
9	.205'	4.193'
S-3 P-2		
1	25° 1.579'	5.014'
2	1.053'	4.942'
3	.394'	4.847'
3a	.207'	4.810'
4	24° 59.902'	4.731'
5	59.444'	4.615'
S-4 P-2		
1	25° 1.801'	68° 2.842'
S-6 P-3		
1	25° 1.306'	68° 4.582'
2	.992'	4.706'
3	.464'	4.922'
3a	.211'	5.074'
4	7.404'	1.237'
5	6.712'	1.738'
6	6.023'	1.690'
7	5.764'	2.304'
8	5.389'	2.351'
9	5.124'	2.531'
10	4.792'	2.614'
11	4.628'	2.828'
12	4.516'	3.225'
13	4.505'	3.544'
14	4.168'	3.636'
17	3.122'	3.660'
18	3.098'	4.023'

	Latitude(N)	Longitude(W)
S-7 P-4		
1	25° 6.583'	68° 3.225'
2	6.543'	1.611'
3	6.546'	1.778'
4	6.557'	1.958'
5	6.557'	2.111'
6	6.570'	2.347'
7	6.571'	2.570'
8	6.581'	2.723'
9	6.600'	2.920'
10	6.575'	3.131'
11	6.580'	3.344'
12	6.560'	3.545'
13	6.601'	3.876'
14	6.627'	4.092'
15	6.631'	4.644'
S-8 C-3		
1	25° 4.964'	68° 1.446'
S-9 C-4		
1	25° 6.564'	68° 1.276'
S-10 C-5		
1	25° 1.301	68° 4.389'

station 3) and those that were obtained as multiple penetrations (remaining 6 penetrations).

We located the first two penetrations using the following physical argument. When the heat flow probe is being lowered, a higher average ship velocity (v) will mean an initially larger ship/fish separation (sf). We knew that the wire was not paid out at the same average rate for all of the lowerings. We attempted to take this factor into account by calculating the rate at which the ship/fish separation increased ($sf/\Delta t$) during the lowering. We also looked at the horizontal deviation (Δ') of the wire from a straight line and the difference (Δ) between the wire out (w) and the ocean depth (d). Finally, we also calculated two nondimensional numbers, q and k, in a somewhat unsuccessful effort to find a quantity which was conserved between stations.

Figure 11 is a schematic diagram showing the various features to be discussed and the formulae used. Table 8 shows this information, when calculable, for all lowerings. The Δx and v values are minimums because they are calculated assuming the ship travels in a straight line between penetrations. Reference to Figure 12 shows that this assumption is usually valid. In Table 9a, we reproduce the relevant information for the 4 pogo probe lowerings during which the fish position was known by

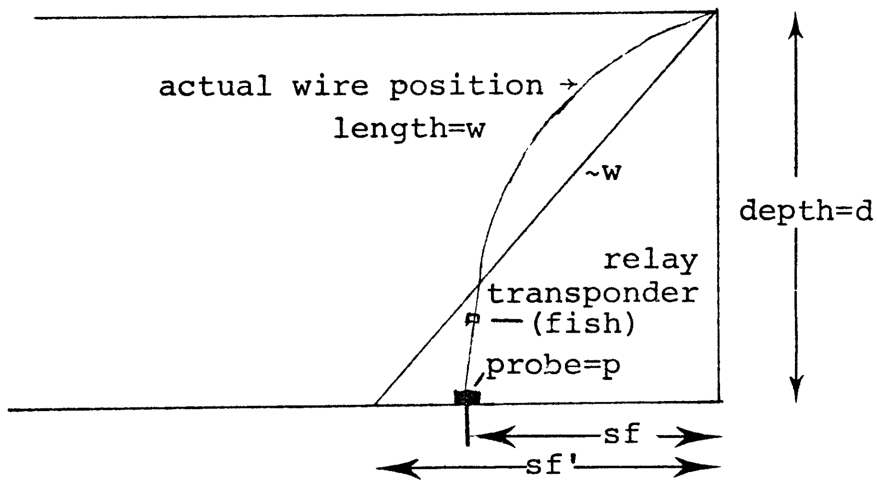

FORMULAE USED

$sf' = ((\text{wire})^2 - (\text{depth})^2)^{1/2}$ $\Delta' = sf' - sf$

$\Delta = (\text{wire}) - (\text{depth})$ $q = sf/\Delta$ $k = q\frac{sf}{sf'} = \frac{sf^2}{sf' \cdot \Delta}$

Δ' is a measure of wire curvature

Δx = distance between penetrations (in minutes)

$v = \Delta x/\Delta t$ = average ship velocity between penetrations (in knots)

Geometry Used to Determine Fish/Ship Separation
for Stations with No Fish Navigation

Figure 11

Table 8

Ship/Fish Separation Data -- First Penetration

sta.#	type	+start time(z)	penetration time(z)	sf(m)	wire(m)	depth(m)	s/f'(m)	Δ'(m)	q	k	Δt(min)	sf/Δt(m/min)	ΔX(min)	V(knots)
1	Core	2114	2232		5980	5484	2382				78			
2a	Pogo	1037	1206	496	5534	5457	918	422	6.5	3.5	90	5.5	.921	.61
2b	Pogo	1913	2032		6127	5509	2670				79		1.549	1.18
3	Pogo	1343	1451		5869	5517	2002				68		1.227	1.08
4	Core	1941	2056		5682	5482	1494				75			
6a	Pogo	1057	1222	3042	6618	5518	3653	611	2.8	2.3	85	35.8	2.278	1.62
6b	Pogo	1821	1924	744	5592	5428	1339	-594	4.6	2.6	63	11.8	.641	.61
7	Pogo	1155	1320	882	5560	5415	1260	379	6.1	4.3	85	10.4	.927	.65
8	Core	1949	2102		5554	5434	1153				73			
9	Core	1050	1243	636	5569	5433	1229	410	4.6	2.4	113	5.6	.283	.15
10	Core	1501	1614	---	5513	5513	---	---	---	---	73	---	---	---

+probe in water

Symbols are defined in figure 11. Some numbers may not be exact due to small depth inaccuracies in the initial calculations.

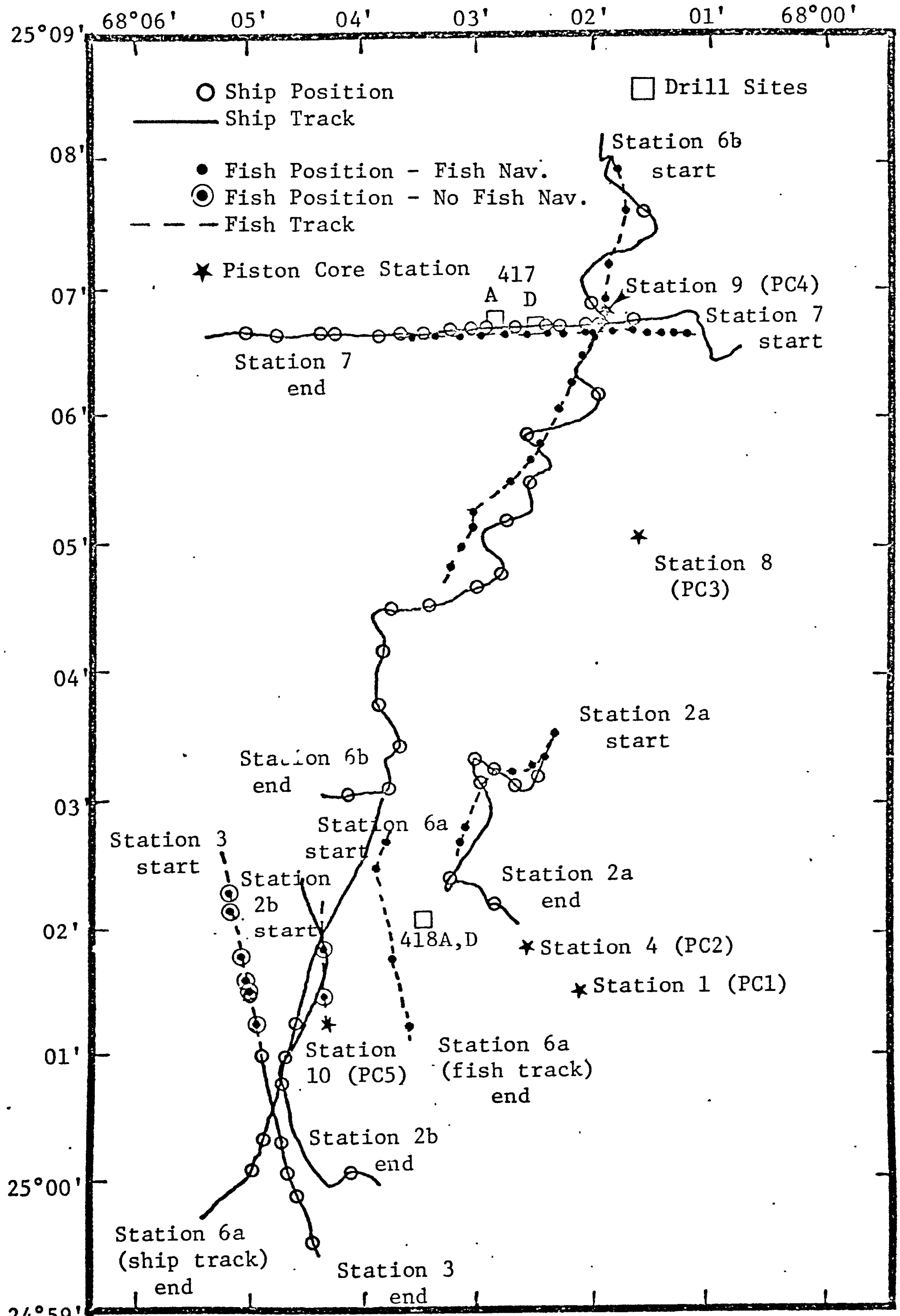

Ship and Fish Tracks During Heat Flow Stations

Figure 12

Table 9a

S/F Pogo Probe First Penetration -- Fish Navigation

station	v(knots)	sf(m)	wire(m)	depth(m)	Δt(min)	s/fΔt(m/min.)
2a	.61	496	5535	5457	90	5.5
6b	.61	744	5591	5502	63	11.8
7	.65	882	5560	5415	85	10.4
average	.62	708				9.2
6a	1.62	3042	6617	5518	85	35.8

Table 9b

S/F Pogo Probe First Penetration -- No Fish Navigation

station	v(knots)	sf(m)	wire(m)	depth(m)	Δt(min)	sf/Δt(m/min)	explanation
2b	1.18	2012	6127	5509	79	25.5	sf interpolated
3	1.08	1555	5869	5517	68	22.9	sf interpolated and reduced to account for sf/Δt

means of acoustic navigation. We see that as the average ship velocity increases, the ship/fish separation does in fact increase. Furthermore, since the wire is paid out an approximately constant rate for the 4 stations, the rate at which the separation increases for a particular station is also larger for a larger ship velocity. Admittedly, our data base is rather sparse. However, we feel comfortable in using it to obtain approximate fish locations for the two pogo probe lowerings during which these locations were not acoustically navigated. For penetration 7, station 2 we have directly interpolated a value of 2012 meters from the observed v/sf relationship. For penetration 1, station 3 we have decreased the directly interpolated value by a small amount to bring the sf/Δt value more in line with the relationship noted in table 9a. These results are shown in table 9b.

We felt that the most important factor in estimating the ship/fish separation once the probe had been lowered was the relationship between ship velocity and the deviation of the wire from a straight line. Tables 10a-c are listings of the values obtained for the quantities described in Figure 11 for all acoustically navigated pogo probe penetrations. Care must be taken in interpreting this data as Ivers and Mudie (1973) have shown that changes in ship speed or direction often take 30 minutes or more to propagate down a long wire. We see that the values of q and

Table 10a

Ship/Fish Separation Data -- Station 2a Pogo 1a

penetration	time(z)	sf(m)	wire(m)	depth(m)	sf'(m)	Δ'(m)	q	k	Δt(min)	Δsf(m)	Δsf/Δt(m/min)	Δx(min)	v(knots)
1	1207	496	5534	5457	918	422	6.5	3.5	90	496	5.5	.921	.61
2	1239.5	699	5531[+]	5464	863	165	10.3	8.4	22.5	203	9.0	.207	.55
3	1305	638	5528	5474	765	126	12.0	10.1	25.5	-60	-2.4	.238	.56
4	1331	636	5525[+]	5484	666	29	15.8	15.1	26	-2	-0.1	.174	.40
5	1357.5	408	5522	5497	530	123	15.9	12.2	26.5	-228	-8.6	.220	.50
6	1533.5	827	5631	5505	1185	358	6.6	4.6	36	419	11.7	.786	1.31
7	1610	977	5631	5505	1185	209	7.7	6.4	36.5	150	4.0	.418	.69

[+]interpolated

start = 1037 Z 2/14/78

Symbols are defined in figure 11. Some numbers may not be exact due to small depth inaccuracies in the initial calculations.

Table 10b

Ship/Fish Separation Data -- Station 6 Pogo 3

penetration	time(z)	sf(m)	wire(m)	depth(m)	sf'(m)	Δ'(m)	q	k	Δt(min)	Δsf(m)	Δsf/Δt(m/min)	Δx(min)	v(knots)
						A							
1	1222	3042	6618	5518	3653	611	2,8	2,3	85	3042	35,8	2,278	1,62
2	1242	3323	6690	5514	3792	468	2.8	2.5	20	281	14.1	.338	.94
3	1309	3327	6917	5502	4192	865	2.4	1.9	27	4	0.1	.570	1.27
3a	1325	3307	6917+	5502	4192	885	2.3	1.8	16	-20	-1.3	.295	1.11
						B							
4	1924	744	5592	5428	1339	594	4.6	2.6	63	744	11.8	.641	.61
5	2019.5	1481	5760	5428	1924	443	4.5	3.4	55.5	737	13.3	.854	.93
6	2103	1845	5942	5432	2409	563	3.6	2.8	43.5	361	8.4	.691	.95
7	2137	2253	6067	5434	2698	444	3.6	3.0	34	408	12.0	.666	1.18
8	2203.5	2374	6116	5434	2808	433	3.5	2.9	33.5	121	3.6	.378	.68
9	2221.5	2648	6244	5436	3073	424	3.3	2.8	18	274	15.2	.320	1.07
10	2242	2828	6446	5448	3444	616	2.8	2.3	21.5	180	8.4	.342	.96
11	2300	2873	6368	5452	3290	417	3.1	2.7	18	45	2.5	.270	.90
12	2322.5	2967	6431	5456	3404	437	3.0	2.7	22.5	94	4.2	.412	1.10
13	2340	3023	6460	5459	3453	430	3.0	2.6	17.5	56	3.2	.319	1.09
14	0000	3151	6478	5461	3484	333	3.1	2.8	20	128	6.4	.356	1.07
15	0019.5	3009	6608	5464	3715	710	2.6	2.1	19.5	-142	-7.3	.396	1.22
16	0033.5	3329	6765	5463	3991	662	2.6	2.1	14	320	22.9	.345	1.48
17	0050	3616	6878	5464	4179	563	2.6	2.2	16.5	287	17.4	.334	1.21
18	0105	3737	6845	5467	4117	380	2.7	2.5	25	121	4.8	.364	.87

+assumed A start = 1057 Z 2/16/79 B start = 1821 Z 2/17/79

Symbols are defined in figure 11. Some numbers may not be exact due to small depth inaccuracies in the initial caculations.

Table 10c

Ship/Fish Separation Data -- Station 7 Pogo 4

pene-tration	time(z)	sf(m)	wire(m)	depth(m)	sf'(m)	Δ'(m)	g	k	Δt(min)	Δsf(m)	sf/ΔtΔ(m/min)	ΔX(min)	V(knots)
1	1320	882	5560	5415	1260	379	6.1	4.3	85	882	10.4	.927	.65
2	1338.5	1086	5586	5417	1361	274	6.5	5.2	18.5	204	11.1	.239	.78
3	1354	1200	5626	5421	1503	304	5.9	4.8	15.5	114	7.4	.167	.65
4	1411	1289	5640	5425	1546	256	6.0	5.0	17	89	5.2	.180	.64
5	1424	1372	5680	5426	1681	309	5.4	4.4	13	83	6.4	.153	.71
6	1443	1502	5717	5429	1794	293	5.2	4.4	19	130	6.8	.236	.75
7	1501.5	1626	5758	5432	1946	320	5.0	4.2	18.5	124	6.7	.223	.72
8	1514.5	1694	5770	5436	1937	243	5.0	4.4	13	68	5.2	.153	.71
9	1531	1767	5800	5439	2012	245	4.9	4.3	16.5	78	4.4	.198	.72
10	1546.5	1917	5840	5441	2122	205	4.8	4.3	15.5	150	9.7	.212	.82
11	1603.5	1942	5861	5441	2177	234	4.7	4.2	17	25	1.5	.213	.75
12	1620	2050	5890	5445	2244	194	4.7	4.3	16.5	108	6.6	.202	.73
13	1643	2237	5952	5455	2391	154	4.5	4.2	23	187	8.1	.334	.87
14	1659.5	2303	5995	5460	2478	176	4.3	4.0	16.5	66	4.0	.218	.79
15	1717	2451	6070	5472	2628	177	4.1	3.8	17.5	148	8.4	.274	.94
16	1734.5	2610	6147	5481	2782	172	3.9	3.7	17.5	159	9.1	.278	.95

start = 1155Z   2/17/78

Symbols are defined in figure 11. Some numbers may not be exact due to small depth inaccuracies in the initial calculations.

k are roughly constant for a given station, but vary from one station to the next. Table 11a shows only the relationship between ship velocity and the deviation of the wire from a straight line. During station 7, we see a small but probably insignificant tendency towards an inverse relationship between v and Δ'. Station 6 shows no correlation and station 2a strongly shows the reverse tendency. From one station to the next, a tendency appears as well for Δ' to increase nonlinearly as v increases. We have used these crude relationships to obtain values of Δ' for stations 2b and 3.

In Table 11b we show our estimated values of Δ' for the remaining 6 unlocated penetrations. In arriving at our values of ship/fish separation, we worked backwards from our knowledge of the wire out, the depth and our estimates of Δ'. This data is given in Table 12. During station 3, the ship/fish separation increases at a faster rate than for other stations because the amount of wire paid out as a function of time is greater than at other stations.

In Figure 12 we have plotted the acoustically navigated ship tracks for all of the pogo probe stations. Also plotted whenever possible is the acoustically navigated path which the fish took as it lagged behind the ship. The noticeable feature is that small changes in ship course

Table 11a

Ship Velocity Versus Wire Curvature -- Fish Navigation

Station 2a		Station 6a		Station 6b		Station 7	
v(knots)	Δ'(m)	v(knots)	Δ'(m)	v(knots)	Δ'(m)	v(knots)	Δ'(m)
First Penetration							
.61	422	1.62	611	.61	594	.65	379
Multiple Penetrations							
.40	29	.94	468	.68	433	.64	256
.50	123	1.11	885	.87	380	.65	304
.55	165	1.27	865	.90	417	.71	309
.56	126	Ave. =	739	.93	443	.71	243
.69	209			.95	563	.72	320
1.31	358			.96	616	.72	245
Ave. =	168			1.07	424	.73	194
				1.07	333	.75	293
				1.09	430	.75	234
				1.10	437	.78	274
				1.18	444	.79	176
				1.21	563	.82	205
				1.22	710	.87	154
				1.48	662	.94	172
				Ave. =	490	Ave. =	238

Table 11b

Ship Velocity Versus Wire Curvature -- No Fish Navigation

First Penetration

Station 2b v(knots)	Station 2b Δ'(m)	Station 3 v(knots)	Station 3 Δ'(m)
1.18	658	1.08	435

Multiple Penetrations

Station 2b v(knots)	Station 2b Δ'(m)	Station 3 v(knots)	Station 3 Δ'(m)
.84	365	1.05	330
		1.08	330
		1.11	330
		1.11	330
		1.14	330

Table 12

Ship/Fish Separation Data--No Fish Navigation

penetration	time(z)	sf(m)	wire(m)	depth(m)	sf'(m)	Δ'(m)	q	k	Δt(min)	Δsf(m)	Δsf/Δt(m/min)	Δx(min)	v(knots)
					Station 2b	Pogo 1b							
8	2032	2012	6127	5509	2670	658	3.3	2.5	79	2012	25.5	1.549	1.18
9	2135	2504	6230	5514	2870	365	3.6	3.1	63	493	7.8	.880	.84
Start 1913Z	2/14/78												
					Station 3	Pogo 2							
1	1451	1555	5869	5517	2002	435	4.5	3.5	68	1555	22.9	1.227	1.08
2	1520.5	2262	6098	5514	2592	330	3.9	3.4	29.5	707	24.0	.531	1.08
3	1556.5	2840	6371	5513	3170	330	3.4	3.0	36	578	16.1	.666	1.11
3a	1606.8	2839	6371	5514	3168	330	3.4	3.0	10	-1	0.1	.191	1.14
4	1624.5	3179	6550	5517	3508	330	3.1	2.8	18	340	18.9	.315	1.05
5	1650	3588	6775	5527	3918	330	2.9	2.6	25.5	409	16.1	.472	1.11

+assumed Start = 1343 Z 2/15/78

Symbols are defined in figure 11. Some numbers may not be exact due to small depth inaccuracies in the initial calculations.

do not necessarily affect the path of the heat flow probe. From an analysis of the known ship paths versus fish paths, we have estimated the fish path when only the ship path was known. These estimated paths are also shown in Figure 12. Given the fish paths and the ship/fish separation at the time of the heat flow measurements, we could straightforwardly plot the positions of the 8 pogo probe measurements discussed. Final locations for all of the heat flow measurements are given in tables 3 and 6.

We tried other methods of locating the heat flow probe, based on slightly different analyses of the data given in tables 10a-c. By this means, we were able to estimate the error of our empirically derived locations to be on the order of ±350 meters. This error is relative to the acoustic navigation net. Ivers and Mudie (1973), using a complex three-dimensional dynamic model of towing a long cable at slow speeds, were able to reduce this error by a factor of two.

Step 7 - Conversion of Digital Pressure Data to Actual Depths

Initially, we felt that the digital pressure data would allow us to determine the depth at which any given measurement was taken with a high degree of accuracy. This was found not to be the case. However, we were able to produce bottom water temperature profiles accurate to within ±15 meters, and with a precision estimated to be on the order of ±1 meter.

We know that over small depth ranges, the relationship between pressure and depth can be taken as linear. Furthermore, the heat flow instrument's electronics are designed such that the relationship between digital counts and actual pressure is as linear as possible. In order to determine the depth sensitivity of the pressure counts, it is necessary to know the actual depth at two times when we also know the pressure counts. Furthermore, to avoid any nonlinearities in the counts/depth relationship, it is best to pick these two depths as close to the actual depth range of interest as possible. For our uses, this depth range is the lowermost few hundred meters of the water column.

Because of the high density of ship tracks in the survey area and the small amount of seafloor relief, we were able to determine the ocean depth to within ±5 meters (from the bathymetry map). Thus, for any particular station, we used the ocean depth as one of our known depths. To determine the other depths, we had recourse to the PGR records. From these records, we could determine to within ±3 seconds, the penetration time, and the times when the direct and reflected signals from the 12 kHz pinger crossed on the PGR record. Hence, a method was developed to calculate the depths to which these crossovers corresponded.

The geometry which we assumed is given in Figure 13. The ship is at a distance h above the seafloor. The pinger (situated next to the heat flow instrument) is at a distance s above the seafloor and is located a distance d away from the ship in a horizontal plane. The length l' is the direct travel distance from the pinger to the ship. The reflected travel distance has a length l, equal to the sum of l_1 and l_2. We will assume that over the distance d, the seafloor is flat. Reference to Figure 2 shows that this is true to within ±25 meters. We could calculate d, the ship/fish separation at the crossover times and at penetration to within ±25 meters for stations with fish navigation.

The PGR was set at a .5 second sweep. The length of time the direct (t') and reflected (t) signals travel are given by,

$$t' = l'/v' \qquad \text{and} \qquad t = 2l_1/v + q/v'$$

where, $q = l_2 - l_1$.

v' is the average sound velocity above the pinger and v is the average sound velocity between the pinger and the seafloor. We expect the direct and reflected arrivals to cross over when the difference in their arrival times is

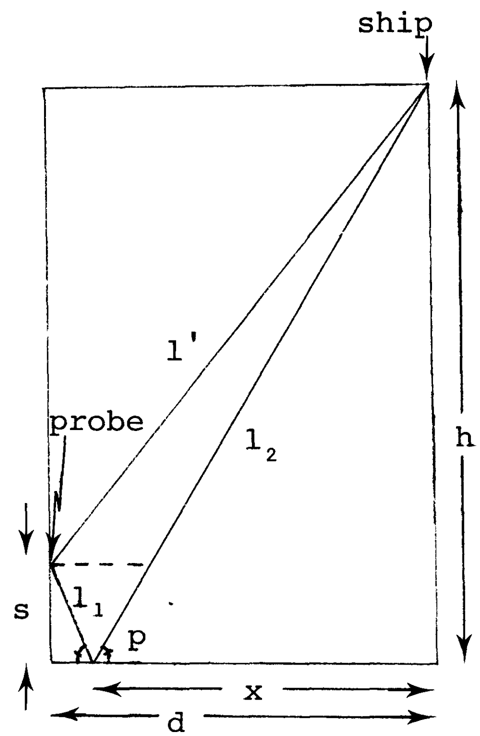

$$l' = (d^2 + (h-s)^2)^{1/2}$$

$$l = l_1 + l_2$$

$$= (s^2 + (d-x)^2)^{1/2} + (h^2+x^2)^{1/2}$$

Geometry Used to Determine Probe Height Above Bottom

Figure 13

equal to an integral multiple of .5 seconds. The PGR converted travel time to meters under the assumption that the average sound velocity was a constant 1463 m/s (800 fm/s). Hence, crossovers occur when the distance between direct and reflected paths (l - l'), is equal to an integral multiple of 1463 $\cdot\Delta t$. Or,

$$1463.\Delta t = 1463 \cdot .5n = 731.5 \text{ m}$$

where Δt is given by,

$$\Delta t = (t - t') = 2l_1/v + (q - l')/v'.$$

Crossover depths occur when,

$$731.5n = 1463.(2l_1/v + (q - l')/v').$$

The travel lengths l' and l are equal to,

$$l' = (d^2 + (h - s)^2)^{1/2}$$

$$l = l_1 + l_2 = (s^2 + (d - x)^2)^{1/2} + (h^2 + x^2)^{1/2}.$$

We can determine x by using the geometrical relationship,

$$\tan(p) = h/x = s/(d - x).$$

This yields, $x = h.d/(h + s).$

The only remaining unknown are v', v and s. As a first approximation, we can assume that $v = v' = 1463$ m/s and that the pinger is directly beneath the ship ($x = d = 0$). Then crossovers would occur when,

$$731.5 = l - l' = 2s \quad \text{or,} \quad s = 365.8 \text{ m (200 fm)}.$$

Using this first order approximation to s, we could calculate the depth to which v' and v corresponded. Using Matthews (1939), we were able to directly interpolate the the value of v' from his tables of harmonic mean vertical sounding velocity versus depth.

The mean sound velocity beneath the pinger, v, was found from Matthews (1939) as well, but by somewhat more indirect means. At 35.00 ‰ salinity and 2.1 °C, near the bottom water temperature, Matthews (1939) gives the velocity of sound as 1455 m/s. The actual salinity will probably be greater than 35.00 ‰ near the bottom, but the salinity correction is negligible (Matthews, 1939).

The pressure (hence, depth) correction was found from Matthews' (1939) Table 5. The depth correction is quite linear in the range of interest; hence, the correction we chose was that corresponding to a depth half way between the pinger and the seafloor. This depth is given by, $h_c = h - \frac{1}{2}s$. The velocity obtained by this method should be similar to that obtained by adding the velocity at (h - s) to that at h and dividing by 2. Or, $v = (v_h + v_{h-s})/2$. This proved to be the case, indicating that in fact the pressure correction is linearly related to depth, at least near the seafloor.

With our estimated values of v' and v, we wanted to solve for s:

$$731.5n = 1463\cdot(2l_1/v + (l_2 - l_1 - l')/v')$$

$$= 1463\cdot(\ 2\cdot(h^2 + x^2)^{\frac{1}{2}}/v + ((h^2 + x^2)^{\frac{1}{2}} - (s^2 + (d-x)^2)^{\frac{1}{2}} - (d^2 + (h-s)^2)^{\frac{1}{2}})\ )$$

with, $x = h\cdot d/(h + s)$.

Rather than spend time on such a problem, we guessed at s and found the value (e) of,

$$731.5n - 1463\cdot(2l_1/v + (l_2 - l_1 - l')/v').$$

We used this value to help modify our estimate of s. The s which we finally used was that which minimized e. With this value of s, it was now possible to refine our estimates of v' and v. Typically, only the first iteration was needed to insure convergence of s. The accuracy of s is on the order of ± 5 meters.

The pressures counts corresponding to the distance s can be found from the digital printout (GEJB - Appendix A). The time interval between penetration and the crossover in question is first determined from the PGR record. This time interval is then converted to a number of cycles (28 seconds = 1 cycle). The penetration time is noted on the digital printout and the number of cycles are either subtracted or added to the penetration cycle time (in counts), corresponding to the probe being lowered or raised. It would be fortuitous if penetration occurred while the pressure variable was being recorded. Thus, it is usually necessary to interpolate the pressure counts. The number of rollovers (r) must be determined and 4096.r added to the pressure counts in order to obtain the total counts. A 3 second error in time corresponds to an error in cycles of .1. At the rate which the probe was moving vertically through the water column, this generally corresponded to an error in estimating pressure counts of 50.

The number of counts corresponding to the ocean depth could be determined from the portion of the digital record corresponding to the heat flow measurement. The error introduced with this determination was due entirely to an instrument drift of typically 10 counts over the course of the measurement. Given the estimates of pressure counts at the seafloor and for at least 1 crossover, we could determine the sensitivity of the pressure sensor in counts/meter.

However, in general, the zero in depth does not correspond to the zero in counts. Hence, a correction term corresponding to this difference must be subtracted from all count readings before converting to depths. The correction term can be determined given the slope (m) of the counts (c) versus depth (d) relationship (i.e. the pressure sensitivity) and one point where both counts and depth are known.

If the entire depth range is used (sea-surface to seafloor), the slope determined from crossovers can be checked. b can be determined from the digital printout while the probe is at the surface. This number, which fluctuates by as much as 40 counts, should be approximately equal to the correction determined from slope-intercept analysis. We would expect the two numbers to be exactly equal if the depth/pressure relationship was linear over its entire range and if we could neglect temperature effects to the instrument.

Over the lowermost 420 meters of the water column, we calculated the pressure sensitivities and corresponding b values given in table 13a. We see that for these stations, the resolution of the pressure sensor is on the order of .11 meters. The actual zero of depth corresponded to approximately 240 counts; the table shows varying degrees of nonlinearity in the counts/ depth relationship. We attempted to use these pressure sensitivities to calculate the depths of nearby heat flow measurements. We found that the amount of instrument drift between penetrations was large enough to make this method of calculating depths less reliable than simply reading the depths from the bathymetry map. For example, the station 6, penetration 6 sensitivity and b values applied to the penetration 7 pressure counts (47849) yield a depth of 5440 meters. Our estimate of the depth from the bathymetry map is 5434 meters, accurate to within ± 5 meters. Over the 440 meter range in which we calculated the pressure sensitivities, we estimate that they are accurate to within $\pm .14$ c/m. This represents a fractional error of less than 1.6 percent, a total error of less than 7 out of 440 meters. However, 1.6 percent of 5434 meters is 87 meters. It is surprising, then, that we did obtain an agreement of 6 meters for penetration 7; as other

Table 13a

The Relationship Between Depth and Pressure Counts Stations 6-10

Station	Penetration	Pressure Sensitivity(c/m)	b(c)	Pressure During Penetration(c)
6	1	8.869	-296	48645
6	4	9.072	-1602	47643
6	6	8.984	-1021	47796
7	16	8.485	1571	48081
9	1	8.776	257	47928

Table 13b

The Relationship Between Depth and Pressure Counts Stations 1-4

Station	Penetration	Pressure Sensitivity(c/m)	b(c)
2	1	11.17	100
3	1	11.07	100

calculations showed, this was the closest agreement we ever obtained.

We could not calculate pressure sensitivities for most pogo probe penetrations because the probe was rarely raised more than a few hundred meters off the seafloor between penetrations. Hence, for the purpose of producing bottom water temperature profiles, we assumed a pressure sensitivity of 8.857 c/m for stations 6 through 10 in all instances when it was not directly calculable. During stations 1 through 4, the pressure sensitivity was greater, causing the pressure counts to go off scale at approximately 5000 meters depth. For these stations, we calculated pressure sensitivities by using the pressure counts at the crossover corresponding to n = 2 (s approximately 797 meters) and the observed value of b while the probe was at the surface. Table 13b shows that the pressure sensitivities calculated for stations 2 and 3 are in good agreement. Figure 14 show bottom water temperature profiles for station 6, penetrations 1, 4, 6, 8, 12 and 17; station 7 penetrations 1, 7 and 16; and piston core stations 8 and 10.

We have noted that in the survey area, the bathymetry map generally proves a more reliable means of estimating ocean depths than the digital pressure counts. All of the depths of the heat flow measurements were initially

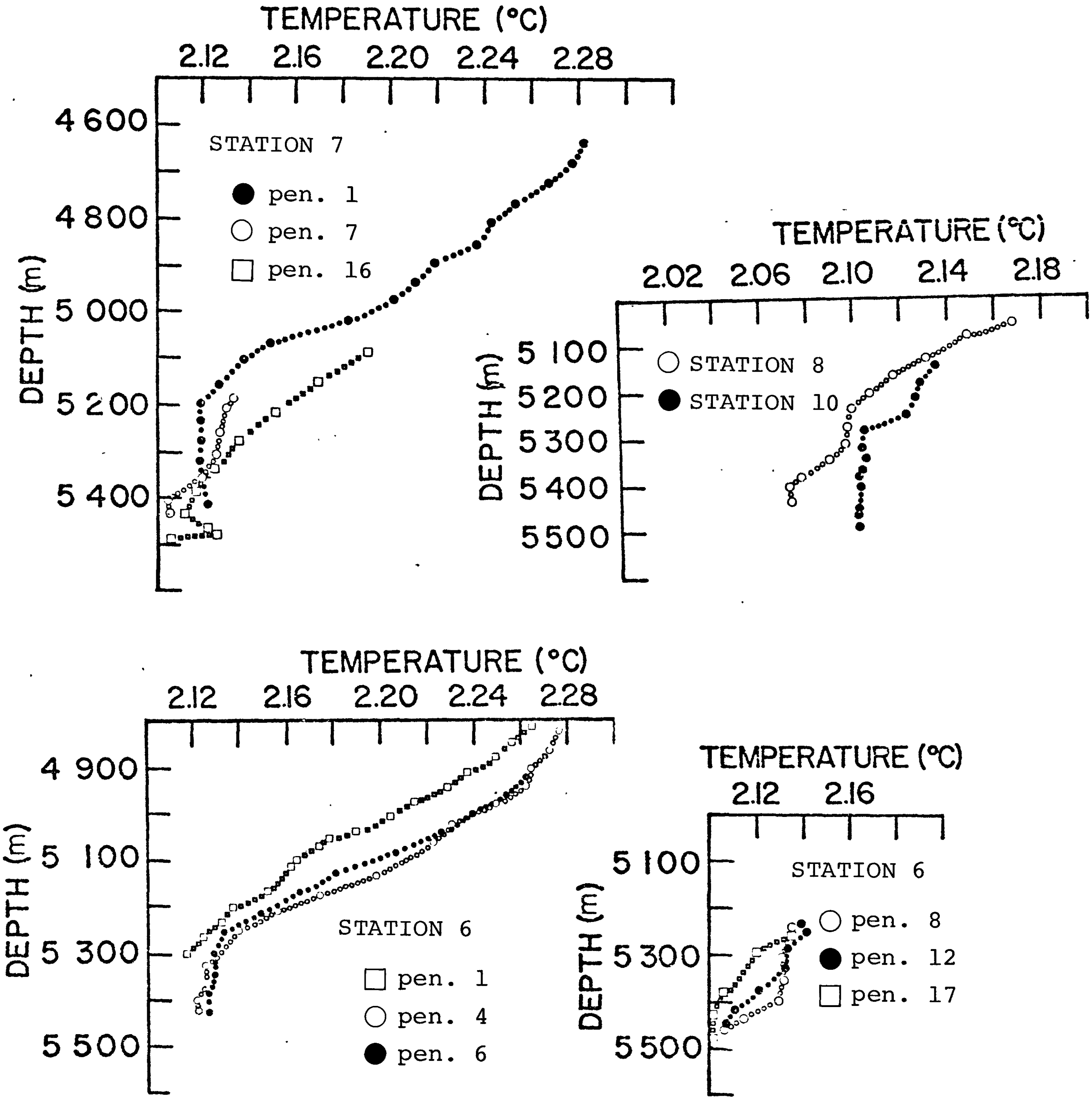

Figure 14

Bottom Water Temperature Profiles

interpolated from the bathymetry map. Because of the high density of ship tracks, most of the measurements were actually crossed over by the ship. Whenever possible we checked the depths obtained from the bathymetry map with those obtained directly from the echo-sounding records. Agreement to within ± 5 meters was obtained in all cases. Tables 3 and 6 list our estimates of the ocean depth at the locations of the heat flow measurements.

IV DISCUSSION AND INTERPRETATION OF THE THERMAL DATA

We have obtained 50 2.5 meter pogo probe and 5 piston core probe heat flow measurements. Two of the piston core probe measurements are not considered reliable because of the large errors associated with their temperature gradients. The 53 reliable measurements range from .92 HFU to 1.40 HFU with the vast majority lying between 1.1 HFU and 1.2 HFU. Their mean and standard deviation are 1.17 HFU and .08 respectively; we are fairly certain that this is representative of the regional heat flux at depth.

Our data compare quite favorably with previous heat flow measurements obtained in the vicinity of the survey area. Reitzel (1963) obtains a mean heat flow form 16 measurements of 1.14 HFU, with a standard deviation of .06. Figure 15 shows the locations of these measurements. The standard deviation of Reitzel's values is unusually low because he has subjectively excluded certain stations based on their anomalous environment or location. The value of 1.17 HFU is located about 100 kms to the west of our survey area (Figure 15). Langseth *et al.* (1966) obtain a mean from 33 measurements of heat flow in the northwest Atlantic basin of 1.17 HFU, with a standard deviation of .24. However, it should be noted that the areal extent of these two surveys is on the order of

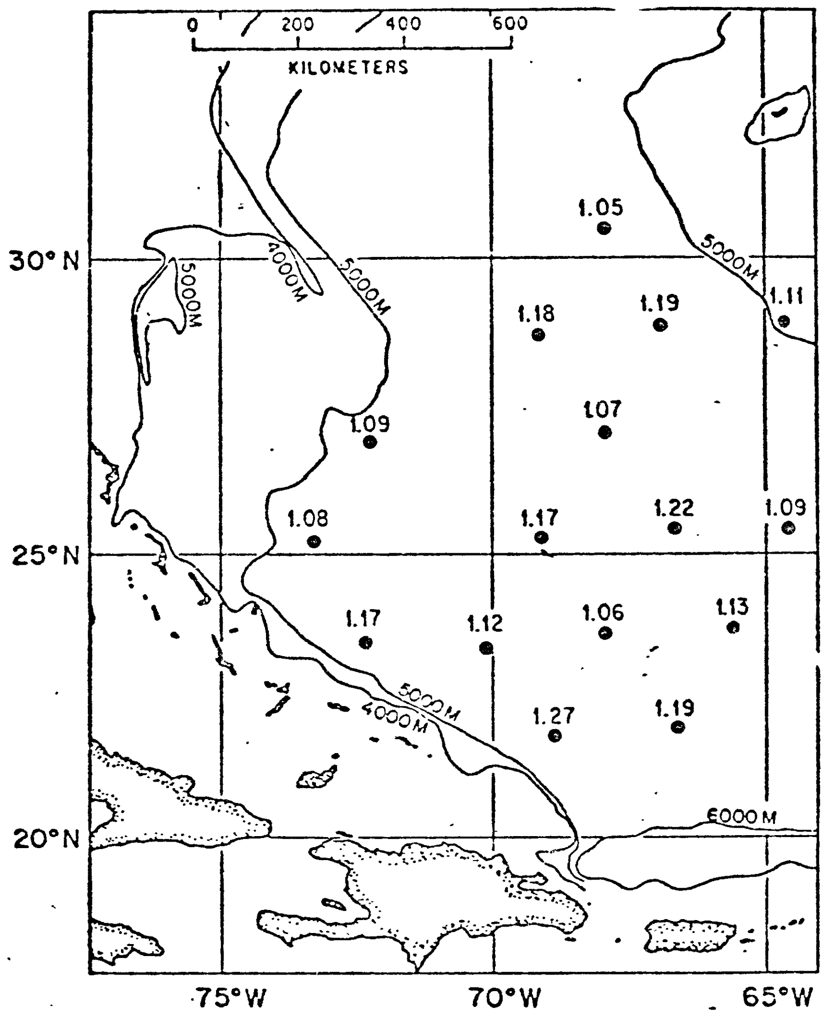

Reitzel's (1963) Northwestern Atlantic Basin

Heat Flow Values

Figure 15

millions of kms whereas our survey is confined to a 10 by 20 km area.

The nonlinearities present in the pogo probe thermal gradients can be explained by a recent temperature perturbation occurring at the sediment-water interface. Von Herzen and Uyeda (1963) discuss the implications for heat flow of recent sedimentation, turbidity currents and landslides and irregular subsurface topography. They note that, generally, these effects all serve to reduce the measured heat flow. Many authors (e.g. Palmasson, 1967; Talwani _et al._, 1971; Lister, 1972) have noted that hydrothermal circulation through the sediments can serve to greatly reduce the measured heat flux. However, we feel that the only plausible explanation of the nonlinear temperature gradients is a recent increase in the bottom water temperature. Figure 16 indicates schematically how this might occur.

Carslaw and Jaeger (1959) derive the formula for the temperature in a half space due to a periodic temperature change ($T_o.\cos(\omega t-\varepsilon)$) at the surface. The temperature is given by,

$$T = T_o.e^{-k.z}.\cos(\omega t - k.z - \varepsilon)$$

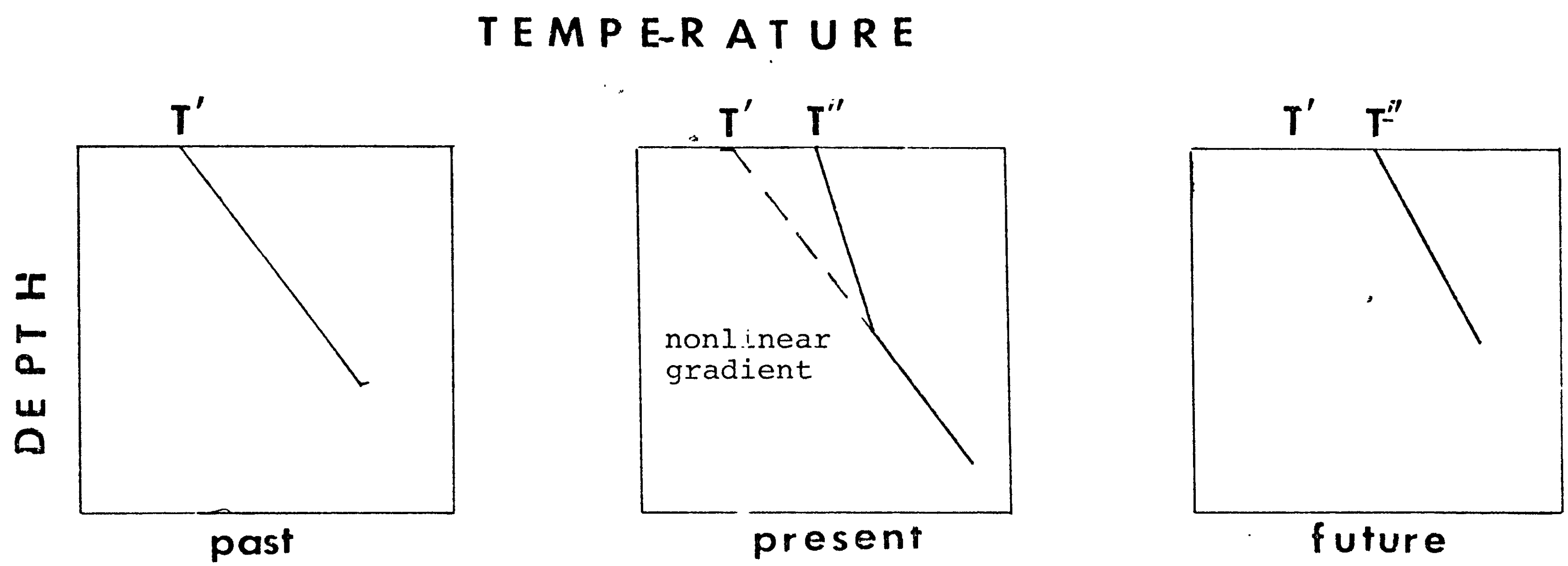

Schematic Showing How a Recent Change in Surface Temperature

Can Affect the Temperature Gradient

Figure 16

where,

z = distance from surface

T_o = initial maximum amplitude of perturbation

$k = (\omega/2K)^{1/2}$

K = thermal diffusivity = conductivity/$(\rho.C_p)$

ρ = density

C_p = heat capacity

and the wavelength λ is,

$\lambda = 2\pi/k = (4.\pi.K.P)^{1/2}$ where P is the period $2\pi/\omega$. If we ignore the phase and consider only the maximum amplitude, the temperature perturbation is $T = T_o.e^{-k.z}$. The perturbation to the temperature gradient will be $dT/dt = -T_o.k.e^{-k.z}$. We know that the mean heat flow is about 1.2 HFU and that the average conductivity in the upper sediments is about 2.10^{-3} cal/°C.cm.s. We have seen that the nonlinearity in temperature gradient at a depth of 1 meter is, on the average, 10 percent of the actual gradient or $.1.(1.2.10^{-6}/2.10^{-3}) = 6.10^{-5}$°C/cm. We can assume that the quantity $\rho.C_p$ is approximately 1 for oceanic sediments (Sclater, 1978). This yields a value of 2.10^{-3} cm^2/s for the thermal diffusivity. Hence, the maximum temperature perturbation at the surface necessary to cause a 10 percent perturbation in the gradient at a depth of 1 meter is given by,

$$T_o = 6.10^{-5}/(k.e^{-100.k})$$

where, $k = (\pi/(K.P))^{1/2} = (\pi/(.002.P))^{1/2}$. For a surface temperature that oscillates with a 1 month period, the maximum temperature perturbation would have to be .03 °C to produce the observed nonlinearities. Furthermore, the wavelength of the oscillation would be about 2.5 meters.

Given this value for T_o, we calculated the expected perturbation in the temperature gradient at a depth of 2 meters as 1 to 2 percent. In the Data Reduction section, by a comparison with the deeper piston core gradients, we postulated that the nonlinearity might very well be on the order of a few percent at this depth (1.5 to 2.5 meters). Further evidence for a maximum surface temperature perturbation of .03 °C is displayed on our bottom water temperature profiles. Note in Figure 14 the tendency for the water temperature to decrease by .02 to .03 °C over the last 150 to 200 meters of the water column. In few cases do we observe a well-mixed isothermal bottom boundary layer. Indeed, that the bottom water had a variable temperature gradient as a function of depth at the time the heat flow measurements were obtained is good reason to suspect that the temperature at the sediment-water interface had been and still was changing. Since the water temperature tended to decrease nonlinearly with depth near the seafloor, there is reason to believe that the bottom water temperature was even colder sometime before the cruise.

If we include the phase of the oscillation in our calculation we find a range of T_o's and periods which would produce similar results. However, this range becomes quite confined if we desire the perturbation to the temperature gradient to decrease from 10 percent at a depth of 1 meter in the sediment column to less than a few percent at a depth of 2 meters in the sediment column. For example, it would be impossible to obtain this behavior with an annual temperature oscillation, regardless of the values of the maximum temperature perturbation T_o, and of the time t since this maximum temperature perturbation occurred.

A periodic temperature change at the surface can explain the thermal gradient data. However, the data can be as equally well explained by invoking a step function increase in the temperature of the bottom water (Figure 16). A step change in temperature (T_o) at the sediment-water interface (z=0) would be propagated downward according to the relation,

$$T = T_o.\mathrm{erf}[z/(4.K.t)^{1/2}]$$

with the same definitions as before (Carslaw and Jaeger, 1959). The temperature gradient that results solely from the change in surface temperature is obtained, as before, by differentiating this equation with respect to z. Or,

$$dT/dz = T_o.(\pi.K.t)^{-1/2}.e^{[-z^2/(4.K.t)]}.$$

Given a K of .002 cm^2/s, we want to know the magnitude of the temperature perturbation and the time it takes for this perturbation to cause a 10 percent error in the gradient (g_1) measured at z = 100 cm and a 2.5 percent error in the gradient (g_2) measured at z = 200 cm. As with the periodic temperature perturbation, we assume a background gradient of 6.10^{-4} °C/cm yielding a g_1 equal to 6.10^{-5} °C/cm and a g_2 equal to $1.5.10^{-5}$ °C/cm. The simultaneous equations which we want to solve for T_o and t are,

$$g_1 = 6.10^{-5} = T_o.(.002.\pi.t)^{-1/2}.e^{(-1.25.10^6/t)}$$

$$g_2 = 1.5.10^{-5} = T_o.(.002.\pi.t)^{-1/2}.e^{(-5.10^6/t)}.$$

Taking the natural logarithm of g_1/g_2 and solving for t yields,

$$t = 3.75.10^6/\ln(g_1/g_2).$$

Then, we can invert the equation for g_1 (or g_2) to find T_o as,

$$T_o = g_1.(.002.\pi.t)^{1/2}.e^{(1.25.10^6/t)}.$$

We see that the propagation time is dependent only on the ratio of g_1 to g_2 and not on the absolute magnitudes of these gradient perturbations. Our initially chosen error contrast of 4 yields a propagation time of 31 days and a surface temperature change of .012 °C. Table 14 gives values of t and T_o as a function of g_2. From this table we see that a gradient contrast of about 4, between a z of 100 and 200 cms, requires the smallest surface temperature perturbation. The data also indicate that the perturbation must be on the order of a few tenths of a degree.

We have seen that the bottom water temperature variations can explain the shallow nonlinearities observed in the thermal gradient. Can other effects also explain the nonlinearities? The small interval over which a significant nonlinearity is present excludes as an explanation rapid sedimentation effects. Sclater et al. (1976) have shown that in well sedimented areas, where the basement material is covered by a layer of impermeable

Table 14

The Relationship Between Bottom Water Temperature Perturbation, Time and Gradient Perturbation at 2 Meters Depth

percent error	g_2 (.10^5°C/cm)	g_1/g_2(error contrast)	t(days)	To(°C)
.01	.006	1000	6	.035
.1	.06	100	9	.020
1	.6	10	19	.013
1.25	.75	8	21	.013
2.5	1.5	4	31	.012
3.33	2	3	40	.013
4	2.4	2.5	47	.013
5	3	2	63	.014
10	6	1	∞	∞

background gradient = $6 \cdot 10^{-4}$ °C/cm

percent error at 1m = 10, g_1 = $6 \cdot 10^{-5}$ °C/cm sediments, hydrothermal circulation effects are not observed. We are confident that all of our heat flow measurements are located in A environments (Sclater *et al.*, 1974). Furthermore, if hydrothermal circulation were occurring, we would expect a much greater scatter in the heat flow data. Thus, we are able to rule out convective heat transfer as a possible perturbing effect to the shallow temperature gradients.

The deep towed hydrophone data are able to resolve a basement high that occurs at approximately 25°06.7'N, 68°02.8'W (Purdy *et al.*, in press). Figure 17 shows the actual reflection data, filtered at two different frequency ranges, and Purdy *et al.*'s (in press) interpretation. Because of the consistency of the heat flow data across this feature (figure 2), it is not readily apparent that thermal refraction has affected the heat flow measurements. Further analysis of the effects of this subsurface topography is planned. If we assume that the basement high is a two-dimensional feature, we can use Sclater and Miller's (1969) finite difference method to compute the surface heat flow across the high.

Hyndman *et al.* (1972) have obtained a value of 1.26 HFU from an 800 meter deep drill hole on Bermuda. This value has been corrected for the topographic effect and radioactive heat generation of the Bermuda seamount and the difference between seafloor and land surface

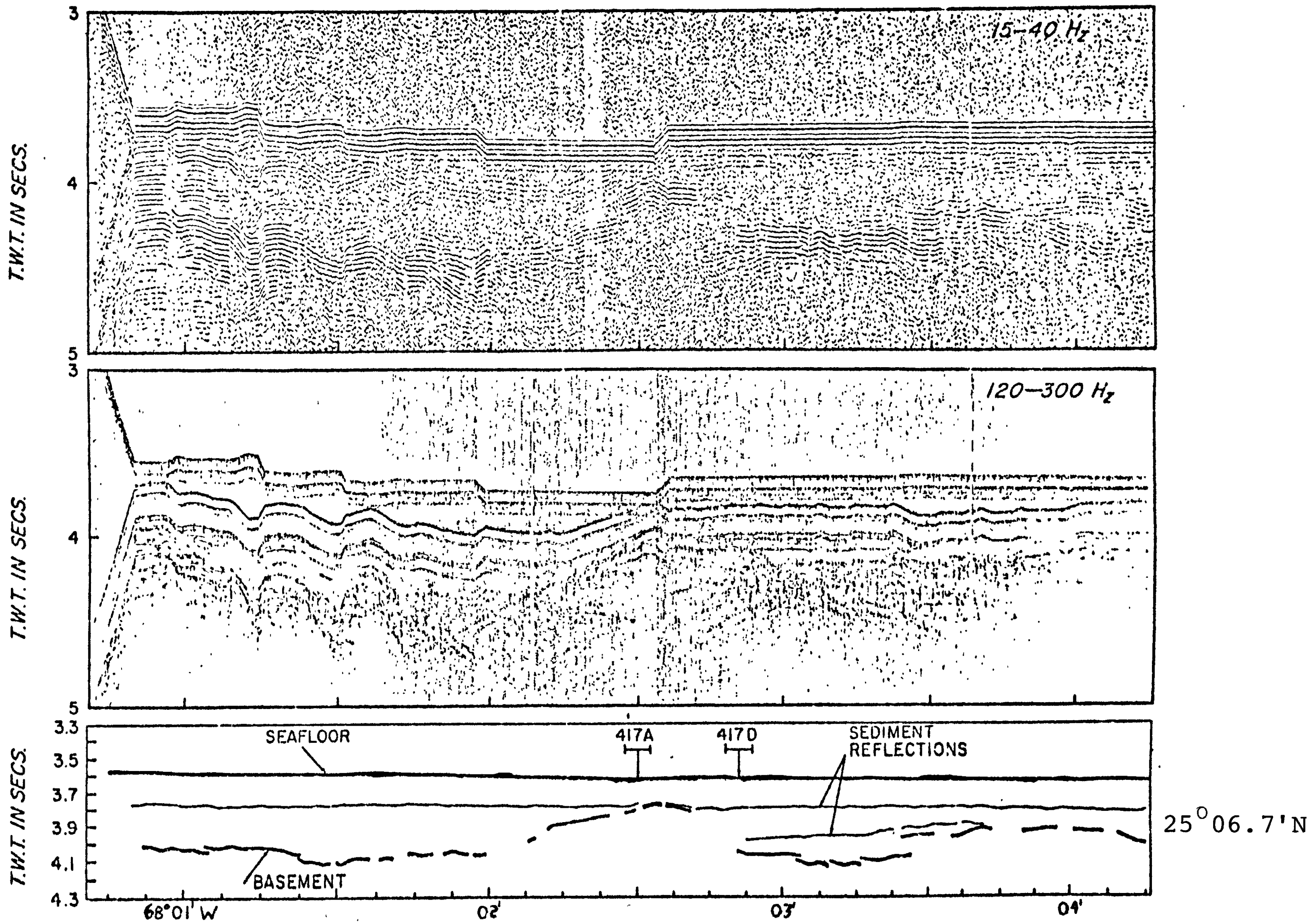

Figure 17 Purdy et al.'s (in press) Interpretation of the Basement High in the Survey Area

temperatures. The value is only slightly greater than our mean of 1.17 HFU. This general agreement supports Crough's (in press) suggestion that the reheating of mid-plate hot-spot swells occurs mostly in the lower part of the lithosphere. Furthermore, as Crough (in press) states, if the heat that supports mid-plate swells is intruded, then it rises vertically from the aesthenosphere and the source of the heat is probably as wide as the surface relief of the swell.

Discrimination between the plate and boundary layer models for the creation of oceanic lithosphere has awaited precise heat flow measurements from older oceanic basins. The age of the oceanic basement underlying the survey area has been calculated from the magnetic time scale of Larson and Hilde (1975) as 110 Ma. A schematic of the thermal boundary layer model showing the material flow (dashed lines) and the concept of a thickening lithosphere is shown in Figure 18a. The solidus temperature T_S is the isotherm that represents the temperature between solid and partially molten states. The solid lithosphere above is cooler than T_s and the aesthenosphere below is hotter. Isothermal surfaces within the cooling lithosphere are indicated by solid lines. ΔH is the elevation of the ridge crest. Parsons and Sclater (1977) derive a

a. The Thermal Boundary Layer Model

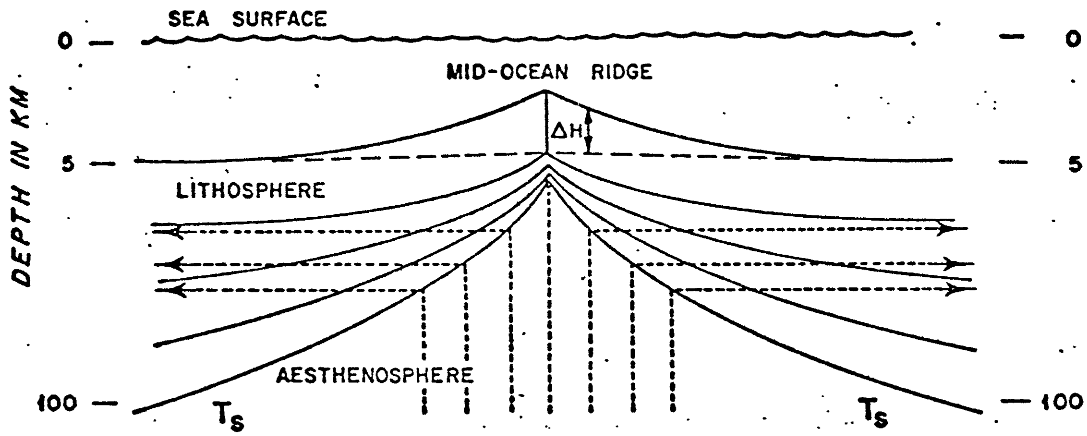

b. The Plate Model

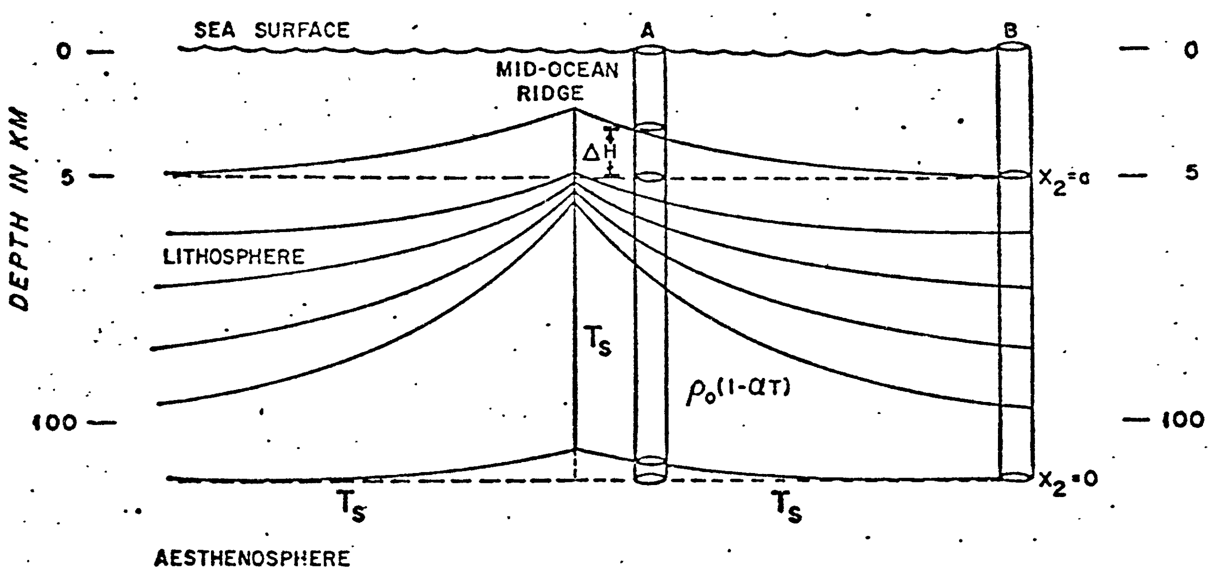

Oceanic Cooling Models

Figure 18

relationship for the heat flow (q_b) as a function of the age of the oceanic basement for the boundary layer model as,

$$q_b = 11.3/(t)^{1/2} \qquad q_b \text{ in HFU, } t \text{ in Ma}$$
$$0<t<120 \text{ Ma}$$

The plate model (a more complex kind of boundary layer model), which assumes a constant temperature T_s at the base of the lithosphere, gives a much better match to the elevation of older oceanic crust (Parsons and Sclater, 1977). Figure 18b is a schematic showing various facets of this model. The elevation ΔH is calculated by assuming that columns A and B of equal cross-sectional area must have equal masses above a common layer $x_2 = 0$. Sclater *et al.* (in press) give the following relationship between heat flow (q_p) and the age of the oceanic basement for the plate model:

$$q_p = .9 + 1.6.e^{-t/62.8} \qquad q_p \text{ in HFU, } t \text{ in Ma}$$
$$t>60 \text{ Ma}$$

Figure 19 is a plot of Sclater *et al.*'s (in press) oceanic heat flow averages superimposed on the plate and

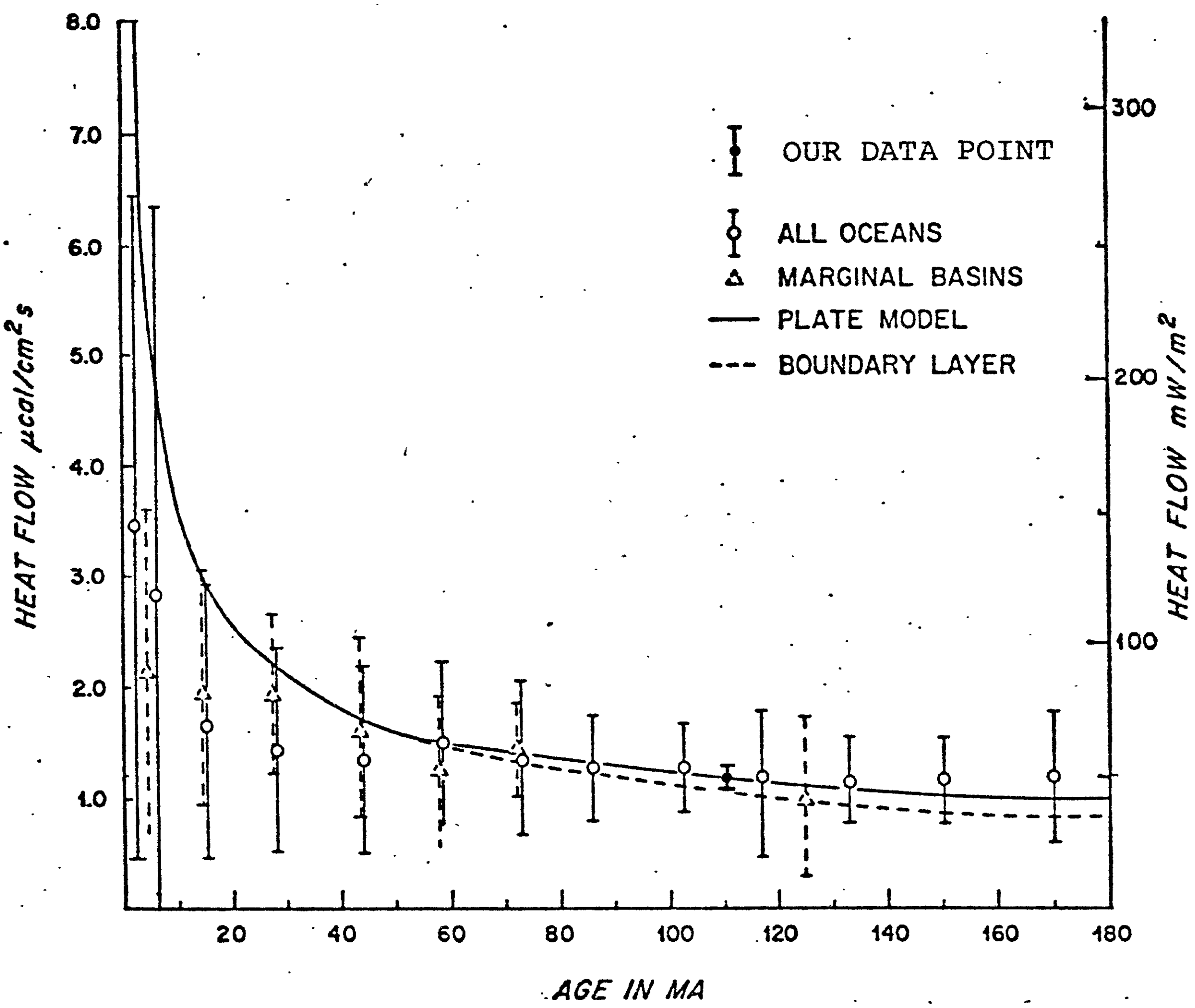

The Cooling of the Oceanic Lithosphere after

Sclater <u>et al</u>. (in press)

Figure 19

boundary layer model cooling curves. Note that for young oceanic ages, the plate and boundary layer models are identical (Parsons and Sclater, 1977) and that the observed conductive heat flow falls well below the predicted values. Sclater et al. (in press) have shown that as much as 28% of the oceanic heat loss is due to hydrothermal circulation through the impermeable sediments which overlie younger oceanic crust. Using an age of 110 Ma yields a q_b of 1.08 HFU and a q_p of 1.18 HFU. Our estimated value of the regional heat flow is 1.17 $\pm$ .08 HFU. This point has been plotted in Figure 19. Our suite of measurements has been obtained over a small area of thick (>300 m) sediment cover on crust of well-defined age. Hence, we believe that our data bear out the validity of the plate model for older oceanic lithosphere.

There have been few well designed (e.g. A environment, well known basement age) closely spaced heat flow surveys carried out on older (>100 Ma) oceanic crust. Our data, although fitting the above criteria cannot be accepted as unreservedly distinguishing between the plate and boundary layer models. We have obtained only 3 reliable measurements that penetrated more than 2.5 meters into the sediment column. Furthermore, because our data lie on the southern part of the Bermuda Rise, we face uncertainties due to the problem of additional heat input at the base of the lithosphere during the formation of the Rise.

Hyndman *et al*. (1972) show that the present island was probably formed about 33 Ma ago by lamprophyric intrusions into a structure that was then some 40 to 80 Ma old. The thermal time constant of the oceanic lithosphere is on the order of 50 to 60 million years (Parsons, personal communication). If the heat transport was entirely conductive, we would not expect to observe a thermal anomaly from a heat intrusion which occurred 33 Ma ago at the base of the lithosphere. However, if the heat intrusion involves material flow to the surface via cracks in the lithosphere or melting of the lithosphere, the thermal time constant could be appreciably smaller.

The time scale of the original formation of the Bermuda Rise (70 to 110 Ma ago), does not preclude the possibility that the original lithospheric reheating still affects the surface temperature gradient. However, Parsons and Sclater (1977) have shown that the depth of the older ocean basins can best be described by the following formula,

$$d(t) = 6400 - 3200\, e^{-t/62.8} \qquad \begin{array}{l} t \text{ in Ma} \\ d \text{ in meters} \end{array}$$

$t > 20$ Ma

This yields an equilibrium depth of 5845 meters for a t of 110 Ma. The depth to the seafloor in our survey area is on the average, 5500 meters. From table 1 it can be seen that there is about 300 meters of sediment overlying the basement in the survey area. Depending on the density of these sediments, the loading effect is on the order of 3/10 to 1/2 of the thickness of the sediments. Following Parsons and Sclater (1977), we choose a correction factor of .3 and arrive at an average depth to basement of 5710 meters. The difference between this depth and the depth predicted from models which account for the conductive cooling of the lithosphere is 135 meters. This is about 1/2 of the estimated scatter expected in the depth-age relationship in the North Atlantic (Parsons and Sclater, 1977). Thus, the argument can be made that if this part of the Bermuda Rise has subsided to a depth near equilibrium, the thermal anomaly which accounted for the initial uplift of the seafloor must also have entirely decayed. On the other hand, it is worth noting that the depth-age relationship derived by Parsons and Sclater (1977) is in part based on depth data from the Bermuda Rise. If the relationship is biased by data from this area, our subsidence argument may be circular. More deeply penetrating (>3 m) heat flow measurements, from old oceanic basins (>110 Ma), far from the sites of more recent upper mantle temperature perturbations (e.g. hot-spots, trenches), would greatly aid our interpretation and arguments.

Finally, we wish to compute the temperature of the upper mantle beneath the survey area. We assume a 10 km thick crustal layer with a heat generation of between 1 and 2 HGU (10^{-13} cal/cm^3). These heat generation values bracket the published estimates for basalt and gabbro (Sclater et al., 1979). Therefore, the corresponding contribution to the surface heat flux is between .1 and .2 HFU. Thus, the heat flow from the mantle (q_m) is 1.02 $\pm$ .13 HFU. The temperature at the base of the crust is given by,

$$T_m = (q_m \cdot d)/K + \int_0^d \int_0^z A(t)\,dt\,dz/K$$

where d is the thickness of the crust, K is the thermal conductivity, assumed to be constant and A(z) is the vertical radioelement distribution function, in this application, also assumed to be constant. The second factor reduces to $Ad^2/2K$. Following Sclater *et al.* (in press), we have chosen an average thermal conductivity for the crust of $6 \cdot 10^{-3}$ cal/^{o}C·cm·s. Thus, with our calculated value of q_m, we arrive at a T_m of 182 $\pm$ 27 ^{o}C.

BIBLIOGRAPHY

Bookman, C.A., I. Malone, and M.G. Langseth, Sea floor geothermal measurements from Vema cruise 26, Columbia University Technical Report, 7-CU-7-73, 1973.

Bryan, W.B., P.T. Robinson, et al., Studying oceanic layers, Geotimes, 22, July/August, 22-26, 1977.

Bullard, E.C., The flow of heat through the floor of the Atlantic Ocean, Proc. Roy. Soc. London, A, 222, 408-429, 1954.

Carslaw, H.S., and J.C. Jaeger, Conduction of Heat in Solids, 510 pages, Oxford Uiversity Press, London, 1959.

Correy, C., C. Dubois, and V. Vacquier, Instrumentation for measuring the terrestial heat flow through the ocean floor, J. Mar. Res., 26, 165-167, 1968.

Crough, S.T., Thermal origin of mid-plate hot-spot swells, Geophys. J. Roy. Astr. Soc., in press.

Crough, S.T., and G.A. Thompson, Numerical and approximate solutions for lithospheric thickening and thinning, Earth and Plan. Sci. Letters, 31, 397-402, 1976.

Donnelly, T.W., J. Francheteau, et al., Mid-Ocean ridge in the Cretaceous, Geotimes, 22, June, 21-23, 1977.

Flower, M.F.J., M.H. Salisbury, et al., DSDP Cretaceous crust sought, Geotimes, 22, September, 20-22, 1977.

Galson, D., Oceanic heat flow, unpublished manuscript, 10 pages, December, 1976.

Gerard, R., M.G. Langseth, and M. Ewing, Thermal gradient measurements in the sater and bottom sediment of the western Atlantic, J. Geophys. Res., 67, 785-803, 1962.

Hoskins, H., and R.C. Groman, Informal report to IPOD site survey management on surveys at IPOD sites A2.2 and 2.3, unpublished manuscript, 21 pages, October, 1976.

Hunt, M.M., W.M. Marquet, D.A. Moller, K.R. Peal, W.K. Smith, and R.C. Spindel, An acoustic navigation system, Woods Hole Oceanographic Institution Technical Report, WHOI-74-6, 1974.

Hyndman, R.D., G.K. Muecke, and F. Aumento, Deep Drill 1972. Heat flow and heat production in Bermuda, Canadian J. of Earth Sci., 6, 809-818, 1974.

Ivers, W.D., and J.D. Mudie, Towing a long cable at slow speeds: A three-dimensional model, Mar. Tech. Soc. Jour., 3, 23-31, 1973.

Langseth, M.G., Techniques of measuring heat flow through the ocean floor, in Terrestial Heat Flow, Geophysical Monograph 8, edited by W.H.K. Lee, Chapter 4, pages 58-77, American Geophysical Union, Washington, D.C., 1965.

Langseth, M.G., X. Le Pichon, and M. Ewing, Crustal structure of the mid-ocean ridges, 5-Heat flow through the Atlantic Ocean floor, and Convection currents, J. Geophys. Res., 71, 5321-5355, 1966.

Larson, R.L., and T.W.C. Hilde, A revised time scale of magnetic reversals for the early Cretaceous and late Jurassic, J. Geophys. Res., 80, 2586-2594, 1975.

Lister, C.R.B., On the thermal balance of a mid-ocean ridge, Geophys. J. Roy. Astr. Soc., 26, 515-535, 1972.

Lister, C.R.B., The dependence of heat flow on age, paper presented at the 16th IUGG General Assembly, Grenoble, 1975.

Lister, C.R.B., Estimators for heat flow and deep rock properties based on boundary layer theory, in Heat Flow and Geodynamics, edited by A.M. Jessop, Tectonophysics, 41, 157-171, 1977.

Matthews, D.J., Tables of the velocity of sound in pure water and sea water for use in echo-sounding and sound-ranging, 2cd ed., Hydrographic Department, Admiralty, London, 52 pages, 1939.

Palmasson, G., On heat flow in Iceland in relation to the Mid-Atlantic Ridge, in Iceland and Mid-Ocean Ridges, edited by S. Bjoinsson, Soc. Sci. Islandia, 38, 111-117, 1967.

Parsons, B., and J.G. Sclater, An analysis of the variation of ocean floor bathymetry and heat flow with age, J. Geophys. Res., 82, 803-827, 1977.

Purdy, G.M., J.I. Ewing, and G.M. Bryan, A deep towed hydrophone seismic reflection survey around IPOD sites 417 and 418, submitted to J. Geophys Res., 1979.

Reitzel, J.S., A region of uniform heat flow in the north Atlantic, J. Geophys. Res., 68, 5191-5196, 1963.

Sclater, J.G., C. Jaupart, and D. Galson, The heat flow through continents and oceans, Reviews of Geophys., in press.

Sclater, J.G., J. Crowe, and R.N. Anderson, On the reliability of oceanic heat flow measurements, J. Geophys. Res., 81, 2997-3006, 1976.

Sclater, J.G., and S.P. Miller, A machine method for computing the effect of a two-layered conductivity structure, Tech. Memo. 198, Mar. Phys. Lab. Scripps Inst. of Oceanogr. La Jolla, CA, 1964.

Sclater, J.G., R.P. Von Herzen, D.L. Williams, R.N. Anderson, and K. Klitgord, The Galapagos spreading center, heat flow low on the north flank, Geophys. J. Roy. Astr. Soc., 38, 609-626, 1974.

Talwani, M., C.C. Windisch, and M.G. Langseth, Reykjanes Ridge crest: A detailed geophysical study, J. Geophys. Res., 76, 473-517, 1971.

Von Herzen, R.P., and R.N. Anderson, Implications of heat flow and bottom water temperature in the eastern equatorial Pacific, Geophys. J. Roy. Astr. Soc., 26, 427-458, 1972.

Von Herzen, R.P., and A.E. Maxwell, The measurement of thermal conductivity of deep-sea sediments by a needle probe method, J. Geophys. Res., 64, 1557-1563, 1959.

Von Herzen, R.P., G. Simmons, and A. Folinsbee, Heat flow between the Caribbean Sea and the Mid-Atlantic Ridge, J. Geophys. Res., 75, 1973-1984, 1970.

APPENDICES

APPENDIX A

Step 1 - Cassette Tape to 9-Track Tape

Each heat flow station, whether a single piston core measurement or a multipenetration pogo probe station, is contained on one side of a cassette tape in binary form. The cassette tape is first transferred via a special interface with the computer to a 9-track magnetic tape. For our data, the tape was labelled GEJA. This tape could then be edited - any sort of gross errors in the data sets could be located and processed. To this end, a computer program was written by Ken Green. The program reads the digital data from tape GEJA and writes it out sequentially on a new 9-track tape (which in the present case, was labelled GEJB). One record on the sequential 9-track tape contains 100 of the 28 second records on the cassette tape. As previously mentioned, each 28 second record contains 14 separate binary numbers. The contents of tape GEJB, the edited 9-track tape, are then printed out on a line printer. A listing of this program and the job control statements necessary to run it are given below. A more precise explanation of what occurs during this step can be found in Green (in prep.)

We also give a sample of the print-out from station 7. Sixteen measurements of heat flow were obtained during this station although only the first two penetrations are shown. A thermistor value of 2049 is an off scale reading. Note that the last column, denoted as delta, contains a quantity which is calculated in the program and is not recorded on the cassette tape. Delta is the difference between the number of counts (F) corresponding to the full scale calibration resistance (R_F) and the number of counts (Z) corresponding to the zero scale calibration resistance (R_Z). Delta is a measure of instrument data quality and it should remain fairly constant during a given station.

```
C     PROGRAM TO READ DHF DATA FROM CARP TAPE AND WRITE BINARY RECORDS
C     OF 1400=100 INPUT RECORDS PLUS SEQUENCE NUMBER
C     MODIFIED TO OUTPUT INPUT RECORDS TO LINE PRINTER 16 MARCH 78
      INTEGER CR/105/,LP/108/,MTI/4/,MTO/5/
      INTEGER IBUF(1000),R/12/,IN(13),OUT(1400)
      CALL SETSKP(IND)
      READ(CR,1)NFIL1,NFIL2
    1 FORMAT(2G)
      IF(NFIL1.EQ.1)GO TO 10
      CALL SKPFIL(MTI,NFIL1-1)
      IF(IND.NE.2)WRITE(LP,2)IND
    2 FORMAT('SKPFIL ERROR IND=',G)
    3 FORMAT('SIGMA7 READ ERROR IN FILE',X,G,X,'RECORD',X,G)
    4 FORMAT('WRITE ERROR IN FILE',X,G,X,'RECORD',X,G,X,'KERR=',G)
   10 CONTINUE
      DO 500 NFIL=NFIL1,NFIL2
      CALL CASSFORM(IBUF,MTI,LP,R,R,R,R,R,R,R,R,R,R,R,R,R)
      CALL CASSERR(ISI,NCHAR,IERR,ISEQ)
      KRECLEN=0
      KCARP=0
      DO 100 NREC=1,2600
      K=1
      DO 50 JREC=1,100
      DO 20 I=1,13
      IN(I)=0
   20 CONTINUE
      CALL CASSREC(IN(1),IN(2),IN(3),IN(4),IN(5),IN(6),IN(7),IN(8),
     $IN(9),IN(10),IN(11),IN(12),IN(13))
      IF(ISI.EQ.1)GO TO 30
      IF(ISI.EQ.2)GO TO 60
      IF(ISI.EQ.3)KRECLEN=KRECLEN+1
      IF(ISI.EQ.4)KCARP=KCARP+1
      IF(ISI.EQ.5)WRITE(LP,3)NFIL,100*NREC+JREC
      GO TO 31
   30 CONTINUE
      ICAL=IN(13)-IN(3)
      WRITE(LP,5)ISEQ,(IN(I),I=1,13),ICAL
    5 FORMAT(1X,15I6)
   31 CONTINUE
      OUT(K)=ISEQ
      K=K+1
      DO 40 I=1,13
      OUT(K)=IN(I)
      K=K+1
   40 CONTINUE
   50 CONTINUE
      JREC=JREC-1
   60 CONTINUE
      CALL BUFF OUT(MTO,1,OUT,14*JREC)
   80 IF(ICHECK(MTO,ISTAT,NPTS,KERR).EQ.1)GO TO 80
      IF(ISTAT.EQ.4)WRITE(LP,4)NFIL,NREC,KERR
      IF(ISI.EQ.2)GO TO 110
  100 CONTINUE
  110 CONTINUE
      END FILE MTO
      WRITE(LP,200)NFIL,NREC
      WRITE(LP,201)KRECLEN,KCARP
  200 FORMAT('FILE NUMBER ',X,G,X,'CONTAINS',X,G,X,'OUTPUT RECORDS')
  201 FORMAT('LENGTH ERRORS=',G,5X,'CARP ERRORS=',G)

  500 CONTINUE
      END FILE MTO
      END
```

Figure A1

Job Control Statements Necessary to Run
Ken Green's program

```
!JOB account,ID
!LIMIT (9T,2),(CORE,10),(TIME,5)
!MESSAGE TAPE GEJA ON 9T  TAPE IN I/O RACK NORING
!MESSAGE GEJB ON 9T  **WRITE**
!FORTRAN LS,GO

-program-

!ASSIGN F:4,(DEVICE,9T),(SN,GEJA),(IN)
!ASSIGN F:5,(DEVICE,9T),(SN,GEJB),(OUT)
!LOAD (GO),(UNSAT,(3))
!RUN
!EOD
```

Table A1

Sample of 9-Track Tape Printout from Station 7 Showing First Two Penetrations

```
JA = FORMAT CODE
33 = EXPECTED NO. OF 4 BIT CHARACTERS PER CASSETTE RECORD
60 = USUAL NO. OF CASSETTE RECORDS PER TAPE RECORD
13 = NO. OF 16 BIT WORDS PER CASSETTE RECORD
AII 97-2 STATION 7 POG9 4
TAPE 106A
RO=5000 OHMS.
```

1	5	114	825	2049	2049	2049	2049	2049	2049	2049	2049	2049	3293	2468
2	6	39	809	2049	2049	2049	2049	2049	2049	2049	2049	2049	3325	2516
3	7	109	848	2049	2049	2049	2049	2049	2049	2049	2049	2049	3359	2511
4	8	233	871	2049	2049	2049	2049	2049	2049	2049	2049	2049	3358	2487
5	9	235	871	2049	2049	2049	2049	2049	2049	2049	2049	2049	3358	2487
6	10	439	870	2049	2049	2049	2049	2049	2049	2049	2049	2049	3360	2490
7	11	631	872	2049	2049	2049	2049	2049	2049	2049	2049	2049	3361	2459
8	12	1006	874	2049	2049	2049	2049	2049	2049	2049	2049	2049	3361	2487
9	13	1397	874	2049	2049	2049	2049	2049	2049	2049	2049	2049	3360	2486
10	14	1800	872	2049	2049	2049	2049	2049	2049	2049	2049	2049	3360	2488
11	15	2204	871	2049	2049	2049	2049	2049	2049	2049	2049	2049	3362	2491
12	16	2613	873	2049	2049	2049	2049	2049	2049	2049	2049	2049	3359	2486
13	17	3014	872	2049	2049	2049	2049	2049	2049	2049	2049	2049	3360	2488
14	18	3394	870	2049	2049	2049	2049	2049	2049	2049	2049	2049	3360	2490
15	19	3798	869	2049	2049	2049	2049	2049	2049	2049	2049	2049	3359	2490
16	20	97	869	2049	2049	2049	2049	2049	2049	2049	2049	2049	3359	2490
17	21	492	868	2049	2049	2049	2049	2049	2049	2049	2049	2049	3359	2491
18	22	904	867	2049	2049	2049	2049	2049	2049	2049	2049	2049	3357	2490
19	23	1318	866	2049	2049	2049	2049	2049	2049	2049	2049	2049	3358	2492
20	24	1726	867	2049	2049	1126	1954	2049	1489	240	1062	1168	3358	2491
21	25	2124	868	3398	3161	1517	2358	2600	1903	537	1434	1693	3357	2459
22	26	2524	866	231	4046	2431	3294	3569	2854	1652	2304	2042	3358	2492
23	27	2926	864	3715	3372	1753	2665	3005	2247	983	1820	2010	3355	2491
24	28	3331	863	3541	3356	1853	2735	3212	2385	1123	1903	2160	3355	2492
25	29	3736	865	3791	3453	1856	2624	2815	2033	857	1604	1954	3355	2490
26	30	38	864	330	286	3415	4035	95	3320	1991	2737	2719	3354	2490
27	31	417	863	550	395	3664	334	1130	596	3733	312	1139	3356	2493
28	32	410	861	746	777	87	636	1246	731	35	659	1497	3354	2493
29	33	400	862	833	918	279	889	1709	1107	138	854	1710	3354	2492
30	34	362	861	1458	1434	432	1086	2042	1507	820	1395	1905	3353	2492
31	35	329	862	1529	1533	844	1549	2330	1518	855	1577	2426	3354	2492
32	36	318	863	1845	1955	1322	1870	2611	2335	1259	1724	2440	3356	2493
33	37	288	864	2502	2521	1706	2359	2960	2514	1827	2549	3230	3354	2490
34	38	268	864	2594	2672	1811	2581	3321	2508	1828	2569	3407	3357	2493
35	39	262	861	2625	2750	2091	2648	3420	2813	1829	2574	3406	3355	2494
36	40	248	864	2851	2891	1942	2589	3406	2820	2094	2631	3418	3355	2491
37	41	246	863	2876	2877	1851	2576	3437	2634	1868	2583	3418	3355	2492
38	42	267	865	2572	2577	1836	2583	3330	2528	1850	2496	3134	3358	2493
39	43	286	864	2531	2535	1636	2326	2821	2529	1687	2257	2573	3357	2493
40	44	306	865	2332	2290	965	1653	2455	2104	957	1515	2441	3356	2491
41	45	326	864	1574	1576	861	1561	2310	1550	839	1514	2323	3355	2491
42	46	337	864	1538	1544	843	1494	2072	1543	797	1433	1985	3358	2494
43	47	333	864	1536	1529	613	1177	1932	1527	803	1336	1977	3356	2492
44	48	349	865	1518	1528	737	1305	1816	1406	510	1137	1980	3357	2492
45	49	352	864	1477	1520	713	1204	1810	1535	557	1172	1761	3359	2495
46	50	337	865	1534	1534	840	1380	1822	1532	559	1540	2163	3359	2494
47	51	322	867	1557	1576	871	1585	2435	1645	870	1588	2434	3358	2491
48	52	302	867	1834	2004	1267	1757	2475	2298	1510	1919	2546	3359	2492
49	53	263	866	2574	2574	1900	2542	3360	2592	1887	2637	3495	3358	2492
50	54	222	868	2831	2892	2083	2707	3532	2921	2239	2930	3738	3358	2490
51	55	193	866	3118	3171	2529	3185	4046	3301	2498	3234	4081	3359	2493
52	56	143	868	3873	3991	3241	3788	507	128	3506	4036	735	3360	2492
53	57	73	867	253	258	3655	298	1146	210	3589	300	1146	3360	2493
54	58	22	868	316	350	3749	358	1194	441	3898	450	1254	3361	2493
55	59	4055	868	559	619	4093	687	1672	809	203	912	1698	3361	2493
56	60	3982	869	930	947	317	1036	1903	1225	557	1209	2048	3362	2493
57	61	3898	870	1625	1682	902	1641	2457	1945	1253	1958	2838	3363	2493
58	62	3824	869	2220	2459	1805	2265	3049	2801	2121	2776	3672	3361	2492
59	63	3736	870	3340	3417	2742	3444	201	3524	2876	3581	298	3361	2491
60	64	3639	871	545	666	4075	520	1304	910	260	924	1789	3362	2491
61	65	3546	871	1540	1689	1023	1647	2523	1872	1150	1901	2729	3362	2491
62	66	3455	872	2392	2460	1746	2369	3170	2553	1882	2574	3330	3363	2491
63	67	3355	871	3359	3397	2536	3378	127	3643	2951	3684	406	3363	2492
64	68	3276	873	71	193	3437	77	878	551	3963	550	1427	3363	2490
65	69	3192	874	1291	1343	593	1310	2172	1598	851	1578	2351	3364	2490
66	70	3117	874	2036	2165	1404	2137	2973	2246	145.	2257	3052	3365	2491
67	71	3043	874	2542	2562	1736	2569	3358	2645	1834	2666	3433	3365	2491
68	72	2979	873	2839	2899	2035	2848	3616	2930	2130	2952	3679	3364	2491
69	73	2942	877	3145	3205	2304	3065	3810	3308	2334	3088	3817	3363	2458
70	74	2927	876	3408	3426	2592	3219	3832	3445	2565	3188	3840	3366	2490

Table A1 (cont.)

71	75	2925	874	3444	3464	2453	3103	3806	3419	2327	3067	3793	3365	2491
72	76	2941	876	3278	3293	2276	3027	3778	3263	2186	3001	3715	3366	2490
73	77	2965	876	2978	2978	2111	2566	3529	2923	2050	2833	3517	3366	2490
74	78	3003	876	2792	2764	1878	2619	3257	2662	1540	2595	3252	3367	2491
75	79	3047	878	2457	2445	1563	2361	3037	2343	1519	2335	3074	3367	2489
76	80	3105	877	2242	2217	1112	1810	2476	1932	822	1601	2181	3367	2490
77	81	3167	875	1415	1312	357	1146	1736	1172	202	881	1453	3367	2492
78	82	3245	877	613	434	3333	22	581	41	3069	3877	405	3365	2491
79	83	3331	879	3672	3664	2536	3292	3912	3260	2352	3125	3659	3367	2488
80	84	3403	876	2700	2631	1757	2460	3104	2460	1573	2290	3064	3368	2492
81	85	3444	879	2314	2331	1558	2253	2825	2249	1451	2178	2989	3365	2489
82	86	3450	876	2225	2247	1472	2133	2698	2209	1265	2011	2661	3366	2490
83	87	3477	876	1813	1760	707	1459	2035	1261	4043	566	599	3366	2490
84	88	3757	877	2138	1840	874	1655	2086	1198	72	761	1402	3366	2489
85	89	103	876	3764	3288	2085	2469	2505	1660	263	797	868	3367	2491
86	90	548	877	2336	2207	1266	1915	2516	1598	670	1438	2098	3366	2489
87	91	1013	876	115	31	3276	3958	482	3646	2744	3397	4045	3365	2490
88	92	1458	876	2323	2126	1292	1939	2514	1592	859	1520	2150	3366	2490
89	93	1904	875	837	779	4026	526	1063	158	3369	3972	434	3365	2490
90	94	2367	876	2776	2601	1657	2363	3062	2101	1278	1894	2424	3366	2490
91	95	2818	874	701	567	3872	427	1120	180	3534	70	860	3365	2491
92	96	3272	874	3347	3240	2334	3019	3707	2758	1990	2606	3270	3365	2491
93	97	3717	874	1856	1759	1033	1695	2487	1500	762	1373	2110	3364	2490
94	98	66	876	614	567	4003	518	1352	367	3819	333	1196	3365	2489
95	99	527	874	3946	3893	3170	3787	554	3638	3014	3518	405	3364	2490
96	100	979	873	3215	3200	2695	3202	4046	3035	2420	2983	3755	3364	2491
97	101	1415	874	2558	2531	1971	2531	3366	2370	1774	2356	3248	3365	2491
98	102	1862	874	2012	1981	1437	2053	3089	2041	1511	2091	3014	3363	2489
99	103	2289	874	1922	1879	1306	1867	2720	1713	1113	1655	2433	3364	2490
100	104	2712	874	1435	1370	802	1382	2240	1237	672	1251	2113	3364	2490
101	105	3169	874	876	805	215	734	1550	518	4092	560	1442	3365	2491
102	106	3599	874	282	283	3838	281	1161	128	3663	133	1016	3363	2489
103	107	4030	872	3833	3793	3277	3821	610	3686	3132	3679	489	3365	2493
104	108	363	874	3494	3441	2903	3467	307	3368	2812	3355	159	3365	2491
105	109	797	874	3073	3037	2515	3065	3994	2962	2479	3022	3937	3365	2491
106	110	1230	875	2833	2813	2264	2812	3736	2701	2198	2720	3619	3365	2490
107	111	1658	875	2375	2345	1854	2387	3308	2264	1748	2293	3208	3365	2490
108	112	2099	875	2084	2059	1543	2085	2987	1940	1412	1956	2897	3366	2491
109	113	2532	874	1659	1628	1120	1650	2541	1493	995	1535	2557	3366	2492
110	114	2950	876	1557	1563	1083	1600	2508	1470	918	1451	2363	3366	2490
111	115	3371	874	1169	1139	626	1152	2082	1038	572	1102	2053	3366	2492
112	116	3803	876	874	857	347	870	1781	733	257	790	1736	3368	2492
113	117	117	875	595	590	143	651	1604	562	58	572	1462	3365	2490
114	118	539	876	374	370	3985	410	1375	317	3951	363	1294	3365	2489
115	119	963	874	146	129	3740	154	1092	41	3633	65	1019	3366	2492
116	120	1371	876	3966	3964	3502	4018	873	3918	3443	3964	807	3367	2491
117	121	1782	876	3711	3703	3208	3720	557	3595	3120	3641	496	3367	2491
118	122	2201	876	3423	3424	2948	3441	285	3323	2853	3362	202	3369	2493
119	123	2598	875	3169	3167	2710	3214	70	3108	2636	3151	20	3368	2493
120	124	3004	878	3011	3004	2556	3063	4020	2967	2514	3014	3954	3369	2491
121	125	3416	876	2830	2823	2341	2845	3806	2743	2285	2784	3739	3368	2492
122	126	3819	879	2581	2571	2100	2607	3570	2505	2050	2554	3510	3369	2490
123	127	132	877	2392	2378	1911	2405	3344	2281	1817	2322	3291	3368	2491
124	128	541	878	2160	2154	1656	2183	3152	2075	1650	2149	3110	3370	2492
125	129	952	877	1951	1956	1507	1995	2940	1876	1418	1913	2862	3369	2492
126	130	1342	879	1720	1715	1245	1747	2715	1651	1220	1714	2663	3369	2490
127	131	1759	879	1478	1464	1004	1500	2457	1391	941	1439	2415	3369	2490
128	132	2161	880	1302	1299	804	1359	2328	1258	835	1322	2268	3371	2491
129	133	2551	878	1176	1180	752	1241	2218	1151	712	1197	2163	3370	2492
130	134	2944	879	1037	1023	576	1062	2032	967	528	1314	1991	3369	2490
131	135	3358	878	886	882	455	944	1930	858	422	900	1849	3370	2492
132	136	3748	879	692	689	248	736	1726	650	212	692	1665	3369	2490
133	137	46	881	567	549	82	557	1537	467	32	517	1498	3369	2488
134	138	447	879	370	393	4059	445	1427	351	4005	398	1381	3370	2491
135	139	837	879	243	223	3863	257	1234	162	3829	218	1196	3371	2492
136	140	1226	879	45	41	3706	59	1070	0	3666	51	1029	3371	2492
137	141	1605	880	3987	3974	3537	4021	883	3902	3488	3968	866	3371	2491
138	142	2013	883	3794	3781	3349	3828	704	3720	3294	3771	659	3371	2488
139	143	2398	881	3631	3637	3221	3697	604	3620	3211	3683	569	3372	2491
140	144	2794	882	3552	3552	3127	3605	489	3504	3049	3548	443	3371	2489
141	145	3194	881	3414	3413	3002	3476	375	3392	2984	3454	352	3371	2490
142	146	3591	881	3314	3317	2849	3362	260	3275	2876	3348	254	3372	2491
143	147	3987	882	3234	3231	2820	3258	191	3206	2738	3263	160	3371	2489
144	148	295	882	3120	3118	2701	3170	59	3072	2665	3140	29	3372	2490
145	149	691	882	2992	2997	2559	3056	4058	2972	2556	3029	4013	3373	2491
146	150	1080	882	2899	2895	2478	2945	3939	2861	2462	2925	3923	3372	2490
147	151	1478	882	2808	2808	2337	2868	3871	2744	2383	2858	3854	3372	2490

Table A1 (cont.)

148	152	1867	885	2755	2765	2364	2832	3844	2756	2357	2820	3822	3372	2487
149	153	2253	865	2710	2705	2305	2771	3776	2692	2296	2757	3751	3372	2487
150	154	2644	884	2650	2657	2254	2718	3719	2635	2239	2711	3712	3374	2490
151	155	3032	864	2601	2606	2206	2671	3644	2599	2200	2665	3669	3374	2490
152	156	3409	863	2572	2574	2173	2637	3644	2561	2162	2629	3631	3372	2489
153	157	3769	863	2534	2540	2141	2606	3617	2533	2147	2609	3617	3374	2491
154	158	71	884	2517	2522	2121	2590	3596	2506	2117	2585	3593	3375	2491
155	159	429	884	2504	2504	2107	2572	3560	2494	2094	2562	3568	3375	2491
156	160	811	863	2473	2478	2092	2548	3553	2471	2075	2545	3552	3373	2490
157	161	1151	863	2458	2459	2064	2527	3540	2454	2057	2526	3526	3374	2491
158	162	1538	885	2439	2439	2046	2508	3518	2430	2039	2507	3516	3374	2489
159	163	1939	886	2410	2419	2020	2458	3438	2403	2002	2472	3479	3374	2488
160	164	2334	865	2379	2387	1932	2455	3462	2374	1980	2445	3454	3375	2490
161	165	2719	865	2363	2373	1968	2435	3451	2361	1975	2443	3450	3374	2489
162	166	3097	865	2348	2359	1963	2424	3431	2349	1955	2422	3425	3375	2490
163	167	3496	884	2330	2334	1937	2400	3398	2316	1917	2352	3385	3377	2493
164	168	3886	885	2276	2285	1845	2343	3347	2262	1870	2334	3343	3375	2490
165	169	181	886	2255	2261	1853	2321	3326	2240	1545	2306	3305	3378	2492
166	170	564	884	2221	2222	1823	2289	3301	2213	1823	2291	3292	3376	2492
167	171	949	885	2187	2194	1795	2244	3237	2151	1758	2224	3233	3377	2492
168	172	1340	887	2117	2114	1633	2157	3158	2059	1681	2143	3158	3375	2488
169	173	1698	886	2043	2033	1634	2089	3058	2004	1610	2072	3061	3375	2489
170	174	2085	885	1997	1989	1588	2051	3062	1972	1579	2036	3039	3375	2490
171	175	2470	885	1919	1920	1507	1962	2943	1860	1462	1928	2927	3375	2490
172	176	2827	887	1824	1828	1426	1885	2859	1803	1417	1875	2879	3375	2488
173	177	3205	886	1761	1759	1365	1828	2842	1750	1345	1808	2803	3375	2489
174	178	3589	886	1669	1668	1266	1727	2718	1631	1235	1696	2700	3375	2489
175	179	3975	887	1506	1480	1065	1524	2514	1426	1025	1491	2497	3374	2487
176	180	273	887	1331	1331	986	1447	2448	1359	961	1421	2422	3373	2486
177	181	650	884	1296	1305	905	1367	2331	1290	901	1363	2379	3374	2490
178	182	1047	885	1279	1282	872	1334	2331	1244	854	1320	2331	3373	2488
179	183	1430	883	1249	1250	862	1319	2336	1244	853	1314	2328	3373	2490
180	184	1819	883	1244	1255	860	1324	2342	1248	861	1327	2342	3375	2492
181	185	2200	884	1246	1242	843	1312	2332	1240	851	1320	2336	3372	2488
182	186	2579	885	1250	1264	1220	2011	3444	1257	1079	1378	3263	3373	2488
183	187	2614	885	1260	1266	938	1771	3135	1259	947	1756	3120	3372	2487
184	188	2620	883	1259	1264	971	1733	3092	1260	945	1729	3084	3375	2492
185	189	2619	883	1262	1265	957	1722	3072	1261	958	1720	3067	3373	2490
186	190	2620	883	1258	1266	949	1712	3061	1258	950	1712	3059	3372	2489
187	191	2625	883	1261	1267	947	1706	3050	1258	946	1708	3055	3373	2490
188	192	2623	882	1259	1264	945	1705	3055	1257	943	1705	3057	3373	2491
189	193	2622	883	1263	1270	944	1708	3054	1264	943	1705	3053	3372	2489
190	194	2628	882	1267	1272	941	1702	3054	1269	943	1704	3055	3372	2490
191	195	2623	883	1272	1279	942	1702	3056	1275	941	1704	3058	3372	2489
192	196	2625	884	1274	1281	942	1701	3057	1283	946	1704	3056	3376	2492
193	197	2628	884	1269	1275	942	1704	3057	1281	947	1704	3056	3374	2490
194	198	2627	883	1290	1297	944	1703	3057	1296	944	1704	3056	3374	2491
195	199	2627	884	1298	1306	945	1702	3057	1296	945	1707	3057	3375	2491
196	200	2629	884	1301	1308	946	1704	3059	1302	945	1708	3055	3375	2491
197	201	2627	886	1296	1301	943	1704	3054	1294	946	1704	3057	3373	2487
198	202	2628	886	1302	1312	943	1703	3057	1304	943	1705	3056	3374	2488
199	203	2629	884	1316	1322	946	1705	3055	1304	943	1706	3058	3375	2491
200	204	2630	885	1302	1310	944	1704	3059	1303	951	1706	3059	3375	2490
201	205	2633	885	1272	1251	1102	2364	3735	1273	847	1634	2360	3374	2489
202	206	2590	883	1249	1271	850	1334	2344	1259	848	1326	2337	3373	2490
203	207	2457	885	1246	1253	840	1313	2329	1245	856	1324	2341	3376	2491
204	208	2048	884	1249	1254	849	1323	2336	1244	842	1316	2327	3374	2490
205	209	1598	885	1238	1248	846	1316	2328	1237	840	1311	2325	3376	2491
206	210	1217	884	1243	1249	847	1317	2329	1246	853	1318	2332	3375	2491
207	211	1217	886	1247	1255	849	1316	2332	1247	846	1318	2329	3375	2489
208	212	1208	886	1246	1258	852	1318	2332	1248	849	1320	2335	3376	2490
209	213	1198	887	1252	1261	853	1323	2336	1254	854	1320	2335	3374	2487
210	214	1169	887	1257	1262	852	1319	2334	1256	859	1325	2334	3375	2488
211	215	1163	887	1262	1265	859	1324	2341	1260	860	1333	2340	3374	2487
212	216	1159	887	1260	1267	862	1329	2345	1262	863	1335	2340	3376	2489
213	217	1167	885	1261	1270	868	1336	2347	1262	864	1337	2346	3377	2492
214	218	1148	886	1265	1270	862	1336	2350	1271	867	1337	2349	3376	2490
215	219	1144	888	1269	1278	870	1337	2350	1270	866	1336	2352	3374	2486
216	220	1147	887	1264	1275	870	1335	2351	1267	868	1338	2350	3376	2489
217	221	1136	887	1267	1273	868	1338	2349	1269	867	1337	2348	3377	2490
218	222	1119	888	1266	1274	867	1334	2351	1266	865	1337	2348	3376	2488
219	223	1275	889	1249	1252	843	1318	2328	1241	851	1322	2330	3376	2487
220	224	1741	889	1243	1251	846	1321	2339	1252	859	1333	2344	3377	2488
221	225	2193	888	1242	1269	865	1332	2331	1244	849	1322	2338	3376	2488
222	226	2658	889	1251	1268	1001	1757	3126	1262	951	1715	3066	3376	2487
223	227	2671	888	1259	1265	926	1679	3027	1260	975	1676	3024	3377	2489
224	228	2673	887	1242	1267	919	1670	3016	1260	916	1670	3014	3379	2492

Table A1 (cont.)

Time	Time	Pressure	Z	T_w	T_w	T_2	T_3	T_4	T_w	T_2	T_2	T_3	F	Δ
225	229	2675	869	1262	1268	916	1669	3009	1263	915	1670	3011	3377	2488
226	230	2677	869	1266	1267	919	1667	3012	1264	917	1668	3010	3378	2489
227	231	2675	869	1264	1270	917	1669	3006	1264	919	1667	3008	3378	2489
228	232	2676	889	1264	1269	918	1667	3010	1265	920	1668	3007	3377	2488
229	233	2674	869	1268	1274	921	1669	3006	1267	918	1669	3008	3377	2488
230	234	2675	888	1266	1274	921	1668	3010	1266	921	1670	3008	3376	2488
231	235	2673	888	1267	1273	919	1666	3011	1266	917	1671	3009	3378	2490
232	236	2674	888	1267	1268	919	1670	3011	1266	918	1674	3009	3379	2491
233	237	2675	867	1264	1275	917	1670	3012	1269	921	1672	3008	3378	2491
234	238	2675	889	1266	1271	920	1670	3009	1262	917	1675	3009	3376	2487
235	239	2675	869	1265	1272	917	1670	3012	1266	918	1681	3014	3378	2489
236	240	2678	887	1275	1285	931	1728	3306	1270	940	1822	2960	3377	2490
237	241	2672	890	1260	1269	855	1343	2351	1259	854	1337	2346	3377	2487
238	242	2574	889	1251	1262	846	1322	2338	1249	847	1322	2337	3377	2488
239	243	2468	887	1240	1247	838	1315	2330	1241	836	1312	2329	3377	2490
240	244	2369	887	1240	1247	839	1311	2327	1239	841	1313	2330	3375	2488
241	245	2268	868	1259	1263	855	1327	2347	1263	858	1331	2348	3379	2491
242	246	2149	868	1258	1263	853	1334	2345	1253	854	1331	2341	3376	2488
243	247	2051	869	1252	1259	853	1325	2341	1256	849	1333	2338	3376	2487
244	248	1952	890	1249	1256	844	1322	2331	1246	847	1321	2336	3377	2487
245	249	1837	889	1239	1245	835	1311	2324	1234	833	1308	2322	3375	2486
246	250	1625	889	1225	1233	831	1303	2327	1232	829	1306	2316	3376	2487
247	251	1395	868	1231	1236	825	1305	2317	1227	827	1301	2316	3377	2489
248	252	1359	868	1229	1236	825	1303	2315	1228	826	1301	2315	3376	2488
249	253	1382	868	1228	1237	827	1297	2314	1231	827	1302	2315	3377	2489
250	254	1382	888	1239	1246	826	1301	2315	1240	827	1307	2314	3377	2489
251	255	1380	869	1230	1235	825	1300	2316	1231	827	1298	2310	337.	2487
252	256	1373	887	1232	1238	825	1305	2311	1232	827	1305	2317	3375	2488
253	257	1403	888	1232	1241	827	1307	2312	1227	815	1300	2312	3379	2491
254	258	1805	888	1240	1248	836	1315	2334	1252	852	1332	2336	3376	2488
255	259	2206	888	1255	1267	858	1335	2342	1255	838	1322	2334	3377	2489
256	260	2596	867	1255	1270	1216	2002	3516	1261	1028	1808	3160	3377	2490
⋮	⋮	⋮	⋮	⋮	⋮	⋮	⋮	⋮	⋮	⋮	⋮	⋮	⋮	⋮
857	861	287	913	2049	2049	2049	2049	2049	2049	2049	2049	2049	3394	2481
858	862	287	911	2049	2049	2049	2049	2049	2049	2049	2049	2049	3393	2482
859	863	286	912	2049	2049	2049	2049	2049	2049	2049	2049	2049	3395	2483
860	864	285	910	2049	2049	2049	2049	2049	2049	2049	2049	2049	3394	2484
861	865	285	910	2049	2049	2049	2049	2049	2049	2049	2049	2049	3393	2483
862	866	286	910	2049	2049	2049	2049	2049	2049	2049	2049	2049	3390	2480
863	867	282	910	2049	2049	2049	2049	2049	2049	2049	2049	2049	3391	2481
864	868	285	909	2049	2049	2049	2049	2049	2049	2049	2049	2049	3391	2482
865	869	287	910	2049	2049	2049	2049	2049	2049	2049	2049	2049	3391	2481
866	870	292	909	2049	2049	2049	2049	2049	2049	2049	2049	2049	3390	2481
867	871	290	909	2049	2049	2049	2049	2049	2049	2049	2049	2049	3391	2482
868	872	287	909	2049	2049	2049	2049	2049	2049	0	2049	0	3391	2482
869	873	290	909	0	0	0	0	0	0	0	0	0	3390	2481
870	874	290	910	0	0	0	0	0	0	0	0	0	3389	2479
871	875	287	906	0	0	0	0	0	0	0	0	0	3389	2483
872	876	286	905	0	0	0	0	0	0	0	0	0	3386	2481
873	877	285	904	0	0	0	0	0	0	0	0	0	3388	2484
874	878	285	903	0	0	0	0	0	0	0	0	0	3389	2486
875	879	290	906	0	0	0	0	0	0	0	0	0	3389	2483
876	880	290	905	0	0	0	0	0	0	0	0	0	3388	2483

FILE NUMBER 6 CONTAINS 9 OUTPUT RECORDS
LENGTH ERRORS=1 CARP ERRORS=0

APPENDIX B

Step 2 - Segmentation of the Digital Data

At this stage, it becomes convenient to segment the 9-track tape for clarity and less expensive disk storage. Typically, the probe was held near the bottom for several cycles both before penetration and after pullout for calibration purposes. For each thermal gradient measurement, we attempted to choose an interval that included these holding periods. For ease in later graphic presentation, we limited the length of each interval to a maximum of 76 cycles or 35.5 minutes. A program entitled GETPEN was written that reads from cards the desired start and end counts for any chosen interval. These intervals are then labelled and sequentially written onto a disk file (named AIIDATA). A listing of program GETPEN and the job control statements necessary to run the program are given below.

The contents of the disk file can easily be output to a line printer using the sequence of job control statements given in Figure B1. A sample of this output consisting of the first chosen interval (penetration 1) for station 7 is given in table B1. We chose a start time count (second column) of 181 and an end time count of 214 in order to include both holding periods. Note that for this station, a change of one count in the pressure column corresponds to a change in depth of about 11 centimeters. Since this is a pogo probe station utilizing one water thermistor and only three sediment thermistors, the water thermistor's temperature is recorded three times and the sediment thermistors' temperatures are recorded twice every 28 second cycle. Penetration occurs during the indicated cycle. Note the sharp jump in the count readings (recall that the counts are approximately linearly proportional to temperature) due to the frictional heating of the sediment thermistors and higher sediment temperatures. It can be seen that the pressure and water temperature remain roughly constant throughout the entire measurement while the temperatures recorded in the sediment column decay from initial values associated with a frictional heating of penetration to constant values that are representative of the sediment temperature at the depth of sampling. Pullout, as indicated in table B1 is characterized by more frictional heating of the sediment thermistors followed by an immediate return to the pre-penetration water temperature.

```
      INTEGER IN(14,1700),SREC
      OUTPUT'PROGRAM GETPEN VERSION 1,JAN.16.79'
      LIN:1
      OUT:2
 1000 FORMAT(10G)
      READ(105,1000)NFIL
      DO 400 KG=1,NFIL
      OUTPUT'NOW READING TAPE GEJB FILE#',KG
      READ(105,1000)SREC,NREC,NPEN
      IF(SREC.LE.0.) GO TO 93
      DO 93 I=1,SREC
      CALL BUFFER IN(LIN,0,IN,1400,ISTAT,NTOT)
   93 CONTINUE
      DO 25 JODY=1,NREC
      CALL BUFFER IN(LIN,0,IN(1,1+100*(JODY-1)),1400,ISTAT,NTOT)
      IF(ISTAT.EQ.4)OUTPUT'READ ERROR',KG; GO TO 25
      IF(ISTAT.EQ.3)OUTPUT'END OF FILE',KG;GO TO 25
   25 CONTINUE
      KSTART=1
      KEND=NREC*100
      DO 40 KN=1,NPEN
      READ(105,1000)ISPEN,IEPEN
      OUTPUT'DHF START AND END COUNT',ISPEN,IEPEN
      DO 20 K=KSTART,KEND
      IF((IN(2,K).GE.ISPEN).AND.(IN(2,K).LE.IEPEN)) GO TO 30
   20 CONTINUE
      OUTPUT'DID NOT FIND FILE KG, PEN KN',KG,KN
      GO TO 40
   30 INC:IEPEN-ISPEN
      WRITE(OUT,3000)KG,KN,ISPEN,IEPEN
      WRITE(OUT,2000)((IN(I,NK),I=1,14),NK=K,K+INC)
      KSTART=K+1
   40 CONTINUE
      DO 100 IKG=1,10
      CALL BUFFER IN(LIN,0,IN,1400,ISTAT,NTOT)
      IF(ISTAT.EQ.3) OUTPUT'END OF FILE KG',KG;GO TO 400
  100 CONTINUE
  400 CONTINUE
 2000 FORMAT(14I5)
 3000 FORMAT('AII-97-2 HEAT FLOW TAPE GEJB FILE',I3,
     $'  PENETRATION',I3,' START',I5,' END',I5)
      END
```

Figure Bl

Job Control Statements Necessary to Run GETPEN

```
!JOB account,ID
!LIMIT (CORE,27),(TIME,3),(9T,1)
!MESSAGE TAPE GEJB ON 9T TAPE IN VAULT NORING
!ASSIGN F:1,(DEVICE,9T),(SN,GEJB)
!ASSIGN F:2,(FILE,AIIDATA),(OUT),(SAVE)
!RUN (LMN,LGET)

-program-

!EOD
```

Figure B2

Job Control Statements Necessary to Output Contents of AIIDATA to Line Printer

```
!JOB account,ID
!LIMIT (ORDER)
!LIMIT (CORE,5),(TIME,1)
!PCL
  COPY DP/AIIDATA TO LP
!EOD
```

AII-97-2 HEAT FLOW TAPE GEJB FILE 6 PENETRATION 1 START 181 END 214

177	181	650	884	1296	1305	905	1367	2381	1290	901	1363	2379	3374	
178	182	1047	885	1279	1282	872	1334	2331	1244	854	1320	2331	3373	
179	183	1430	883	1249	1250	862	1319	2336	1244	853	1314	2328	3373	hold
180	184	1819	883	1244	1255	860	1324	2342	1248	861	1327	2342	3375	
181	185	2200	884	1246	1242	843	1312	2332	1240	851	1320	2335	3372	
182	186	2579	885	1260	1264	1220	2011	3444	1257	1079	1878	3263	3373	
183	187	2619	885	1260	1266	998	1771	3138	1259	987	1756	3120	3372	pen.
184	188	2620	883	1259	1264	971	1733	3092	1260	965	1729	3084	3375	
185	189	2619	883	1262	1265	957	1722	3072	1261	958	1720	3067	3373	
186	190	2620	883	1258	1266	949	1712	3061	1258	950	1712	3059	3372	
187	191	2625	883	1261	1267	947	1706	3060	1258	946	1708	3055	3373	
188	192	2623	882	1259	1264	945	1705	3058	1257	943	1705	3057	3373	
189	193	2622	883	1263	1270	944	1708	3054	1264	943	1705	3053	3372	
190	194	2628	882	1267	1272	941	1702	3054	1269	943	1704	3055	3372	equilibrium
191	195	2623	883	1272	1279	942	1702	3056	1275	941	1704	3058	3372	
192	196	2625	884	1274	1281	942	1701	3057	1283	946	1704	3056	3376	
193	197	2628	884	1269	1275	942	1704	3057	1281	947	1704	3056	3374	
194	198	2627	883	1290	1297	944	1703	3057	1296	944	1704	3056	3374	
195	199	2627	884	1298	1306	945	1702	3057	1296	945	1707	3057	3375	
196	200	2629	884	1301	1308	946	1704	3059	1302	945	1708	3055	3375	
197	201	2627	886	1296	1301	943	1704	3054	1294	946	1704	3057	3373	
198	202	2623	886	1302	1312	943	1703	3057	1304	943	1705	3056	3374	
199	203	2625	884	1316	1322	946	1705	3055	1304	943	1706	3058	3375	
200	204	2630	885	1302	1310	944	1704	3059	1303	951	1706	3059	3375	
201	205	2633	885	1272	1281	1102	2364	3735	1273	867	1634	2380	3374	pullout
202	206	2590	883	1269	1271	850	1334	2344	1259	848	1326	2337	3373	
203	207	2457	885	1246	1253	840	1313	2329	1245	856	1324	2341	3376	
204	208	2048	884	1249	1254	849	1323	2336	1244	842	1316	2327	3374	
205	209	1598	885	1238	1248	846	1316	2328	1237	840	1311	2325	3376	
206	210	1217	884	1243	1249	847	1317	2329	1246	853	1318	2332	3375	
207	211	1217	886	1247	1255	849	1316	2332	1247	846	1318	2329	3375	
208	212	1208	886	1246	1258	852	1318	2332	1248	849	1320	2335	3376	hold
209	213	1198	887	1252	1261	853	1323	2336	1254	854	1320	2335	3374	
210	214	1169	887	1257	1262	852	1319	2334	1256	859	1325	2334	3375	

Segmented Digital Data - Station 7 Penetration 1

Table B1

APPENDIX C

page

Step 3 - Plotting of the Digital Data

Plots were made of each interval contained in the disk file AIIDATA. The plotting program entitled TOWP, was designed to be run on a remote terminal - the only necessary input being the total number of desired plots (equal to the number of intervals in AIIDATA) and a logical input unit (LIN). TOWP, currently stored on cards, can be input to a disk file by utilizing the series of job control statements shown in figure Cla. TOWP can then be run from a terminal by following the sequence shown in figure Clb. Each plot will be stored as a separate output file on a disk named PLOT1. A section of the keyboard printout from TOWP is shown in Figure Clc. A complete listing of TOWP is given below.

Once the plot files are generated from TOWP, it remains to print them. Both Tektronix and Versatec plots were made initially for a few of the plot files. We decided that the added clarity and size obtainable through use of the Versatec plotter more than compensated for its slightly greater expense and inconvenience. To minimize waste in case of error, it is recommended that no more than five plots be made during one job. The job control statements necessary to use the Versatec plotter are given in Figure C2. The PLOTV statement is to be interpreted as follows: the first number is a scale factor and should always be set to 1.0, the second and third numbers are the start and end plot files. In the example chosen, plot files 1 through 5 are to be plotted. It is important that the word SAVE be used on line 4 because otherwise the entire PLOT1 file would be destroyed after only the first 5 plot files had been accessed.

Figure C3 is a typical example of a plot generated from AII DATA - again we have chosen the first penetration from station 7. The abscissa has units of cycles (28 seconds) and the ordinate has units of counts. Because of the nearly linear relationship between counts and both temperature and pressure, the plots serve as an excellent first order indicator of measurement quality. For example, pressure is seen to increase as the probe is lowered to the bottom and to rise abruptly to a constant value ($\pm$.7 meters) during penetration. Also refer to the discussion given of table B1.

We felt that it would not be possible to obtain substantial quantitative information from these plots. Hence, as an aid in representation, we have chosen to make the counts axis serve only as a relative indicator of the actual counts for each of the 14 variables. Furthermore, the counts shown for any given variable is unrelated to any of the other 13 variables.

```
      INTEGEP YIN(13,75),Y1TITLE(9),X1TITLE(9)
      DIMENSION IBUF(1000)
      OUTPUT' PPOGPAM TOWP JAN. 79','INPUT UNIT=?'
      READ(105,1000)LIN
      OUTPUT LIN,'NUMBEP OF PLOTS='
      READ(105,1000)NPLOT
      CALL PLOTS(IBUF,-1000)
      DO 100 KG=1,NPLOT
      CALL PLOT(1.,9.5,-3)
C EACH PLOT WILL BE A SEPARATE OUTPUT PLOT FILE
      YSCALE=682.6667
      XSCALE=8.0
      PEAD(LIN,2000)X1TITLE,Y1TITLE,NSTART,NSTOP
      WRITE(108,4000)X1TITLE,Y1TITLE
      NTOT=NSTOP-NSTART+1
      OUTPUT NTOT
      XLEN=NTOT/XSCALE
      READ(LIN,3000,END=10)((YIN(L,M),L=1,13),M=1,NTOT)
   10 CALL AXIS(0.,0.,Y1TITLE,36,12.,0.,0.,YSCALE)
      START=NSTART
      CALL AXIS(0.,0.,X1TITLE,-36,9.5,270.,START,XSCALE)
      DO 700 JC=1,13,2
      IPEN=3
      DO 800 KC=1,NTOT
      Y=YIN(JC,KC)/YSCALE +JC/2. -.5
      X=(KC-1)/XSCALE
      CALL PLOT(Y,-X,IPEN)
      IPEN=2
  800 CONTINUE
      IF(JC.LE.3 .OR. JC.GE.13)GO TO 805
      INTEQ=JC+108
      GO TO 825
  805 IF(JC.NE.1)GO TO 810
      INTEQ=99
      GO TO 825
  810 IF(JC.NE.3)GO TO 820
      INTEQ=105
      GO TO 825
  820 INTEQ=70
  825 YY=Y-.125
      XX=-X-.2
      CALL SYMBOL(YY,XX,.25,INTEQ,-90.,-1)
      IPEN=3
      IF (JC+1.GE.13) GO TO 700
      DO 900 KC=1,NTOT
      KB=NTOT-KC+1
      Y=YIN(JC+1,KB)/YSCALE +JC/2.
      X=XLEN - KC/XSCALE
      CALL PLOT(Y,-X,IPEN)
      IF(KC.NE.1)GO TO 850
      INTEQ=JC+109
      IF(JC.EQ.1)INTEQ=87
      YY=Y-.125
      XX=-X-.2
      CALL SYMBOL(YY,XX,.25,INTEQ,-90.,-1)
      CALL PLOT(Y,-X,IPEN)
  850 IPEN=2
  900 CONTINUE
  700 CONTINUE
      CALL PLOT(-1.,-9.5,-3)
      CALL PLOT(0.,0.,999)
  100 CONTINUE
      OUTPUT' IT IS FINISHED'
 1000 FORMAT(5G)
 2000 FORMAT(9A4,9A4,T59,I5,T68,I5)
 3000 FORMAT(5X,13I5)
 4000 FORMAT(1X,9A4)
 5000 FORMAT(9A4)
      END
```

Figure C1a

Job Control Statements Necessary to Transfer TOWP from Card Deck Storage to Disk Storage

```
!JOB account,ID
!LIMIT (CORE,5),(TIME,1)
!PCL
  COPY CR/TOWP TO DP

-program TOWP-

!EOD
```

Figure C1b

Job Control Statements Necessary to Run TOWP from a Terminal

```
!FORT4 TOWP OVER PTOWP
 EXT. FORTRAN IV, VERSION F01
OPTIONS >NS

!SET F:95/PLOT1;OUT

!SET F:1/[illegible]DATA;[illegible]

!LYNX RTOWP OVER LTOWP, PLOTDFER.8;.3
:P1 ASSOCIATED.
   * * ALLOCATION SUMMARY * *
PROTECTION        LOCATION    PAGES

DATA <00>           A000        7
PROCEDURE <01>      B000        3
DCB <10>            AE00        1

!START LTOWP
```

Figure C1c

Section of the Keyboard Printout from TOWP

```
 PROGRAM TOWP JAN. 79
·INPUT UNIT=?
?1
 LIN = 1
 NUMBER OF PLOTS=?46
 AII-97-2 HEAT FLOW TAPE GEJB FILE  2
   PENETRATION  7 START  771 END  810
 NTOT = 40
 AII-97-2 HEAT FLOW TAPE GEJB FILE  2
   PENETRATION  8 START 1340 END 1364
         .           .           .
         .           .           .
         .           .           .

AII-97-2 HEAT FLOW TAPE GEJB FILE  8
  PENETRATION  1 START  449 END  508
NTOT = 60
AII-97-2 HEAT FLOW TAPE GEJB FILE  9
  PENETRATION  1 START  229 END  272
NTOT = 44
 IT IS FINISHED
```

Figure C2

Job Control Statements Necessary to Use the Versatec Plotter

```
!JOB account,ID
!LIMIT (CORE,20),(TIME,2),(ACCOUNT)
!MESSAGE USES VERSATEC
!SET F:95/PLOT1;SAVE
!PLOTV 1.0,1,5
```

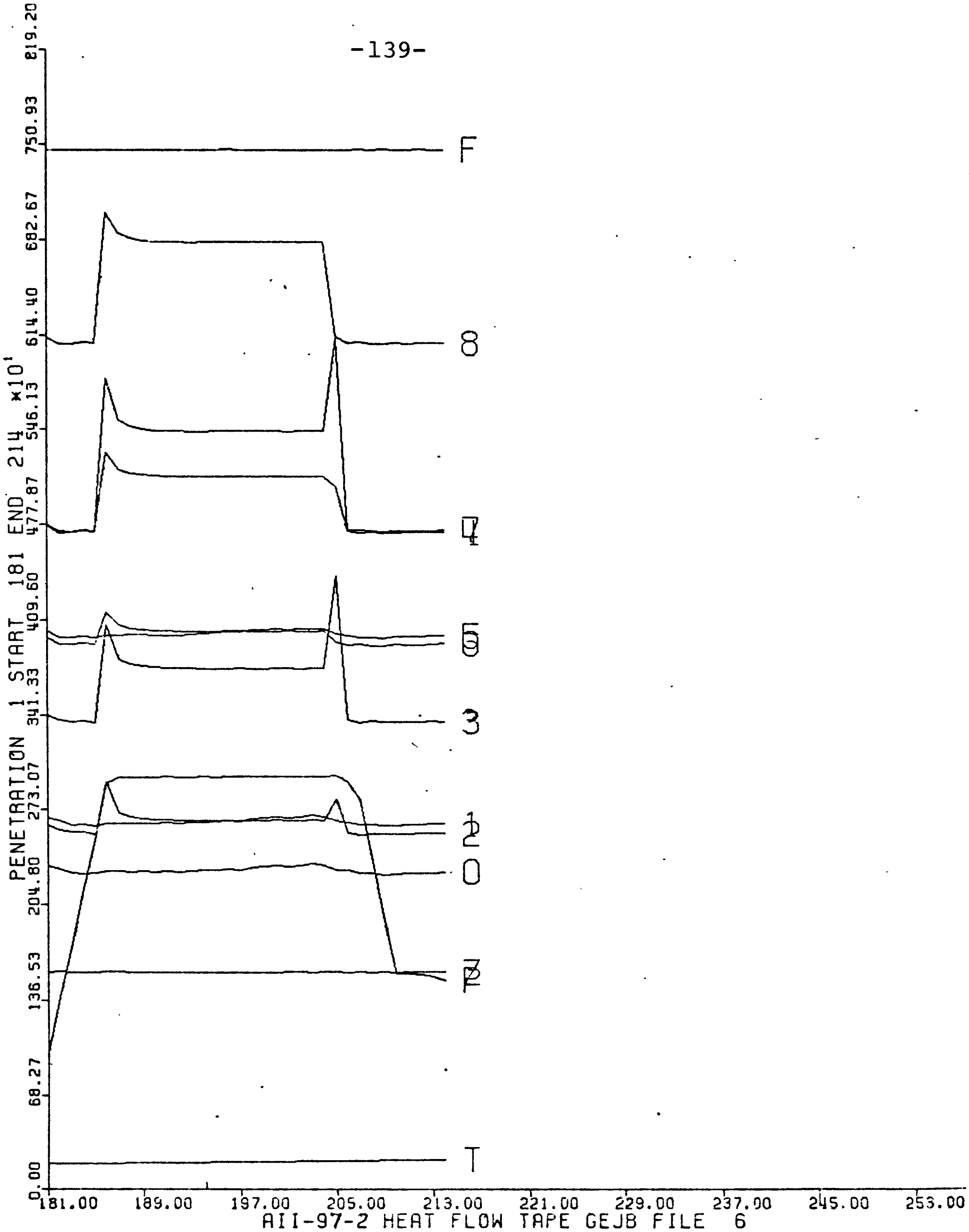

Plot Produced by TOWP - Station 7 Penetration 1

Figure C3

APPENDIX D

page

Step 4 - Conversion of Digital Thermistor Data to Temperature Data

A program was written entitled CONVERT that would convert the digital thermistor data located in file AIIDATA to actual temperature data using the equations given in the Instrumentation and Methods section. The program is designed to be run on a terminal; hence, it must first be stored as a disk file. The job control statements which accomplish this task are given in Figure Cla, with CONVERT replacing TOWP. As inputs, the program requires a logical input unit, a logical output unit, the total number of stations, the total number of thermistors used, the α, β and γ values for each thermistor and a value for R_O. Furthermore, for each station the program requires values for R_Z and R_F, the number of penetrations (1 for piston core stations), the specific thermistors used, and the multiplicative factor for the counts (F) corresponding to R_F. The multiplicative factor takes into account whether or not the F value has rolled over. For example, if Z is 900 and F is 3400 (computed delta would be 2500), the multiplicative factor would be 0. On the other hand, if Z is 2100 and F is 500 (computed delta would be -1600), the multiplicative factor would be 1. Then, all F values would automatically be increased by 4096 counts for use in the thermistor counts to resistance conversion equations. The real value of delta would be F (augmented) - Z = (500 + 4096) - 2100 or approximately 2500 counts. As can be seen, R_Z and R_F have a similar separation for both examples.

A test run of CONVERT is shown in Figure D1. For the purposes of a test run, the data from the second penetration of station 2 was copied from the AIIDATA file to a file named SAMPLE. The data from this penetration occupies lines 110 through 144 of AIIDATA. Figure D2 shows the procedure necessary to accomplish this task from a terminal. The last command returns AIIDATA to the unlined mode (not accessible for editing), which lessens the storage cost of this typically large file. Note that in Figure D1, when options are asked for, the user response was 'ADP, NS'. ADP specifies that CONVERT should be run in the double precision mode; a mode which allows for more accurate results in the conversion process. The job control statements further specify that the output of CONVERT should be stored on a file named TEMP.

A listing of program CONVERT is given below. In this more general case (with AIIDATA specified as the input file), the output of CONVERT was stored on a file named TEMPDATA. The contents of TEMPDATA can be dumped to the line printer in a similar manner as were the contents of AIIDATA. Table D1 gives the section of TEMPDATA corresponding to the part of AIIDATA shown in table B1 and Figure C3 and described earlier in the text. Note that CONVERT is not capable of dealing with cases in which the temperature counts rollover.

We decided that the contents of both TEMPDATA (thermistor readings given in degrees Centigrade) and AIIDATA (thermistor readings given in counts) were of enough future value to permanently save on a labelled 9-track magnetic tape. This was accomplished for the initial file AIIDATA by submitting the job control statements shown in Figure D3a. Once the tape, which we titled GEDG, was initially used, the sequence of job control statements shown in Figure D3b had to be submitted. On the labelled tape, the contents of each disk file was given the name of the file from which it was copied.

In retrospect, due to the small nonlinearity between thermistor temperatures and thermistor counts, it may have been better to have done the plotting with the contents of TEMPDATA. With only minor revisions in TOWP (the plotting program), this change in data processing could be made. We felt that because of the extra cost involved, replotting was not justified.

```
      DIMENSION DATA(14),THERM(3,25),NARRAY(9),KK(10),TITLE(18)
      OUTPUT 'PROGRAM CONVERT FEB. 79', INPUT UNIT=?'
      READ(105,1000)LIN
      OUTPUT LIN, NUMBER OF STATIONS=?'
      READ(105,1000)NSTAT
      OUTPUT NSTAT, OUTPUT UNIT=?'
      READ(105,1000)LOUT
      OUTPUT LOUT, NUMBER OF THERMISTORS USED=?'
      READ(105,1000)NTHERM
      OUTPUT 'I WILL ASSIGN THE THERMISTORS NUMBERS'
      OUTPUT 'YOU TYPE IN THE A, B & C CALIBRATION VALUES IN TH
AT ORDER'
      OUTPUT 'EXPONENTS OF -2, -3 & -6 ARE ASSUMED IN THE CALCU
LATIONS'
      OUTPUT 'INPUT ONLY THE FRACTIONAL PART OF THE CALIBRATION
 VALUE'
      OUTPUT 'SKIP A SPACE BETWEEN EACH OF THE THREE NUMBERS'
      DO 50 I=1,NTHERM
      OUTPUT 'THERMISTOR   NUMBER ',I,' CALIBRATION VALUES ARE?
'
      READ(105,1000) (THERM(J,I),J=1,3)
   50 CONTINUE
      DO 60 I=1,NTHERM
      WRITE(108,2000)I,(THERM(J,I),J=1,3)
   60 CONTINUE
      OUTPUT 'TO EDIT, INPUT THE ASSIGNED THERMISTOR NUMBER FOL
LOWED BY'
      OUTPUT 'THE THREE NEW CALIBRATION VALUES'
      OUTPUT 'SKIP A SPACE BETWEEN EACH OF THE NUMBERS'
    5 OUTPUT 'TYPE 1 TO EDIT, 0 TO CONTINUE'
      READ(105,1000)M
      IF(M.EQ.0)GO TO 30
      KG=0
   10 OUTPUT 'EDIT'
      KG=KG+1
      READ(105,1000)KK(KG),(THERM(K,KK(KG)),K=1,3)
      OUTPUT '1 OR 0?'
      READ(105,1000)M
      IF(M.EQ.1)GO TO 10
      OUTPUT 'YOUR NEW VALUES ARE:'
      DO 20 KB=1,KG
      WRITE(108,2000)KK(KB),(THERM(K,KK(KB)),K=1,3)
   20 CONTINUE
      GO TO 5
   30 OUTPUT 'THERMISTOR NUMBERS WILL BE ASKED FOR BEFORE STATI
ONS'
      OUTPUT 'WHEN ASKED, LIST IN ORDER THE EIGHT THERMISTORS U
SED'
      OUTPUT 'BEGIN WITH THE THERMISTOR RECORDING TWICE CONSECU
TIVELY'
      OUTPUT 'SKIP A SPACE BETWEEN EACH THERMISTOR NUMBER'
      OUTPUT 'ZERO CALIBRATION RESISTANCE=?'
      READ(105,1000)R0
      OUTPUT R0
      DO 700 I=1,NSTAT
      OUTPUT 'STATION ',I, 'NUMBER OF PENETRATIONS=?'
      READ(105,1000)NPENS
      OUTPUT 'ZERO SCALE RESISTANCE=?'
      READ(105,1000)RZERO
      OUTPUT 'FULL SCALE RESISTANCE=?'
      READ(105,1000)RFULL
      C=1./(1.+R0/RFULL)
      D=1./(1.+R0/RZERO)
      CD=C-D
      OUTPUT NPENS,RZERO,RFULL,C,D
      OUTPUT 'THERMISTORS USED?'
      READ(105,1000) (NARRAY(J),J=2,9)
      NARRAY(1)=NARRAY(2)
      DO 500 J=1,9
      JJ=J-1
      WRITE(108,2000)JJ,(THERM(K,NARRAY(J)),K=1,3)
  500 CONTINUE
      OUTPUT 'MULTIPLICATIVE FACTOR FOR FULL SCALE CALIBRATIONS
?'
      OUTPUT '0 IF FULL SCALE COUNTS O-K AS IS'
      READ(105,1000)IFACTOR
      DO 600 J=1,NPENS
      READ(LIN,4000)TITLE,NSTART,NSTOP
      WRITE(LOUT,5000)TITLE
      NTOT=NSTOP-NSTART+1
      WRITE(108,5000) ITLE
      OUTPUT NTOT
      DO 575 K=1,NTOT
      READ(LIN,6000) (DATA(L),L=1,14)
      FULL=DATA(14)+(4096*IFACTOR)
      A=(FULL-DATA(4))/CD
      B=((DATA(4)*C)-(FULL*D))/CD
      DO 550 L=5,13
      DATA(L)=R0/((A/(DATA(L)-B))-1.)
      Q=ALOG(DATA(L))
      N=NARRAY(L-4)
      X=THERM(1,N)*.01
      Y=THERM(2,N)*Q*.001
      Z=THERM(3,N)*Q*Q*Q*.000001
      DATA(L)=(1./(X+Y+Z))-273.15
  550 CONTINUE
      WRITE(LOUT,7000) (DATA(L),L=1,14)
  575 CONTINUE
  600 CONTINUE
  700 CONTINUE
 1000 FORMAT(10G)
 2000 FORMAT(I4,3(5X,F10.7))
 4000 FORMAT(18A4,T59,I5,T68,I5)
 5000 FORMAT(18A4)
 6000 FORMAT(14I5)
 7000 FORMAT(4I5,9F9.5,I5)
      END
```

```
!  FORT4 CONVERT OVEP RVERT
 EXT. FORTPAN IV, VERSION F01
OPTIONS :   ADP,NS

!SET F:1/SAMPLE;IN

!SET F:2/TEMP;OUT

!LYNX RVEPT OVEP LVERT
:P1 ASSOCIATED.
   * * ALLOCATION SUMMARY * *
PROTECTION        LOCATION    PAGES

DATA (00)           A000        3
PROCEDURE (01)      AA00        2
DCB (10)            A600        2

!START LVEPT
 PROGPAM CONVERT FEB. 79
 INPUT UNIT=?
?1
 LIN = 1
 NUMBER OF STATIONS=?
?1
 NSTAT = 1
 OUTPUT UNIT=?
?2
 LOUT = 2
 NUMBER OF THERMISTORS USED=?
?4
 I WILL ASSIGN THE THERMISTCRS NUMBERS
 YOU TYPE IN THE A, B & C CALIBRATION VALUES IN THAT ORDER
 EXPONENTS OF -2, -3 & -6 APE ASSUMED IN THE CALCULATIONS
 INPUT ONLY THE FRACTIONAL PART OF THE CALIBRATION VALUE
 SKIP A SPACE BETWEEN EACH OF THE THREE NUMBERS
 THERMISTOR    NUMBER
 I = 1
  CALIBRATION VALUES ARE?
?.1315576 .2622218 .1399615
 THERMISTOR    NUMBER
 I = 2
  CALIBRATION VALUES ARE?
?.1266464 .2686491 .1310889
 THERMISTOR    NUMBER
 I = 3
  CALIBRATION VALUES ARE?
?,\.1322545 .2610160 .1457364
 THERMISTOR    NUMBER
 I = 4
  CALIBRATION VALUES ARE?
?.1323985 .2611319 .1454189
    1       .1315576       .2622218       .1399615
    2       .1266464       .2686491       .1310889
    3       .1322545       .2610160       .1457364
    4       .1323985       .2611319       .1454189
 TO EDIT, INPUT THE ASSIGNED THERMISTOR NUMBER FOLLOWED BY
 THE THREE NEW CALIBPATION VALUES
 SKIP A SPACE BETWEEN EACH OF THE NUMBERS
 TYPE 1 TO EDIT, 0 TO CONTINUE
?0
 THERMISTOR NUMBERS WILL BE ASKED FOR BEFORE STATIONS
 WHEN ASKED, LIST IN OPDER THE EIGHT THERMISTORS USED
 BEGIN WITH THE THERMISTOP RECORDING TWICE CONSECUTIVELY
 SKIP A SPACE BETWEEN EACH THERMISTOR NUMBER
 ZERO CALIBRATION RESISTANCE=?
?20000
 R0 = 20000.0000000000
 STATION
 I = 1
 NUMBER OF PENETRATIONS=?
?1
 ZERO SCALE RESISTANCE=?
?4968.2
 FULL SCALE RESISTANCE=?
?4877.5
 NPENS = 1
 RZERO = 4968.20000000000
 RFULL = 4877.50000000000
 C = .196060697417345
 D = .198981103964243
 THERMISTORS USED?
?1 2 3 4 1 2 3 4
    0       .1315576       .2622218       .1399615
    1       .1315576       .2622218       .1399615
    2       .1266464       .2686491       .1310889
    3       .1322545       .2610160       .1457364
    4       .1323985       .2611319       .1454189
    5       .1315576       .2622218       .1399615
    6       .1266464       .2686491       .1310889
    7       .1322545       .2610160       .1457364
    8       .1323985       .2611319       .1454189
 MULTIPLICATIVE FACTOR FOR FULL SCALE CALIBRATIONS?
 0 IF FULL SCALE COUNTS 0-K AS IS
?0
AII-97-2 HEAT FLOW TAPE 6EJB FILE  2  PENETRATION  2 START  326 END  358
 NTOT = 33
 *STOP* 0
```

Test Run of CONVERT - Station 2 Penetration 2

Figure D1

Figure D2

Procedure Necessary to Copy Station 2 Penetration 2 from AIIDATA to SAMPLE

```
!COPY AIIDATA OVER AIIDATA(LN)
 -terminal responds-
!COPY AIIDATA(110-144) OVER SAMPLE
 -terminal responds-
!COPY AIIDATA OVER AIIDATA(NLN)
 -terminal responds-
```

Figure D3a

Job Control Statements Necessary to Store File AIIDATA on a Labelled 9-Track Magnetic Tape

```
!JOB account,ID
!LIMIT (CORE,5),(TIME,1),(9T,1)
!MESSAGE USES NEW TAPE GEDG ON 9T
!PCL
  COPY /AIIDATA.account TO LT#GEDG/AIIDATA
!EOD
```

Figure D3b

Job Control Statements Necessary to Store File TEMPDATA on a Labelled 9-Track Magnetic Tape

```
!JOB account,ID
!LIMIT (CORE,5),(TIME,1),(9T,1)
!MESSAGE USES GEDG ON 9T  **WRITE RING**
!PCL
  COPY /TEMPDATA.account TO LT#GEDG/TEMPDATA
!EOD
```

AII.97.2 HEAT FLOW TAPE GEJB FILE 6 PENETRATION 1 START 181 END 214

177	181	650	884	2.12765	2.12911	2.05513	2.11900	2.11526	2.12668	2.05447	2.11834	2.11494	3374	
178	182	1047	885	2.12478	2.12526	2.04953	2.11353	2.10713	2.11908	2.04637	2.11125	2.10713	3373	
179	183	1430	887	2.12017	2.12034	2.04822	2.11135	2.10808	2.11936	2.04674	2.11054	2.10677	3373	hold
180	184	1819	883	2.11931	2.12110	2.04789	2.11211	2.10887	2.11996	2.04806	2.11260	2.10887	3375	
181	185	2200	884	2.11957	2.11892	2.04492	2.11011	2.10745	2.11860	2.04624	2.11141	2.10811	3372	
182	186	2579	885	2.12169	2.12234	2.10694	2.22389	2.28958	2.12120	2.08367	2.20218	2.25984	3373	-pen.
183	187	2619	885	2.12171	2.12269	2.07031	2.18478	2.23946	2.12155	2.06850	2.18233	2.23650	3372	
184	188	2620	887	2.12175	2.12256	2.06616	2.17863	2.23150	2.12191	2.06517	2.17797	2.23019	3375	
185	189	2619	887	2.12229	2.12277	2.06386	2.17695	2.22852	2.12212	2.06403	2.17662	2.22770	3373	
186	190	2620	887	2.12166	2.12296	2.06255	2.17537	2.22686	2.12166	2.06271	2.17537	2.22653	3372	
187	191	2625	887	2.12212	2.12310	2.06222	2.17434	2.22655	2.12164	2.06205	2.17466	2.22573	3373	
188	192	2623	882	2.12194	2.12275	2.06205	2.17428	2.22624	2.12161	2.06172	2.17428	2.22608	3373	
189	193	2622	887	2.12247	2.12361	2.06173	2.17472	2.22571	2.12264	2.06156	2.17423	2.22554	3372	
190	194	2628	882	2.12326	2.12407	2.06139	2.17385	2.22573	2.12359	2.06172	2.17418	2.22589	3372	equilibrium
191	195	2623	887	2.12394	2.12508	2.06140	2.17374	2.22604	2.12443	2.06123	2.17407	2.22636	3372	
192	196	2625	884	2.12402	2.12516	2.06122	2.17325	2.22561	2.12549	2.06188	2.17374	2.22544	3376	
193	197	2628	884	2.12326	2.12424	2.06123	2.17365	2.22589	2.12521	2.06205	2.17385	2.22573	3374	
194	198	2627	887	2.12681	2.12795	2.06172	2.17380	2.22591	2.12779	2.06172	2.17396	2.22575	3374	
195	199	2627	884	2.12795	2.12925	2.06172	2.17347	2.22575	2.12762	2.06172	2.17428	2.22575	3375	
196	200	2629	884	2.12844	2.12957	2.06188	2.17380	2.22608	2.12860	2.06172	2.17445	2.22542	3375	
197	201	2627	886	2.12741	2.12822	2.06107	2.17368	2.22550	2.12708	2.06157	2.17368	2.22599	3373	
198	202	2628	886	2.12836	2.12998	2.06107	2.17347	2.22585	2.12868	2.06107	2.17379	2.22569	3374	
199	203	2629	884	2.13087	2.13185	2.06188	2.17396	2.22542	2.12892	2.06139	2.17412	2.22591	3375	
200	204	2630	885	2.12846	2.12976	2.06139	2.17369	2.22606	2.12863	2.06255	2.17401	2.22606	3375	
201	205	2633	885	2.12361	2.12508	2.08745	2.28150	2.33728	2.12377	2.04871	2.16233	2.11504	3374	-pullout
202	206	2590	887	2.12342	2.12375	2.04624	2.11379	2.10939	2.12180	2.04591	2.11249	2.10824	3373	
203	207	2457	885	2.11934	2.12047	2.04427	2.11002	2.10651	2.11918	2.04690	2.11181	2.10847	3376	
204	208	2048	884	2.12001	2.12082	2.04591	2.11184	2.10792	2.11920	2.04476	2.11070	2.10545	3374	
205	209	1598	885	2.11804	2.11966	2.04526	2.11051	2.10635	2.11788	2.04427	2.10970	2.10586	3376	
206	210	1217	884	2.11901	2.11999	2.04558	2.11084	2.10668	2.11950	2.04657	2.11100	2.10717	3375	
207	211	1217	886	2.11938	2.12069	2.04558	2.11041	2.10703	2.11938	2.04509	2.11073	2.10654	3375	
208	212	1208	886	2.11920	2.12115	2.04608	2.11070	2.10694	2.11952	2.04558	2.11103	2.10743	3376	hold
209	213	1198	887	2.12008	2.12155	2.04607	2.11144	2.10771	2.12041	2.04523	2.11095	2.10753	3374	
210	214	1169	887	2.12087	2.12169	2.04591	2.11076	2.10729	2.12071	2.04706	2.11174	2.10729	3375	

Converted Temperature Data - Station 7 Penetration 1

Table D1

APPENDIX E

Conversion of Pogo Probe Temperature Data to Temperature Gradients

For the 4 pogo probe stations, a computer program was developed that calculates the interval gradients and the total gradient. The program requires inputs on cards for each station in the format indicated in table Ela. The format of the output is shown in table Elb. An important use of the output was in determining the magnitude of thermistor leakage. The quantity (TC1 - TC2) gives the change between the two holding periods of thermistors 2, 3, and 4 with respect to the water thermistor. Table Elc is a sample of the program's output for the first penetration of station 7.

A listing of the program is given below. For operation from a terminal, it is first necessary to copy the program and the data to separate disk files. This can be accomplished in a similar manner as was done for TOWP and CONVERT (Figure Cla). We named our program file FILE and our data file FILE1. Figure E1 shows how FILE would be run from a terminal. The output is written onto a file named HEATFLOW. It is then necessary to have the contents of HEATFLOW printed. This can be done on the line printer as was done for files AIIDATA and TEMPDATA (Figure B1) or it can be done on the terminal by issuing the single command, COPY HEATFLOW.

At the time this program was written, file TEMPDATA had not been created. It represents an initial attempt to obtain thermal gradient information from the pogo probe measurements. In some cases, such as when holding periods were not well defined or when the sediment thermistors failed to reach equilibrium, we had to modify the output from the program. Furthermore, it would definitely have been easier to use TEMPDATA (actual temperature data) to calculate the gradients, rather than start with AIIDATA (digital data).

```
      DIMENSION T(4),TC1(4),TC2(4),TC12(4),RA(4),RB(4),RC(4)
      DATA KR,LP/105,108/
      DATA R0/20000./
    5 READ(KR,10)N,RZ,RF
   10 FORMAT(I10,2F10.0)
      C=1./(1.+R0/RF)
      D=1./(1.+R0/RZ)
      WRITE(LP,15)C,D
   15 FORMAT('1',F10.7,5X,F10.7)
      DO 25 J=1,4
      READ(KR,20)RA(J),RB(J),RC(J)
   20 FORMAT(3F10.0)
   25 CONTINUE
      DO 140  II=1,N
      CALL HFLOW (T,II,RA,RB,RC,C,D)
      CALL HFLOW (TC1,II,RA,RB,RC,C,D)
      CALL HFLOW (TC2,II,RA,RB,RC,C,D)
      DO 100 I=2,4
      TC1(I)=TC1(I)-TC1(1)
      TC2(I)=TC2(I)-TC2(1)
      TC12(I)=(TC2(I)+TC1(I))/2.
      WRITE(LP,90)II,I,TC1(I),TC2(I),TC12(I)
   90 FORMAT(' ',I4,5X,I4,3(5X,F10.7))
  100 CONTINUE
      TC12(1)=0.
      DO 120 I=1,4
      T(I)=T(I)-TC12(I)
      WRITE(LP,110)II,I,T(I)
  110 FORMAT(' ',I4,5X,I4,5X,F10.7)
  120 CONTINUE
      GRAD1=(T(3)-T(2))/100.
      GRAD2=(T(4)-T(3))/100.
      GRAD12=(T(4)-T(2))/200.
      WRITE(LP,130)GRAD1,GRAD2,GRAD12
  130 FORMAT(/3(5X,E15.7)/)
  140 CONTINUE
      READ(KR,150)NSTA
  150 FORMAT(I10)
      IF(NSTA .EQ. 1) GO TO 5
      STOP
      END
      SUBROUTINE HFLOW (T,II,RA,RB,RC,C,D)
      DIMENSION RA(4),RB(4),RC(4),AN(4),R(4),T(4)
      DATA R0/20000./
      DATA KR,LP/105,108/
      CD=C-D
      READ(KR,40)Z,F,(AN(I),I=1,4)
   40 FORMAT(6F10.0)
      A=(F-Z)/CD
      B=((Z*C)-(F*D))/CD
      RN=-R0/(A/B+1.)
      WRITE(LP,45)II,A,B,RN
   45 FORMAT(' ',I4,5X,E15.7,5X,E15.7,5X,F10.2)
      DO 60 I=1,4
      R(I)=R0/((A/(AN(I)-B))-1.)
      Q=ALOG(R(I))
      T(I)=(1./((RA(I)*(10.**(-9)))+(RB(I)*Q*(10.**(-10)))+
     C(RC(I)*Q*Q*Q*(10.**(-13)))))-273.15
      WRITE(LP,50)II,I,R(I),T(I)
   50 FORMAT(' ',I4,5X,I4,5X,F10.2,5X,F10.6)
   60 CONTINUE
      RETURN
      END
```

Table E1a

Input Format for Heat Flow Program (FILE)

Explanation

column	1	10	11	21	31	41	51	
		n	R_Z	R_F				
W	$\alpha\cdot 10^9$		$\beta\cdot 10^{10}$	$\gamma\cdot 10^{13}$				
2	$\alpha\cdot 10^9$		$\beta\cdot 10^{10}$	$\gamma\cdot 10^{13}$				
3	$\alpha\cdot 10^9$		$\beta\cdot 10^{10}$	$\gamma\cdot 10^{13}$				
4	$\alpha\cdot 10^9$		$\beta\cdot 10^{10}$	$\gamma\cdot 10^{13}$				
equilibrium	Z		F	Nw	N_2	N_3	N_4	repeat
pre-penetration hold	Z		F	Nw	N_2	N_3	N_4	n
post-pullout hold	Z		F	Nw	N_2	N_3	N_4	times
	. . .							
	1 (if another station follows)							

w=water thermistor

2=sediment thermistor located .5 meters below the weight stand

3=sediment thermistor located 1.5 meters below the weight stand

4=sediment thermistor located 2.5 meters below the weight stand

α,β,γ=thermistor calibration constants (in Real format)

n=number of measurements that use the given R_z,R_f,α's, β's and γ's (generally one station) - must be right justified to column 10 and in Integer format

N_w,N_2,N_3,N_4,Z,F=number of counts (in Real format) corresponding to the W,2,3 and 4 thermistors, R_z and R_f respectively

Table E1b

Format for Heat Flow Program Output (HEATFLOW)

Explanation

	1	C 5x	D						
	I_n	5x	A	5x	B	5x	R_n		
	I_n	5x	1	5x	R_w	5x	T_w		
equilibrium	I_n	5x	2	5x	R_2	5x	T_2		
	I_n	5x	3	5x	R_3	5x	T_3		
	I_n	5x	4	5x	R_4	5x	T_4		

repeat for pre-penetration and post-pullout holds

temperature corrections	I_n	5x	2	5x	$TC1_2$	5x	$TC2_2$	5x	$TC12_2$
	I_n	5x	3	5x	$TC1_3$	5x	$TC2_3$	5x	$TC12_3$
	I_n	5x	4	5x	$TC1_4$	5x	$TC2_4$	5x	$TC12_4$

corrected equilibrium temperatures	I_n	5x	1	5x	T_w
	I_n	5x	2	5x	T_2
	I_n	5x	3	5x	T_3
	I_n	5x	4	5x	T_4

skip a line

5x GRAD 23 5x GRAD 34 5x GRAD 24

repeat entire process n times for each station

repeat entire process again if another station follows

I_n = integer count which is set equal to the measurement number

5x = skip 5 spaces

R_n = resistance corresponding to 0 counts

TC1 = temperature correction calculated for pre-penetration hold

TC2 = temperature correction calculated for post-pullout hold

$TC1_2$ = average of TC1 and TC2 - used to calculate the corrected equilibrium temperatures

GRAD23, GRAD34, GRAD23 = temperature gradients calculated between thermistors 2 and 3, 3 and 4, and 2 and 4.

Table Elc

Sample Heat Flow Program Output - Station 7 Penetration 1

1	.1960769	.1999811		
1	-.8573645E 06		.1714813E 06	5000.31
1	1	4954.14	2.123587	
1	2	4965.96	2.061722	
1	3	4938.35	2.174175	
1	4	4889.45	2.225893	
1	-.8573645E 06		.1714823E 06	5000.34
1	1	4955.08	2.119361	
1	2	4969.29	2.046735	
1	3	4952.54	2.110540	
1	4	4915.78	2.106772	
1	-.8573645E 06		.1714853E 06	5000.45
1	1	4955.05	2.119524	
1	2	4969.55	2.045582	
1	3	4952.43	2.111029	
1	4	4915.63	2.107425	
1	2	-.0726262	-.0739412	-.0732837
1	3	-.0088211	-.0084958	-.0086585
1	4	-.0125891	-.0120984	-.0123438
1	1	2.1235668		
1	2	2.1350057		
1	3	2.1828337		
1	4	2.2382363		

.4782794E-03	.5540269E-03	.5161532E-03

Figure E1

Job Control Statements Necessary to Run FILE from a Terminal

```
!FORT4   FILE OVER RFILE
 EXT. FORTRAN IV, VERSION F01
OPTIONS >NS·BC,ADP

!SET F:105/FILE1:IN

!SET F:108/HEATFLOW:OUT

!LYNX RFILE OVER LFILE
:P1 ASSOCIATED.
    * * ALLOCATION SUMMARY * *
PROTECTION        LOCATION   PAGES

DATA <00>           A000        2
PROCEDURE <01>      A900        1
DOB <10>            A400        2

!START LFILE
 *STOP* 0
```